Physics

with a High Intensity Proton Source
at Fermilab

Draft Version 1.0
February 3, 2008

Contributors to this document

(under construction)

If there is anyone missing, e-mail ykkim@fnal.gov, or your working group conveners.

Please contribute (read it, send your comments etc.) or in other forms, and join the contributor list.

Jeffrey Appel (Fermilab)
David Asner (Carleton University)
Ikaros Bigi (University of Notre Dame)
Douglas Bryman (University of British Columbia)
Andrjez Buras (Technical University of Munich)
Marcela Carena (Fermilab)
Roberto Carosi (INFN, Pisa)
Dave Christian (Fermilab)
Janet Conrad (Columbia University)
Milind Diwan (Brookhaven National Laboratory)
Craig Dukes (University of Virginia)
Estia Eichten (Fermilab)
David Finley (Fermilab)
Peter Fisher (MIT)
Bonnie Fleming (Yale University)
Steve Geer (Fermilab)
Andre de Gouvea (Northwestern University)
Keith Gollwitzer (Fermilab)
Deborah Harris (Fermilab)
David Hertzog (University of Illinois, Urbana-Champaign)
Christopher Hill (Fermilab)
Stephen Holmes (Fermilab)
Gino Isidori (INFN, Frascati)
David E. Jaffe (Brookhaven National Laboratory)
Boris Kayser (Fermilab)
Edward Kearns (Boston University)
Young-Kee Kim (Fermilab and University of Chicago)
Andreas Kronfeld (Fermilab)
Kenneth Lande (University of Pennsylvania)
Kevin Lesko (Lawrence Berkeley National Laboratory)
Laurence Littenberg (Brookhaven National Laboratory)
Byron Lundberg (Fermilab)
Joseph Lykken (Fermilab)
Michelangelo Mangano (CERN)
David McGinnis (Fermilab)
Mark Messier (Indiana University)
James Miller (Boston University)
Sanjib Mishra (University of South Carolina)
William Molzon (University of California, Irvine)
Pier Oddone (Fermilab)
Vaia Papadimitriou (Fermilab)
Stephen Parke (Fermilab)
Klaus Peters (GSI)
Roberto Petti (CERN)
Kevin Pitts (University of Illinois, Urbana-Champaign)

Stephen Pordes (Fermilab)
Chris Quigg (Fermilab)
Thomas Phillips (Duke University)
Regina Rameika (Fermilab)
Lee Roberts (Boston University)
Jonathan Rosner (Univerwity of Chicago)
Alan Schwartz (University of Cincinnati)
Niki Saoulidou (Fermilab)
James Siegrist (UC Berkeley and Lawrence Berkeley National Laboratory)
Giulio Stancari of INFN Ferrara
Rex Tayloe (Indiana University)
Robert Tschirhart (Fermilab)
Taku Yamanaka (Osaka University)
Peter Yamin (Brookhaven National Laboratory)

Contents

1 Introduction

Perspective

Within the next ten years the Standard Model will likely have to be modified to encompass a wide range of newly discovered phenomena, new elementary particles, new symmetries, and new dynamics. These phenomena will be revealed through experiment with high energy particle accelerators, mainly the LHC. This will represent a revolution in our understanding of nature, and will either bring us closer to an understanding of all phenomena, through existing ideas such as supersymmetry to superstrings, or will cause us to scramble to find new ideas and a new sense of direction. We are thus entering a dramatic and important time in the quest to understand the fundamental laws of nature and their role in shaping the universe.

The energy scales now probed by the Tevatron, of order hundreds of GeV, will soon be subsumed by the LHC and extended up to a few TeV. We expect the unknown structure of the mysterious symmetry breaking of the Standard Model to be revealed. We will then learn the answer to a question that has a fundamental bearing upon our own existence: "What is the origin of mass?"

All modern theories of "electroweak symmetry breaking" involve many new particles, mainly to provide a "naturalness" rationale for the weak scale. Supersymmetry (SUSY) represents extra (fermionic) dimensions of space, leading to a doubling of the number of known elementary particles and ushering in many additional new particles and phenomena associated with the various symmetry breaking sectors. The possibility of additional bosonic dimensions of space would likewise usher in an even greater multitude of new states and new phenomena. Alternatively, any new spectroscopy may indicate new principles we have not yet anticipated, and we may see new strong forces and/or a dynamical origin of mass. The wealth of new particles, parameters, *CP*-phases, and other phenomena carries important implications for precision quark flavor physics experiments that are uniquely sensitive probes of new phenomena.

We have already begun to see the enlargement of the Standard Model in the leptonic sector. Neutrino masses and mixing angles, which in the early 1990's were unknown, must now be incorporated into our full description of nature. In a minimal scenario of Majorana masses and mixings amongst the three known left-handed neutrinos, we see a strong hint of a new and very large mass scale, possibly associated with grand unification or the scale of quantum gravity, the Planck mass. We are not yet sure what the proper description of neutrino masses and mixing angles will be. Experiments may reveal additional unexpected particles coupled to the neutrino sector. New phenomena, such as leptonic *CP*-violation, will be major focal points of our expanding understanding of the lepton sector. There is much to be done with experiment to attack the issues that neutrinos now present.

Already, developments in neutrino physics and the possibility of a novel source of *CP*-violation in the lepton sector have spawned hopes that the cosmic matter-antimatter

asymmetry may be explained through *leptogenesis*. Neutrino physics, together with the search for new energy frontier physics, offers the possibility of experimental handles on the questions of dark matter and dark energy. Without the discovery of new particles in accelerator experiments, the telescope-based cosmological observations of the early universe would remain unexplained puzzles. The process of understanding the laws of physics in greater detail through accelerator-based high energy physics will potentially have incisive impact on our understanding of dark matter and dark energy.

Precision flavor physics in both the quark and the lepton sectors offers a window on the sensitive entanglement of beyond-the-Standard-Model physics with rare processes, through quantum loop effects involving known or new states. Flavor physics offers sensitive indirect probes and may be the first place to reveal additional key components of the post-Standard Model physics. The main arenas for quark flavor physics include strange, charm and beauty, hence kaons, *D*-mesons, *B*-mesons and heavy baryons. A remarkable historical paradigm for the importance of flavor physics is the well known suppression of flavor-changing neutral currents. The analysis of the K_L–K_S mass difference by Gaillard and Lee, 35 years ago in the Fermilab Theory Group, led to the confirmation of the GIM mechanism and predicted the mass of the charm quark, $m_c \sim 1.5$ GeV, definitively and prior to its discovery. This, today, implies an astonishing constraint on SUSY models, e.g., that the down and strange squarks are mass degenerate to $1{:}10^5$. This, in turn, has spawned a new working hypothesis called "Minimal Flavor Violation" (MFV). But is MFV really a true principle operating in nature and, if so, where does it come from? Such questions can only be addressed in precision flavor physics experiments.

Modes in rare *K* and *B* decays have been calculated to a high degree of precision within the framework of the Standard Model. Hypothetical new phenomena coming from physics beyond the Standard Model can lead to departures from these precise predictions. In the lepton sector there remains a large unexplored territory in rare muon decays accessible to modern experiments with similar sensitivity to new physics. The spirit of the approach remains very much the same as in the era of Gaillard and Lee.

Flavor dynamics and the origin of quark and lepton masses and mixings are amongst the least understood topics in elementary particle physics, representing the darkest corner of the Standard Model. There is a plausible "string-inspired" view that the ultimate understanding of flavor dynamics will come only from a more fundamental theory at the inaccessible GUT or Planck scale. Yet, we do not know definitively the scale of and origin of these phenomena. Plausible theories abound in which flavor dynamics could be rich at scales of order hundreds of TeV and accessible to *K*, *B*, *D*, and rare muon transition experiments. In fact, rare decays provide a method to address the ultra high energy > 100 TeV scale in nature. The discovery of new physics in the study of *CP*-violating and rare decay processes would play a fundamental role in sculpting a revolutionary new view of the physical world.

Creating Opportunities

Experimental particle physics advances by synthesizing insights won by many techniques. Collider experiments have taken us to the energy frontier with proton-antiproton collisions at the Tevatron and electron-positron interactions at LEP and SLC. Colliders have enabled measurements of great delicacy at the *B* factories and CLEO. Fixed-target experiments have been major contributors to flavor physics, our knowledge of nucleon structure, and our understanding of neutrino properties and interactions. However, many of the accelerator experiments that have helped define the diversity and scale of our program, and have helped drive the past decades of discovery, are coming to an end.

Beyond the Tevatron Collider program, we look forward to the Large Hadron Collider, which will place experiment squarely in the heart of the TeV scale essential to the understanding of electroweak symmetry breaking. Fermilab is a key player in the LHC program, as a developer of superconducting magnets, the headquarters of U.S. CMS, and the site of the LHC Physics Center. The high-energy frontier is part of Fermilab's heritage, and remains an essential element of its future.

Doing good science and making new scientific tools available is critical to our challenging future. This requires the broadband energy frontier assault that the LHC provides, followed by the incisiveness of the ILC. We must also explore the energy frontier beyond the ILC via a multi-TeV scale lepton collider, such as CLIC or the muon collider. Both of these machines pose extreme technical challenges and have comparable degrees of unproven technological viability. Bold new concepts in overcoming some of these challenges have evolved in recent years and need to be tested.

This document describes a framework for constructing an adaptable program that will bring world-class science in the short term, can evolve toward world-leading experiments in the medium term, and prepares the technological ground for ambitious energy frontier accelerator initiatives in the future. While providing views of more than one possible long-term future, the program develops in stages, allowing for multiple decision points that refine and optimize the ultimate path and destinations. Scientific opportunities and the state of technology will inform each decision. Our overarching goal is to create a diversity of possibilities as we continue our tradition of discovery.

Above all, it is imperative that we adopt a realistic view and understanding of what can be done now, as well as a strong vision of regaining the energy frontier in the future. A new high-luminosity proton source, Project X (a national project with international collaboration), could provide a diverse interim physics program, and could potentially drive long range future accelerator initiatives. This would form the basis for the U.S. leadership in neutrino physics, and a parallel program of world-class kaon and muon experiments. The first phase could be developed with some of these experiments prior to the availability of Project X, using enhanced, existing facilities at Fermilab. As Project X becomes available, these experiments could enter a next phase in which the ultimate capabilities are achieved.

Project X calls for the development of the same superconducting radio-frequency technology as will be used in the ILC. Thus the pursuit of Project X would spur U.S. industrialization in this vital area while also providing a system test for key ILC components. The expertise gained through this work would position the U.S. and Fermilab to contribute significantly to the global ILC effort and would help position Fermilab to host the ILC.[1]

We focus here on a menu of experiments at the sensitivity frontier that work coherently with the laboratory's committed program in neutrino physics (MINOS through NOvA) to opportunities of next-generation neutrino experiments of great sensitivity to leptonic *CP* violation that would require a multi-MW proton source and a very large, longer baseline detector. Prominent examples are studies of the charged and neutral rare kaon decays $K \rightarrow \pi\nu\nu$ and the search for lepton-flavor violation in muon-electron conversion. These experiments, each with the capability to affect dramatically our understanding of the fundamental interactions, can produce world-class results with modest reconfiguration and improvement of the existing accelerator complex. Enhanced by a new bright proton source, Project X, they would become world-leading experiments. The superconducting linac would demonstrate the superconducting RF technology of the ILC and may ultimately provide a platform for developing an evolutionary path to a muon-storage-ring neutrino factory and a multi-TeV muon collider.

Not every item on the experimental menu will be chosen. The possibility of mounting some experiments early will be explored and R&D resource needs to investigate these possibilities are modest. The resource scope of a new high intensity proton source that drives this research program into the future is comparable to the Main Injector project (http://projectx.fnal.gov/RnDplan/).With the flexibility to construct a coherent program, we can deliver discovery science, renew the user community by encouraging young scientists to bring new ideas, and create possibilities for the future of particle physics.

[1] The ILC's opportunities for discovery have motivated the global particle physics community to come together in an effort to design the accelerator and its experimental program. Fermilab has contributed strongly to this effort: the design of the accelerator; the development of SCRF technology in the U.S.; the design of the physics and experimental program; the site studies necessary for hosting the ILC at or near Fermilab; and the establishment of a test-beam facility for the development of ILC detectors. The ILC and related SCRF efforts at Fermilab make up by far the laboratory's largest future program.

2 The Proton Source Roadmap for Fermilab

Fermilab is embarked upon a program of continuous performance improvements to the proton complex in support of the ongoing needs of the neutrino program. This program is being implemented in phases, with the "Proton Plan" currently underway, to be followed by accelerator upgrades implemented as part of the NOνA project. The Proton Plan aims to deliver roughly 340 kW of beam power to the NuMI target, coincident with 70 kW to the antiproton production target in early FY 2009. Following completion of Run II the total, 410 kW, would be available on the NuMI target. The NOνA Project includes accelerator and NuMI target station upgrades aimed at delivery of 700 kW of beam power to the NuMI target.

Following completion of the Proton Plan there are several paths to further increase the proton beam power available at Fermilab that have been considered. These paths include evolution and further upgrade of the existing complex to "Super-NuMI" (SNuMI), construction of a new rapid cycling synchrotron, and construction of a high-power linac based on Superconducting RF technology (SCRF) developed for the ILC. The path based on a new SCRF linac is referred to as "Project-X" and has been identified by the Fermilab Steering Group as the most compelling path forward. The Project-X path described below provides the greatest flexibility toward a very high power facility while simulataneously advancing energy-frontier accelerator technology.

The table below compares performance of the present complex with the SNuMI path forward and the Project-X path forward. The first three columns represent current performance and improvements now underway. The last two columns list SNuMI and Project X parameters. All columns are based on injecting beam from the existing 8 GeV Booster, except for Project X, which eliminates the need for the Booster. While the table does not list any beam power availability at 8 GeV in SNuMI, protons could be made available at this energy at the expense of availability at 120 GeV.

	Current	Proton Plan	NOvA	SNuMI	Project X	Unit
Batch intensity (8 GeV)	3.0E12	4.3E12	4.1E12	4.5E12	5.6E13	protons/pulse
Rep rate	9	9	12	13.5	5	Hz
Protons / hour	9.7E16	1.4E17	1.8E17	2.2E17	1.0E18	
Main Injector batches	11	11	12	18	3	
MI batches to pbar target	2	2	0	0	0	
MI cycle time	2.4	2.2	1.33	1.33	1.4	Second
NuMI beam power (120 GeV)	216	338	710	1169	2304	kW
8 GeV beam power (available)	14	17	16	0	205	kW
Injection energy (1st synch)	400	400	400	400	8000	MeV
βy^2	1.45	1.45	1.45	1.45	90.30	
Injection emittance	10	10	10	10	20	πmm-mr
Injection space charge tune shift	0.15	0.22	0.21	0.23	0.07	

Table 1 Proton sources at Fermilab. NOvA column includes a potential upgrade of the Booster repetition rate to support simultaneous delivery of 2×10^{20} protons / year at 8 GeV. NOvA itself requires Booster operations at 9 Hz.

2.1 Project X

Project X is identified in the Fermilab Roadmap as described in the Fermilab Steering Group Report as the preferred route forward for the proton based program at Fermilab. (http://www.fnal.gov/pub/directorate/steering/index.shtml).

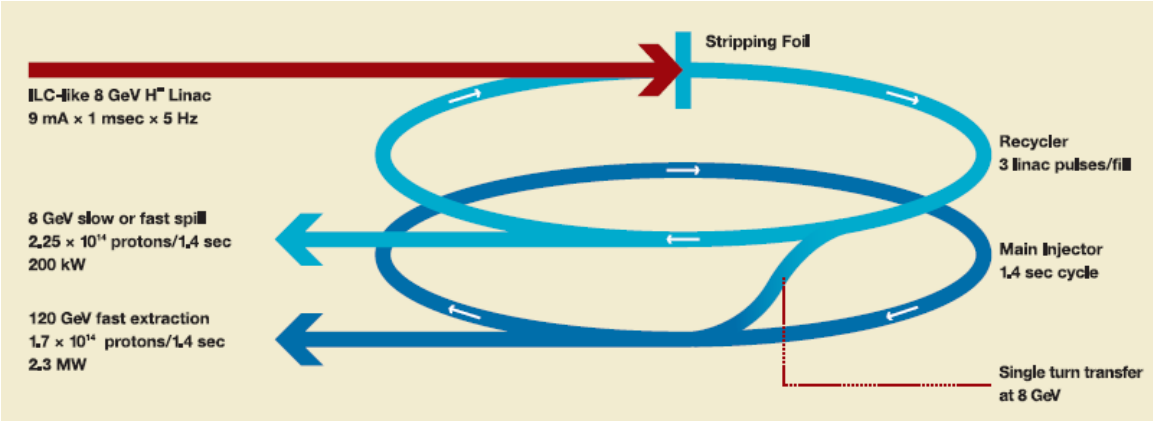

Figure 2.1: Schematic view of Project X

Project X is based on an 8 GeV superconducting H^- linac, paired with the existing (but modified) Main Injector and Recycler rings, to provide in excess of 2 MW of beam power throughout the energy range 60 – 120 GeV, simultaneous with at least 100 kW of beam power at 8 GeV. The linac utilizes technology in common with the ILC over the energy range 0.6 – 8.0 GeV. Beam current parameters can be made identical to those of ILC resulting in identical RF generation and distribution systems. This alignment of ILC and Project X technologies allows for a shared development effort. The initial 0.6 GeV of the linac draws heavily on technology developed by Argonne National Laboratory for a facility for rare isotope beams. It is anticipated that the exact configuration and operating parameters of the linac will be defined through the R&D program and will retain alignment with the ILC plan as it evolves over this period.

Utilization of the Recycler Ring as an H^- stripper and accumulator ring is the key element that provides the flexibility to operate the linac with the same beam parameters as the ILC. The linac operates at 5 Hz with a total of 5.6×10^{13} H^- ions delivered per pulse. H^-'s are stripped at injection into the Recycler in a manner that "paints" the beam both transversely and longitudinally to reduce space charge forces. Following the 1 ms injection, the orbit moves off the stripping foil and circulates for 200 msec, awaiting the next injection. Following three such injections a total of 1.7×10^{14} protons are transferred in a single turn to the Main Injector. These protons are then accelerated to 120 GeV and fast extracted to a neutrino target. The Main Injector cycle takes 1.4 seconds, producing approximately 2.3 MW of beam power at 120 GeV. At lower proton energies Main Injector cycle times can be shorter, allowing a beam power above 2 MW in the range of proton energy between 60 GeV and 120 GeV. In parallel, because the loading of the Recycler only requires 0.6 seconds, up to four linac cycles are available for accumulation

and distribution of 8 GeV protons from the Recycler. Total available 8 GeV beam power lies in the range of 100-200 kW, depending on the energy in the Main Injector.

It is anticipated that Project X configured as described above would initially support high intensity neutrino beams to the NOνA experiment, in parallel with a rare-decay research program driven with the intense 8 GeV proton source. Depending upon future directions, flexibility is retained for delivering neutrinos toward the DUSEL site and/or protons into the Tevatron.

2.2 Rare Decay Experiment Requirements of the 8 GeV Proton Complex

The next generation of rare-decay experiments requires kaon and muon beams of extraordinary quality. These experiments operate at the intensity frontier, where conventional decay and interaction processes can conspire in a high-rate environment to mimic the sought-after rare decay signatures. The principal weapon to control these backgrounds is the partnership of detectors that deliver excellent time resolution with high duty-factor beams which minimize the instantaneous rates that the detectors must face. Project-X is an exceptional opportunity to build a high intensity 8-GeV proton beam complex with nearly 100% duty factor and high availability (nominally 5000 hours per year). This complex could be realized with the intrinsically high duty factor SCRF 8-GeV linear accelerator driving a series of stacking and stretcher rings configured to deliver the RF structure required by the experiments. The joint potential of high duty factor and high availability would make the Fermilab complex a unique resource for rare-decay experiments.

Both the muon and kaon rare decay programs could have Phase I operation before the high-power Project X era (Phase II). A conceptual scheme has been developed to establish the required RF structure for Phase-I operation for both programs with an evolution of the existing Accumulator and Debuncher complex into an 8-GeV "stretcher ring". The scheme is described in some detail in the Fermilab Steering Group report. The proton beam RF train requirements for the kaon and muon programs are listed below in Table 2.

	Train Frequency (MHz)	Pulse Width (nanoseconds)	Inter-Pulse Extinction
Kaon experiments	20-30	0.1-0.2	10^{-3}
Muon conversion experiment	0.5-1.0	50	10^{-9*}
Muon g-2 experiment	30-100	50	---

*muon conversion extinction is achieved by a combination of extinction in the circulating beam/extraction and in an external device in the proton beam transport

Table 2: RF train requirements for the kaon and muon rare decay programs.

The average Phase-I beam current in an Accumuator/Debuncher stretcher ring would be about two amperes, comparable to B-factory currents and manageable with now standard accelerator instrumentation and techniques. Phase-II operation with the Accumulator /

Debuncher stretcher complex would lead to an order of magnitude higher circulating current which may lead to beam instabilities (driven by electron cloud effects for example) that could compromise the integrity of the RF train or the high duty factor required by the experiments. This can be mitigated by more rapid cycling of the 8 GeV Recycler/Debuncher/Accumulator complex, more sophisticated beam instrumentation and feedback, or evolution and construction of another stretcher ring in the complex for Phase-II operation. More rapid cycling of the 8 GeV complex would come at the expense of duty factor, but is relatively straightforward. Advanced instrumentation and feedback is possibly a solution but does not scale well to even higher power in the complex. A larger stretcher ring based on the Recycler or Tevatron infrastructure would reduce the circulating beam current by a factor of six and twelve, respectively. It has the best scaling properties for the complex, thereby reducing technical risk but comes with a greater initial capital cost. A larger stretcher ring also preserves the Fermilab antiproton complex for possible future experiments. A study group of experimenters and accelerator physicists is now actively reviewing these options to determine the best path forward for a Phase-II stretcher ring complex.

2.3 Comparison to Other Facilities.

The intensity frontier physics potential has motivated investments world-wide in next generation proton facilities. How the evolution of the Fermilab proton complex fits in this context is summarized here.

For long-baseline neutrino physics the principal metric is high-energy beam power where the Fermilab Main Injector and the new JPARC proton facility in Japan will be leading the next decade. The JPARC facility has a near term goal of >400 kW, comparable to the NOvA-era Proton Plan. JPARC is considering upgrades to 1.6 MW with 50 GeV protons by the end of the next decade. Project X would be able to deliver over 2 MW in the wide range of proton energy between 50 and 120 GeV in a similar time scale.

For rare-muon and rare-kaon decay physics the facility metric is more nuanced than neutrino facility metrics. Beam power, duty factor, beam availability and the ease of implementing necessary RF beam structures are all important elements. After the Tevatron collider program is complete, the existing multiple rings in the Fermilab accelerator complex can be redeployed as elements of a unique high duty factor and high availability facility with an order of magnitude higher sensitivity than other facilities world-wide. As an example, the comparative power of Project X among world-wide facilities for kaon physics is tabulated in Section 4.

For physics driven by antiproton beams, the existing Fermilab facility already exceeds the intensity goals of the GSI antiproton facility projected to come online late in the next decade. With the construction of a new accelerator ring dedicated for experiments, the current antiproton source will then be able to drive an antiproton based research program with an expected yearly antiproton yield of an order of magnitude higher than the one at GSI. In Section 5 the existing/projected Fermilab and projected GSI antiproton facilities are compared.

3 Neutrinos

3.1 Introduction

3.1.1 Neutrino Oscillations

During the past decade, we have found compelling evidence that neutrinos oscillate between flavors, which implies that they have nonzero masses. Laboratory and astrophysical data indicate that these masses are extremely small. Their small size suggests, through the "see-saw" mechanism, that new physics occurs at an ultra-high mass scale very close to the grand unification scale. Thus, neutrino masses provide a tantalizing window on physics way beyond the purview of the Standard Model.

Neutrino oscillation also implies that leptons mix, just as quarks do. As with quark mixing, leptonic mixing can lead to *CP* violation, which is a key requirement of theories that try to explain the baryon-antibaryon asymmetry of the universe. While *CP* violation in the CKM quark mixing matrix cannot explain this asymmetry, there is the remarkable prospect that, through "leptogenesis," leptonic *CP* violation can explain it.

To learn more about the new physics to which neutrino masses point and about the possibility of leptogenesis, we need to answer two qualitative questions:

1. Is the neutrino mass hierarchy normal (i.e., quark-like) or inverted?
2. Do neutrino interactions violate CP?

Also important is a quantitative third question:

3. What is the approximate size of the small leptonic mixing angle θ_{13}?

In the past decade, dramatic insights into the nature of neutrinos have been gained from experiments with naturally-occurring neutrinos. However, answering these new questions will require experiments with man-made neutrinos, from accelerators and reactors. In particular, answering the qualitative questions *1* and *2* will almost certainly require intense neutrino beams from accelerators. An important first step in this direction will be made by the NOvA experiment, using a beam from Fermilab.

In this section, we briefly review what has been learned so far about the neutrinos, discuss the importance of the open questions *1–3*, and consider how these questions can be answered, while recognizing that as in the past, neutrinos may bring us unexpected surprises in the future.

What we have learned so far

Neutrinos come in three "flavors": ν_e, ν_μ, and ν_τ. Each of these is coupled only to the charged lepton of the same flavor: ν_e to the e, ν_μ to the μ, and ν_τ to the τ. If there are additional neutrino flavors, they must be very massive or have non-Standard-Model

couplings. Neutrino oscillation is the remarkable morphing of a neutrino of one flavor into that of another. The leptonic mixing implied by this oscillation means that each neutrino of definite flavor, ν_α, is not a neutrino of definite mass, ν_i, but a superposition of such neutrinos. This superposition is given by $\nu_\alpha = \sum_i U^*_{\alpha i} \nu_i$, where U is the unitary *leptonic mixing matrix*. Conversely, each neutrino of definite mass is a superposition of the neutrinos of definite flavor, given by $\nu_i = \sum_\alpha U_{\alpha i} \nu_\alpha$.

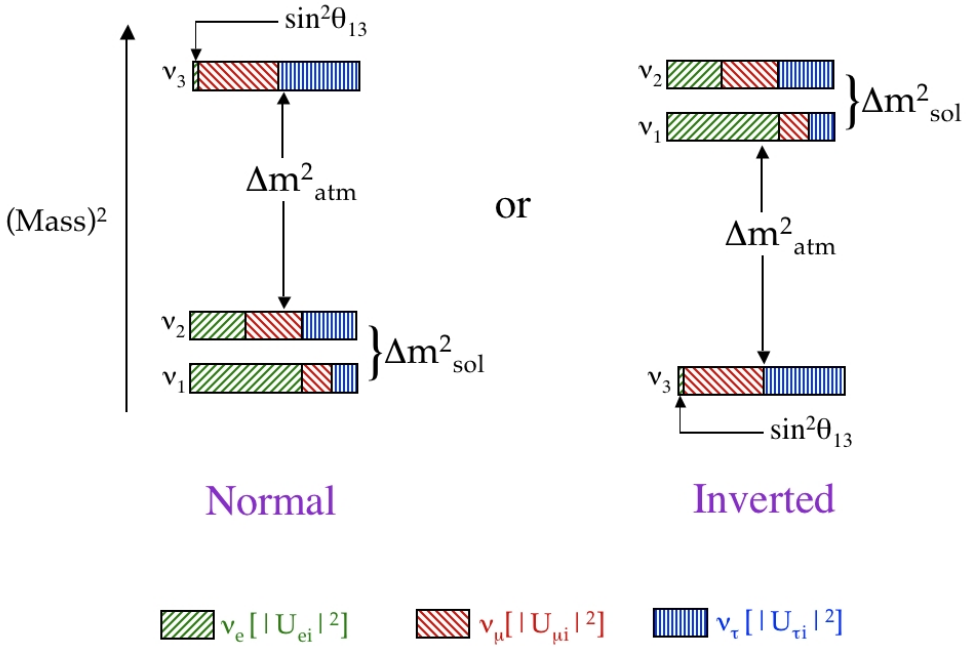

Figure 3.1 The neutrino (Mass)^2 spectrum.

Since there are three neutrinos of definite flavor, there must be at least three of definite mass: ν_1, ν_2, and ν_3. Oscillation data tell us that the (Mass)^2 spectrum of these neutrinos is one of the two spectra shown in Figure 3.1. The spectrum on the left, with the closely-spaced pair at the bottom, resembles the charged lepton and quark spectra, and so is referred to as a "normal" spectrum or hierarchy, while the very unusual one on the right, with the closely-spaced pair at the top, is referred to as an "inverted" spectrum or hierarchy.

The atmospheric (Mass)^2 splitting in Figure 3.1, $\Delta m^2_{\rm atm} \cong 2.4 \times 10^{-3}$ eV^2, drives the observed behavior of atmospheric neutrinos, while the thirty-times smaller solar (Mass)^2 splitting, $\Delta m^2_{\rm sol} \cong 7.6 \times 10^{-5}$ eV^2, drives the behavior of solar neutrinos. The approximate ν_e, ν_μ, and ν_τ fractions of each neutrino are shown by different color/hatching. However, the ν_e fraction shown for the isolated neutrino ν_3 is just an illustration of the possibilities. At present, we know only that, at 2σ, this fraction, whose size is the mixing parameter $\sin^2\theta_{13}$, is no larger than 0.032.

Neglecting phases irrelevant to neutrino oscillation, the leptonic mixing matrix can be written in the form

$$U = \underbrace{\begin{bmatrix} 1 & 0 & 0 \\ 0 & c_{23} & s_{23} \\ 0 & -s_{23} & c_{23} \end{bmatrix}}_{\text{Atmospheric}} \times \underbrace{\begin{bmatrix} c_{13} & 0 & s_{13}e^{-i\delta} \\ 0 & 1 & 0 \\ -s_{13}e^{i\delta} & 0 & c_{13} \end{bmatrix}}_{\text{Cross-Mixing}} \times \underbrace{\begin{bmatrix} c_{12} & s_{12} & 0 \\ -s_{12} & c_{12} & 0 \\ 0 & 0 & 1 \end{bmatrix}}_{\text{Solar}} \qquad \textbf{(1)}$$

Here, $c_{ij} \equiv \cos\theta_{ij}$ and $s_{ij} \equiv \sin\theta_{ij}$. The first, "Atmospheric," matrix factor dominates atmospheric neutrino oscillation, and from the atmospheric neutrino data, $37^\circ \leq \theta_{23} \leq 53^\circ$ at 90% CL. The last, "Solar," factor dominates solar neutrino flavor change, and from the solar (and to some extent the KamLAND reactor) data, $\theta_{12} = (33.9^{+2.4}_{-2.2})^\circ$. In striking contrast to the small quark-mixing angles, the atmospheric and solar neutrino mixing angles, θ_{23} and θ_{12}, are both very large. Indeed, the value of θ_{23} that fits the data best is 45° — maximal mixing. The middle, "Cross-Mixing," factor involves the mixing angle θ_{13}, which is constrained by upper limits from reactor data to $\leq 10^\circ$, corresponding to $\sin^2 2\theta_{13} \leq 0.12$. The Cross-Mixing factor also contains the *CP*-violating phase δ, which, if not 0° or 180°, leads to a *CP*-violating difference between the probabilities for corresponding neutrino and antineutrino oscillations. However, as the expression above for U makes clear, δ enters leptonic mixing only in the (θ_{13}, δ) combination $\sin\theta_{13}\exp(-i\delta)$. Thus, the size of any δ-induced *CP*-violating difference between neutrino and antineutrino oscillation will depend on the value of θ_{13}. In addition, our ability to tell whether the neutrino mass spectrum is normal or inverted will depend on θ_{13}. Consequently, it is important to know for how small a value of θ_{13} any proposed experimental facility can still show that neutrino and antineutrino oscillations violate *CP*, and still determine the nature of the neutrino mass spectrum.

The importance of the open questions

1. Is the neutrino mass spectrum normal or inverted?

The most plausible explanation for the extreme lightness of neutrinos is the "see-saw mechanism." Given this lightness, the see-saw mechanism suggests that neutrino masses come from physics near the grand unification energy scale, 10^{16} GeV. Needless to say, physics from $\sim 10^{16}$ GeV is far beyond the scope of the Standard Model. From the standpoint of the Grand Unified Theories (GUTs) that describe physics at this scale, we expect the neutrino spectrum (or "hierarchy") to resemble the charged lepton and quark spectra. The reason is simply that, in GUTs, the neutrinos, charged leptons, and quarks are all related – they belong to common multiplets of the theory. On the other hand, some classes of string theories lead one to expect an inverted neutrino spectrum. Thus, in working toward a theoretical understanding of the origin of neutrino mass, we would certainly like to know whether the mass spectrum is normal or inverted.

The nature of the spectrum can also help us determine whether, as is widely expected, neutrinos are their own antiparticles. The only known practical approach to confirming this expectation is to show that neutrinoless double beta decay occurs. The rate for this process is proportional to the square of an effective neutrino mass, $\langle m_{\beta\beta} \rangle$. If the mass spectrum is inverted, then $\langle m_{\beta\beta} \rangle$ must be larger than 10–15 millielectron volts (meV). Thus, if the spectrum should be found to be inverted, and a search for neutrinoless double beta decay can establish that the rate for this process is less than the rate that would correspond to $\langle m_{\beta\beta} \rangle$ = 10 meV, then we will have learned that, contrary to prejudice, neutrinos are distinct from their antiparticles. Looking at the matter in another way, if the spectrum should be found to be inverted, and neutrinos are their own antiparticles, then an experimental search for neutrinoless double beta decay is guaranteed to see a signal if its reach extends to $\langle m_{\beta\beta} \rangle$ = 10 meV.

The question of the character of the spectrum may involve more than the issue of whether it is normal or inverted. The LSND experiment reported an antineutrino oscillation whose short wavelength calls for a $(\text{Mass})^2$ splitting much larger than either of those in the three-neutrino spectra of Fig. 3.1.1. Confirmation of the reported oscillation would require that the neutrino spectrum be revised altogether to include one or more additional states. The MiniBooNE experiment, aimed at testing LSND, does not confirm the LSND oscillation in neutrino running. However, it is possible that the LSND signal may still be confirmed in antineutrino running. Furthermore, MiniBooNE has observed an excess of events at low energies which could suggest new physics. The interpretation of this excess may be addressed through future precision low energy neutrino experiments. In this report, we have assumed a three-neutrino spectrum in making our plans, but with a watchful eye on future developments.

2. Do neutrino interactions violate CP?

We would like to know why the universe contains baryons, of which we are made, but almost no antibaryons, which, had they been present, would have annihilated us. An explanation for this crucial feature of the universe is suggested by the see-saw mechanism. This mechanism gives the light neutrinos ultra-heavy (perhaps GUT-scale) neutrino "see-saw partners." Both the light neutrinos, ν, and their heavy see-saw partners, N, are their own antiparticles. The heavier the N are, the lighter the ν are. The heavy neutrinos N would have been created in the hot Big Bang, and would then have decayed via the modes $N \to \ell + H$ and $N \to \bar{\ell} + \overline{H}$, where ℓ is a lepton, and H is the Standard-Model Higgs boson. If today's light neutrinos violate *CP*, then quite likely so do their heavy see-saw partners, since both *CP* violations arise from the same matrix of Yukawa coupling constants. With *CP* violated, the *CP*-mirror-image decays $N \to \ell + H$ and $N \to \bar{\ell} + \overline{H}$ have different rates, so that N decays in the early universe would have produced a world with different numbers of leptons and antileptons. Standard-Model processes would then have converted some of this lepton-antilepton asymmetry into a baryon-antibaryon asymmetry, producing the matter-antimatter asymmetric world that we see today. Clearly, to explore the possibility that this scenario, known as leptogenesis, was indeed the origin of the matter-antimatter asymmetry of the universe, we must find out whether the light neutrinos violate *CP*.

3. What is the approximate size of θ_{13}?

While we know that the mixing angle θ_{13} is small, we do not know *how* small. A compilation of the θ_{13} predictions of 63 models of neutrino masses and leptonic mixing shows very wide variation, with predictions for $\sin^2 2\theta_{13}$ ranging from values slightly above the present upper bound all the way down to 10^{-5}. Thus, learning the actual size of θ_{13} will discriminate among the models. Quite apart from specific models, from the mathematics of mixing it can easily be shown that it is highly unlikely for θ_{13} to be very different from the other, large mixing angles unless there is some physical mechanism making it so. Hence, should we find that $\sin^2 2\theta_{13}$ is less than, say, 10^{-2}, there will be strong motivation to seek a reason, such as a new symmetry, for this behavior. Clearly, learning the size of θ_{13} will be important to our quest for an understanding of the origin of neutrino mass.

As we have already noted, and will see in greater detail shortly, the size of leptonic *CP* violation and our ability to determine whether the neutrino mass spectrum is normal or inverted both depend on the value of θ_{13}. Thus, knowledge of this value would be of help in the planning of experiments to probe *CP* violation and the nature of the mass spectrum. However, this knowledge is not essential if, as here, the approach being contemplated is appropriate for any value of $\sin^2 2\theta_{13}$ within a broad range covering several orders of magnitude.

How the questions can be answered

The determination of θ_{13} will be a major focus of accelerator and reactor experiments already under construction. Here we shall concentrate on the determination of the neutrino mass hierarchy and the search for *CP* violation – objectives of a longer- term program.

The mass hierarchy and *CP* violation can both be probed via accelerator neutrino experiments that study the oscillations $\nu_\mu \to \nu_e$ and $\overline{\nu}_\mu \to \overline{\nu}_e$. The appearance probability for ν_e in a beam that is initially ν_μ can be written for $\sin^2 2\theta_{13} < 0.2$

$$P\left[\nu_\mu \to \nu_e\right] \cong \sin^2 2\theta_{13}\, T_1 - \alpha \sin 2\theta_{13}\, T_2 + \alpha \sin 2\theta_{13}\, T_3 + \alpha^2\, T_4$$

Here, $\alpha \equiv \Delta m^2_{21} \big/ \Delta m^2_{31}$ is the small (~ 1/30) ratio between the solar and atmospheric $(\text{Mass})^2$ splittings, and

$$T_1 = \sin^2\theta_{23}\,\frac{\sin^2\left[(1-x)\Delta\right]}{(1-x)^2}$$

$$T_2 = \sin\delta \sin 2\theta_{12}\sin 2\theta_{23}\sin\Delta\,\frac{\sin(x\Delta)}{x}\,\frac{\sin\left[(1-x)\Delta\right]}{(1-x)}$$

$$T_3 = \cos\delta \sin 2\theta_{12}\sin 2\theta_{23}\cos\Delta\,\frac{\sin(x\Delta)}{x}\,\frac{\sin\left[(1-x)\Delta\right]}{(1-x)}$$

$$T_4 = \cos^2\theta_{23}\sin^2 2\theta_{12}\,\frac{\sin^2(x\Delta)}{x^2}$$

In these expressions $\Delta \equiv \Delta m^2_{31}L/4E$, with L the distance between the neutrino source and the detector and E the neutrino energy, is the kinematical phase of the oscillation. The quantity $x \equiv 2\sqrt{2}G_F N_e E/\Delta m^2_{31}$, with G_F the Fermi coupling constant and N_e the electron number density, is a measure of the importance of the matter effect resulting from coherent forward scattering of electron neutrinos from ambient electrons as the neutrinos travel through the earth from the source to the detector.

In the appearance probability $P(\nu_\mu \to \nu_e)$, the T_1 term represents the oscillation due to the atmospheric mass scale, the T_4 term represents the oscillation due to the solar mass scale, and the T_2 and T_3 terms are the *CP*-violating and *CP*-conserving interference terms, respectively. At the first atmospheric oscillation maximum, $\left[(1-x)\Delta\right] = \pi/2$, the atmospheric T_1 term and the solar T_4 term are equal when $\sin^2 2\theta_{13} = 0.002$. The solar term leads to ν_e appearance even if $\sin^2 2\theta_{13} = 0$.

The probability for the corresponding antineutrino oscillation, $P\left(\overline{\nu}_\mu \to \overline{\nu}_e\right)$, is the same as the probability $P(\nu_\mu \to \nu_e)$ given by the equations above, but with the signs in front of both x and $\sin\delta$ reversed: both the matter effect and *CP* violation lead to a difference between the $\nu_\mu \to \nu_e$ and $\overline{\nu}_\mu \to \overline{\nu}_e$ oscillation probabilities. In view of the dependence of x on Δm^2_{31}, and in particular on the sign of Δm^2_{31}, the matter effect can reveal whether the neutrino mass hierarchy is normal or inverted. However, to determine the nature of the hierarchy via the matter effect, and to establish the presence of *CP* violation in neutrino oscillation, it obviously will be necessary to disentangle the matter effect from *CP* violation in the neutrino-antineutrino probability difference that is actually observed. To this end, complementary measurements will be extremely important. These can take advantage of the differing dependences on the matter effect and on *CP* violation in $P(\nu_\mu \to \nu_e)$.

Given that $\left|\Delta m^2_{31}\right| \cong 2.4\times10^{-3}\,\mathrm{eV}^2$, the matter-effect parameter $|x| \cong E/(12\,\mathrm{GeV})$. With this in mind, we imagine, as one illustration, measurements made at accelerator neutrino

energies of ~ 1 GeV, and at the L/E corresponding to the first maximum of the atmospheric oscillation term, $\sin^2 2\theta_{13} T_1$, of $P(\nu_\mu \to \nu_e)$. Then, from the equations for $P(\nu_\mu \to \nu_e)$, we see that — at this given L/E — the effect of matter on the T_1 term, $1/(1-x)^2 \cong 1 \pm (E/6\,\mathrm{GeV})$, grows with energy, enhancing (suppressing) the term if the mass hierarchy is normal (inverted). In contrast, at this same fixed L/E, the *CP*-violating T_2 term in $P(\nu_\mu \to \nu_e)$ is approximately proportional to Δ, hence to L/E, so that it grows with L and decreases with E. At fixed L/E, it does not vary with energy or distance. Hence, two detectors, at two different distances L and two different energies E, but at the same L/E, will see the same *CP* violation but different matter effects.

As a second illustration, if we go from the first atmospheric oscillation maximum to the second one by reducing the energy a factor of three with L fixed, the effect of matter on the $\sin^2 2\theta_{13} T_1$ term is reduced by a factor of three, while the *CP*-violating term proportional to $\sin\delta$ is tripled. In a broadband neutrino beam, the required reduction of E by a factor of three can be achieved by simply probing a lower-energy part of the neutrino spectrum. In a narrowband off-axis beam, the reduction can be achieved by going further off axis at a given L.

The violation of *CP* can either enhance $\nu_\mu \to \nu_e$ and suppress $\bar{\nu}_\mu \to \bar{\nu}_e$, or *vice versa*, depending on the value of the phase δ. Similarly, the matter effect can either enhance $\nu_\mu \to \nu_e$ and suppress $\bar{\nu}_\mu \to \bar{\nu}_e$, or *vice versa*, depending on the sign of Δm^2_{31}. For a given θ_{13}, the neutrino-antineutrino asymmetry obviously is easiest to observe when *CP* violation and the matter effect happen to add together in the same direction.

In Section 3.1.2 (A) we outline an experimental program to address these important measurements.

3.1.2 Neutrino Scattering Physics

Measurements of neutrino scattering have played an important role in both the development of the Standard Model as know it, and in providing evidence that the Standard Model does not suffice. The first measurements of the weak neutral current were made with neutrino scattering measurements on both electrons and nuclei, and neutrinos have probed the quark structure of the nucleon and provided measurements of the strong coupling constant across a range of momentum transfers. More recently, the discovery that neutrinos change flavor and therefore have mass has forced the field to rethink completely the notion of mass and its origin.

The previous section discusses how oscillation measurements will need to be made at hundreds of kilometers from the neutrino production location. This section will discuss the questions that can be answered with neutrino scattering measurements at short distances. A clear need for scattering measurements comes from the fact that neutrino oscillation experiments rely on precise knowledge of neutrino scattering cross sections. The 2004 *APS Multidivisional Neutrino Study Report* which set a roadmap for neutrino

physics predicated its recommendations on a set of assumptions about current and future programs including: "determination of the neutrino reaction and production cross sections required for a precise understanding of neutrino-oscillation physics and the neutrino astronomy of astrophysical and cosmological sources. Our broad and exacting program of neutrino physics is built upon precise knowledge of how neutrinos interact with matter."

Neutrino Scattering Measurements from Low to High Energy

At neutrino energies below about 1GeV, the quasi-elastic process dominates the cross section. With a current uncertainty of 15-20%, this process is one of the best measured cross sections in neutrino physics. The upcoming generation of cross section experiments will make significant inroads in understanding the form factor for this process as a function of momentum transfer, and make first measurements of possible nuclear effects of this cross section. However, a whole new suite of measurements would be possible with additional proton power in the beamline. This process will dominate any signal of muon to electron neutrino oscillations, and recent studies have shown that for the long term oscillation experiments, not only the cross section itself must be known but eventually, uncertainties on the ratio between electron and muon neutrino cross sections will become important, and the field must measure that ratio accurately.

At higher energies, deep inelastic scattering processes dominate, offering the opportunity to probe the quark distributions in the nuclei themselves. Using the high statistics samples that would be accessible in the Project X era as well as with special attention to minimizing neutrino beam uncertainties, it should be possible to measure separately the four different structure functions $F_2^{\nu N}$, $F_2^{\nu \mathrm{bar} N}$, $F_3^{\nu N}$ and $F_3^{\nu \mathrm{\ bar\ } N}$.

At energies above 10's of GeV, on shell charm can be produced, which can result in new precise measurements of the strange sea. Although we know that the net strangeness in the proton and neutron must be equal to 0, neutrino scattering measurements provide our best knowledge of whether or not the strange quark distribution equals that of the strange anti-quark distribution as a function of momentum transfer. These measurements will require high statistics of both neutrino and antineutrino data, and at the current time only a very small number of nuclei have been probed.

At neutrino energies above about 30 GeV, the neutrino electron scattering cross section becomes large enough to provide a suite of new measurements. One exciting possibility with the advent of a high energy high statistics neutrino and antineutrino run would be that of a new measurement of $\sin^2\theta_W$, the weak mixing angle, using neutrino-electron scattering. There is currently a 3 sigma discrepancy between the most precise measurement in neutrino nucleon scattering and the value coming from precision electroweak observables at the Z mass.

With the advent of neutrinos obtaining a mass comes the possibility that neutrinos have magnetic moments. If the neutrino mass were 1 eV, the resulting magnetic moment would be about $3e^{-19}$ μ_b, where $\mu_b = e/2m_e$. This value is too small to be detected, but that means that any measurement of a non-zero magnetic moment would be a striking signal

of new physics. By measuring the elastic scattering rate as a function of recoil energy, in the Project X era one can probe well past current experimental limits. In the next section we outline the Fermilab experiments, current and future, that can contribute to this important area of neutrino physics.

3.1.3 Proton Decay and Related Deep Underground Physics

One of the central consequences of grand unification is the prediction of proton decay. Its observation would lend credence to the general picture of coupling constant unification and the merging of the standard gauge interactions into a common simple gauge group, such as SU(3) x SU(2) x U(1) → SU(5), with a telescoping pathway to → SO(10) → E6 → ... E8 x E8. This phenomenon is central to SUSY, and Superstring Theory, and we may already be seeing hints of the effects of unification in the tiny nonzero neutrino masses as anticipated by the neutrino seesaw mechanism.

Very large detectors future are being contemplated for neutrino oscillation physics, with accelerator neutrinos and atmospheric neutrinos, supernova neutrino detection, dark matter searches and a renaissance of searches for nucleon decay. One possibility is a water Cherenkov detector, similar to Super-Kamiokande, with mass in the range of 1000 kton. Another is a liquid Argon detector, similar to the ICARUS liquid Argon TPC for the Gran Sasso Laboratory. Both have various advantages, the water Cherenkov detector mass providing great fiducial volme sensitivity, and the liquid Argon detector providing resolution through tracking similar to a bubble chamber. Both are being contemplated in a deep underground facility, such as DUSEL, to operate in the very low cosmic ray background at depths as great as 6000 feet.

Very large detectors would be extremely sensitive to nucleon decay. Such detectors would extend the limits on proton decay into modes such as $p \rightarrow e^+ \pi^0$ to sensitivities of 10^{35} yr or beyond and will have complimentary sensitivity to the scalar mediated mode p $\rightarrow K^+ \nu^0$ at a sensitivity of a few 10^{34} yr. Although the kaon is too slow to produce Cherenkov radiation in a water detector, the 2π decay modes can be reconstructed in low background environment. This level is suggested by gauge boson mediated proton decay in super-symmetric GUTs.

The complementarity to the neutrino long baseline program and the study of leptonic CP-violation suggests that these programs should operate in tandem in a common detector. In addition, there is sensitivity to the neutrinos produced from galactic supernovae. A supernova event is expected on a 40 year time scale within the galaxy and could produce of order 10^5 detectable neutrinos. Large, isotropically sensitive, general-purpose detectors can also probe many other physics targets. This includes exploration of subjects ranging from the temporal variation of the solar neutrino flux, searches for neutrinos from individual or aggregate sum over all supernovae and other cataclysmic events, to cosmic ray composition (where the depth is advantageous), dark matter searches annihilation neutrinos, searches for cosmic exotic particles (e.g., quark nuggets, monopoles, monopolonium, etc.), and point source neutrino astronomy. In all instances, the capability

potentially exceeds Super-Kamiokande by virtue of lower energy thresholds, better energy loss rate resolution, momentum, angle, sign and event topology resolution.

3.2 Experimental Program

The compelling questions in neutrino physics today drive a worldwide program of forefront neutrino experiments. The operating, approved, and proposed experiments constitute a program such that Fermilab is, and will continue to be, a leader in this exciting field. The experiments which comprise this program are described below and the strategy to realize it is described in the "The Neutrino Strategy" section.

3.2.1 Neutrino Oscillation Measurements

Fermilab is home to two operating neutrino beamlines, the Booster Neutrino Beam and the NuMI Neutrino Beam. An exciting program of short and long baseline neutrino oscillation experiments is presently underway. With experiments using these beams, together with upgrades such as Project X, we envision a vibrant future in neutrino oscillation physics at Fermilab.

The Booster Neutrino Beamline (BNB) produces a narrow band, 800 MeV peak energy, primarily muon neutrino beam, from 8 GeV protons from the Fermilab Booster. The MiniBooNE short baseline neutrino oscillation experiment, running since 2002 on the BNB, has ruled out a two neutrino interpretation of the LSND neutrino oscillation signal in neutrino mode. However, a low energy excess observed by MiniBooNE is still not understood. Results in anti-neutrino mode may provide an important clue both to oscillations across a broad range of energies, and to the low energy excess. A proposed new liquid Argon TPC experiment, MicroBooNE, will definitively address this low energy excess, measure low energy neutrino cross sections on Argon, and perform important R&D necessary for larger liquid Argon detectors.

Fermilab is presently operating the world's highest intensity neutrino beam for long baseline neutrino oscillation physics, the NuMI beam. In the near term, the MINOS experiment is NuMI's flagship long baseline program, providing definitive evidence for the oscillatory behavior of neutrinos as well as the best measurement of Δm^2_{23}. Although not optimized for ν_e appearance, MINOS has sensitivity to θ_{13} that reaches beyond the benchmark limit by CHOOZ. As such, it will provide valuable input, positive or negative, in the search for θ_{13}.

After 2011, the NuMI beamline will have the main objective of delivering neutrinos to the NOvA detector. In recent studies and reviews NOvA has been classified as one of the Phase I experiments which are searching for the small mixing angle θ_{13}. The other experiments are the reactor neutrino experiments Double CHOOZ and Daya Bay, as well as the T2K experiment which will use the new neutrino beam from JPARC and the Super-Kamiokande detector. While the Double CHOOZ experiment will achieve a

maximum sensitivity to $\sin^2 2\theta_{13} \sim 0.03$ (90% CL), the Daya Bay and T2K experiments hope to reach a sensitivity of $\sin^2 2\theta_{13} \sim 0.01$ (90% CL) after several years of running.

NOvA was recommended for CD-2 approval in October 2007 based on a schedule that has 15 kilotons of detector mass complete by January of 2013. The project scope includes an accelerator upgrade to take the NuMI intensity to 700 kW. NOvA plans to run for six years, three using neutrinos and three using anti-neutrinos. NOvA will extend the search for $\nu_\mu \to \nu_e$ oscillations down to $\sin^2 2\theta_{13} = 0.02$ (3σ) and obtain information about the sign of Δm^2_{23} and δ_{CP}. For favorable values of the phase δ_{CP}, NOvA can determine the mass hierarchy for values of $\sin^2 2\theta_{13} > 0.06$ (at the 95% C.L.). In addition, NOvA will improve on the measurements of $\nu_\mu \to \nu_\tau$, measuring $\left|\Delta m^2_{23}\right|$ to roughly 3% and $\sin^2 2\theta_{23}$ to roughly 2-3 %, providing a sensitive test of μ-τ symmetry in neutrinos.

Project X Neutrino Physics

A flagship neutrino program for Project X could be a new long baseline beam directed toward a very large detector. The physics motivations and experimental strategies have been previously outlined in detail in the report by NuSAG to NSAC/HEPAP and the accompanying study by the joint BNL/FNAL working group [arXiv:0705.4396 hep-ph].

Here we recapitulate the essential points that relate to the experimental strategy for long baseline neutrino oscillation physics. In all cases, an intense neutrino beam based on 2.3 MW proton beam power driven by Project X is assumed. That leaves the following fundamental experimental choices to be determined: the choice of detector technologies, the baseline of the neutrino beam, and the neutrino beam configuration (wide band vs. off-axis, narrow band). Connected to these choices are scientific and practical considerations. The scientific considerations are mainly related to how the choice of detector technologies will influence a broader program that includes proton decay, astrophysics, and other non-accelerator opportunities. Another important scientific consideration will be the evolving knowledge of θ_{13} as the experimental program advances. The practical considerations are driven by cost, schedule, and risk. Phase II accelerator based programs have also been proposed for neutrino beams from JPARC (T2KK) and CNGS (ModuLAr). In all programs major improvements in proton intensity and detector mass are required.

Project X Neutrino Detectors

For the massive detectors required for *CP* violation searches the choice of detector technology has been narrowed to three possible configurations: a 100 kiloton liquid argon TPC (LAr100), a 300 kiloton water Cherenkov detector (WC300), or some combination of the two. These detector configurations are estimated to be roughly comparable in sensitivity, where the larger mass of the WC300 compensates for lower efficiency and higher background compared to the assumptions made for LAr100. An advantage of the water Cherenkov option is that it is a known and tested technology on large scales, though several R&D issues remain.

The liquid argon option shows great promise for reach in accelerator and non-accelerator physics, but the technology has not yet been demonstrated for a large mass (>100 ton) in a physics experiment. There is necessary R&D to accomplish in order to realize detectors on this mass scale. For both technologies, if sited below ground. This includes R&D on construction of large caverns.

Water Cherenkov Detectors

The long and successful history of the operation of the Super-Kamiokande detector makes the water Cherenkov detector technology an excellent candidate for scaling to even larger sizes. The critical technical issues that need to be studied for construction of such a detector are discussed below.

First, since the detector needs to be sited underground, there are two concepts for constructing a water Cherenkov detector in the 300-500 kton scale. These can be classified as single horizontal chamber (the concepts for the proposed Hyper-Kamiokande and the UNO detectors), and multiple vertical cylinders (the concepts for MEMPHIS in Frejus or the Multi-Modular, 3M, detector in Homestake). In either case, the feasibility of the chamber is determined by the span – the width of the horizontal chamber or the diameter of the vertical cylinder. The cavern stability and feasibility must be examined at the specific proposed location, depth, and rock type. Detailed geo-technical measurements and modeling should be carried out so that questions about cavern configurations can be resolved.

The second issue in regard to water detectors is the choice of phototube. Recent developments have led to the option of selecting smaller diameter (10 – 12 inch) but more efficient tubes than used in Super-Kamiokande (20 inch). The smaller PMTs are also mechanically stronger than the larger PMTs and, in case of implosion, have only 1/8 the stored energy of the larger PMTs. The smaller tubes are also shorter allowing for a larger fraction of the water volume to be fiducial.

Because the water detectors do not need to be prototyped on a small scale they do not feature prominently in the near term plans for the Fermilab accelerator complex. Nevertheless, if they are to be part of the long term neutrino program, attention to the specific R&D needs of this technology must be considered in planning the future program.

Liquid Argon TPC Detectors

Liquid argon detectors show great promise with excellent efficiencies and background rejection for a variety of physics goals. An extensive R&D program culminating in the success of the ICARUS T600 program has illustrated the capabilities of the detector. However, further R&D is necessary to consider massive detectors, on the scale of tens of kilotons.

For several years there have been efforts both in the U.S. and Europe to carry out an R&D plan for large detectors and several different design ideas for massive detectors have emerged. These include a modularized detector, a single detector but with modularized drift regions, and a single open volume, very long drift detector combining charge and light collection. In addition to conceptual designs for massive detectors, small scale test stands have been constructed to address the technical issues of liquid argon purity and electronics.

Regardless of the configuration, the major challenges for running a liquid argon detector include:

- Achieving and maintaining argon purity adequate to support electron drift times on the order of 10 msec in industrially built vessels
- Achieving a high signal to noise ratio with wires of lengths up to 10 meters
- Optimizing the detector size, configuration, and internal detectors for constructability and cost scaling
- Developing fully automated simulation, reconstruction and particle identification techniques, and data reduction algorithms for liquid argon detectors

In recent months, progress on how to bridge the gap between test stands and the ultimate massive detector has emerged. A staged evolution of the liquid argon detector technology for use in neutrino experiments, as suggested by the NuSAG committee, has come into focus.

Detectors ranging in mass from the ton to kiloton scale can be deployed in existing Fermilab neutrino beams. At each stage, key issues in detector development will be addressed at the relevant scale, as well as producing physics results. The shift from R&D to physics will evolve with the size of the detector. The R&D goal of the program is to develop a clear concept of how to construct a detector with total mass in the one hundred kiloton range. Along the way, exciting and timely physics questions will be addressed.

The R&D strategy of developing a series of liquid argon TPCs for neutrino experiments is already underway, with the 0.3 ton ArgoNeuT detector being installed in the NuMI-MINOS near detector hall. This small detector will be able to record more than 150 neutrino interactions per day, providing a valuable data set for developing reconstruction and particle ID algorithms.

The next detector in the series would be a 170 ton total volume, installed in the Booster Neutrino beam as has been proposed for the MicroBooNE experiment. This detector will insure that progress in the program continues smoothly by developing components needed for a larger detector. At the same time the MicroBooNE experiment addresses the MiniBooNE low energy excess and measures neutrino cross sections on argon.

For the next step, installation of liquid argon detector modules in the Soudan Laboratory (LAr5 at Soudan) on the NuMI beam (~5000 ton) is being explored. This effort would address all of the issues related to underground operation. At the same time, a detector of

this mass has sensitivity to measuring $\sin^2 2\theta_{13}$ and the mass hierarchy with reach comparable to that of the NOvA experiment. Combination of the results from both detectors would maximize the investment made in the NuMI beam. A simple analysis to determine the physics reach of an evolving NuMI program with the NOvA and liquid argon detectors has been done. The results show this detector combination to be very advantageous. The NOvA experiment will have sensitivity down to $\sin^2 2\theta_{13} \sim 0.02$. The addition of the LAr5 detector will double that sensitivity. Operation of these detectors with Project X intensity will extend the reach to observing $\sin^2 2\theta_{13}$ to well below 0.01.The actual limit achievable will depend on the knowledge of the intrinsic and neutral current backgrounds. Using both detectors and Project X, ultimate sensitivity to the mass hierarchy for a large region of phase space can extend down to well below $\sin^2 2\theta_{13} \sim 0.04$. A full simulation of the liquid argon detector including measured efficiencies and background measurements from the ArgoNeuT detector will be done in the near future. Preliminary considerations also indicate that the underground liquid argon detector may also have competitive sensitivity to the proton decay in the $K\nu$ channel.

The above outlined program makes progress in both the R&D and physics phases continuously throughout this and the next decade, leading to a flagship program with excellent reach in the exploration of neutrino mass and mixing. The sensitivities for the above scenarios are shown in Figure 3.2.

Building on Project X: A Neutrino Factory

The next-to-next generation of neutrino physics, clearly an uncertain extrapolation from our current state of knowledge, is typically envisioned to be based on a radically different neutrino source, either on muon decay in a storage ring (neutrino factory), or radioactive nuclear decay in a storage ring (beta beam). It is worth noting that Project X ties into the development plans for a neutrino factory. As one illustrative example, consider a 4 GeV Neutrino Factory. This facility could be developed by (i) upgrading the Project X beam power at 8 GeV to 2 MW, (ii) adding an intense muon source that could also serve as a Muon Collider front end test facility, and (iii) adding acceleration to 4 GeV and a racetrack shaped muon storage ring. The costs associated with the Muon Collider test facility is believed to be of the same scale as the Project X cost, as is the cost of the additional upgrade to a Neutrino Factory. Hence, Project X offers a potentially attractive path to a facility which, in principle, could determine the neutrino mass hierarchy even if θ_{13} was exactly zero, or if θ_{13} were large, could determine the oscillation parameters with unprecedented precision. To keep this option open, it is important that the Project X beam power at 8 GeV be upgradeable to 2 MW or more.

DUSEL

The proposed Deep Underground Science and Engineering Laboratory (DUSEL) at the Homestake Mine in Lead, South Dakota offers an option for the neutrino community to plan for the next generation of long baseline neutrino oscillation detectors to be located deep underground. The DUSEL-Homestake site is located at a distance of 1300 km from Fermilab. Over this baseline, a beam of neutrinos in the energy range of a few GeV is

well suited to extend the sensitivity to measurement of neutrino mass and mixing parameters, including the search for *CP* violation. Proton intensities envisioned for the Project X era will be essential for such a program.

DUSEL also offers the opportunity to construct large caverns at a depth suitable for placement of multiple detectors, each on the scale of 10-100 kton. A program of constructing and deploying these detectors such that the ultimate mass will approach one megaton can give an ultimate sensitivity to nucleon decay of order 10^{35} years in the $p \rightarrow e^{+}\pi^{0}$ mode and for $p \rightarrow K^{+}\pi^{0}$ at a sensitivity of a few 10^{34} years. A combination of detectors, water Cherenkov and liquid argon may be an appropriate way to maximize discovery potential.

In addition, there is sensitivity to the neutrinos produced from galactic supernovae. A supernova event is expected on a 40 year time scale within the galaxy and could produce of order 10^{5} detectable neutrinos. Large, isotropically sensitive, general-purpose detectors can also probe many other physics targets. This includes exploration of subjects ranging from the temporal variation of the solar neutrino flux, searches for neutrinos from individual or aggregate sum over all supernovae and other cataclysmic events, to cosmic ray composition (where the depth is advantageous), dark matter searches annihilation neutrinos, searches for cosmic exotic particles (e.g., quark nuggets, monopoles, monopolonium, etc.), and point source neutrino astronomy. In all instances, the capability potentially exceeds Super-Kamiokande by virtue of lower energy thresholds, better energy loss rate resolution, momentum, angle, sign and event topology resolution.

Such a program would be a significant achievement for the scientific community. Exploring the synergy that can be achieved by constructing a multi-purpose detector which can lead to the accomplishment of multiple science goals is an important element in planning the DUSEL facility.

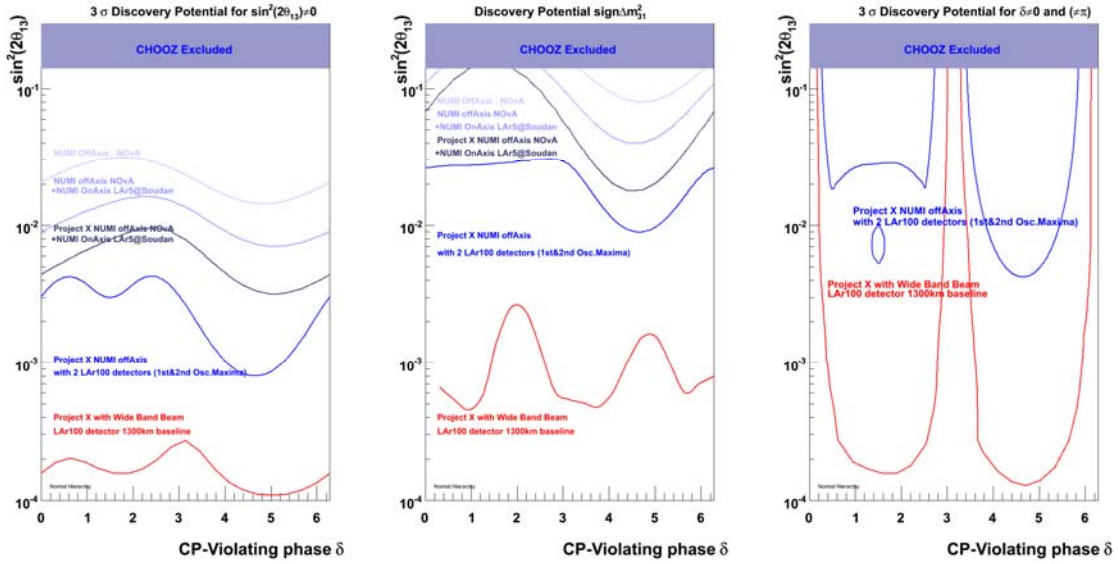

Figure 3.2 Sensitivities as a function of the *CP* violating phase δ for discovering $\sin^2 2\theta_{13}$, neutrino mass hierarchy and *CP* violation for a staged evolution of the neutrino program, starting with the NOvA experiment (Phase I) and culminating with a neutrino beam to very massive detectors (Phase II). As examples we show the potential of two massive detectors in the NuMI off-axis location, and the reach of a single massive detector at a 1300 km baseline with a wide band neutrino beam. (Note : The reactor experiments, Double CHOOZ and Daya Bay aim to achieve sensitivity to $\sin^2 2\theta_{13}$ to the 90% CL of 0.03 and 0.01 respectively, but have no sensitivity to the mass ordering or *CP* violation.)

3.2.2 Neutrino Scattering Measurements

The intense neutrino beams currently running at Fermilab (BNB, NuMI) and possible additional near-future scenarios (e.g., the Tevatron neutrino beam) offer the possibility for exciting on-site neutrino scattering experiments in these beams. These experiments could provide insight into electroweak and strong-interaction physics via the use of electrons, quarks, nucleons, and nuclear targets.

The BNB and NuMI Neutrino Scattering Programs

The MiniBooNE experiment, located 500 meters from the BNB target, has produced an important physics result on neutrino oscillations. In addition, neutrino charged- and neutral-current scattering has been investigated in the 1 GeV energy with world-record sized data samples. Results from these measurements are providing better understanding of neutrino interactions on carbon which will greatly help with extracting precise neutrino oscillation parameters from future experiments such as T2K and NOvA. More data on antineutrino interactions is currently being collected by MiniBooNE in order to understand the antineutrino sector.

The SciBooNE experiment is located at a near location on the BNB 100 meters from the BNB neutrino beam target. This neutrino scattering experiment uses a fine-grained tracking detector and was commissioned in 2007. It will collect 1 x 10^{20} protons on target in both neutrino and antineutrino modes. The data collected by SciBooNE will enable more precise measurements of multiple neutrino and antineutrino scattering processes,

furthering the understanding of the underlying physics at 1 GeV. Upgrades and further running with the SciBooNE detector are currently being considered in order to extend the physics reach of the detector and BNB. One possibility is a precise measurement of neutrino neutral current elastic scattering. This process is uniquely sensitive to the spin of the nucleon carried by an isoscalar component in the nucleon (such as strange quarks) and can provide an answer to part of the nucleon spin puzzle.

The MINERvA experiment will be located on axis on the NuMI beamline, and will run concurrently with both MINOS with a low energy beam (peaked at about 3.5 GeV) and also with NOvA with a medium energy beam (peaked at about 7 GeV). The goal of the MINERvA experiment is to study neutrino interactions in this broad energy range in unprecedented detail by constructing a fine-grained hermetic detector with several different nuclear targets.

The aforementioned MicroBooNE experiment, with excellent tracking capabilities and low energy sensitivity will also provide rich neutrino scattering data from both the BNB and NuMI neutrino spectra.

Although the intense neutrino beam from Project X is driven by the requirements for long baseline neutrino oscillations, there is also a relatively new proposal for an on-site experiment that would build on the cross section measurements made by SciBooNE and MINERvA. The proposal, HiResMν, is to build a high-resolution neutrino detector within a dipole magnetic field (B ~ 0.4T) and a fiducial mass of 7.4 tons. The experiment could run with long-baseline neutrino oscillation experiments in the Medium-Energy configuration of the NuMI-beam. In addition to contributing to the understanding of the systematic limits of the neutrino oscillation experiments, such an experiment can address a broad range of measurements ranging from measurement of the weak mixing angle to searches for weakly interacting massive particles with electronic, muonic and hadronic decay modes with unprecedented sensitivity.

Tevatron Neutrino Program

Using the Tevatron, Fermilab can create a unique ultra-high-energy neutrino facility. The facility would target 800 GeV protons on a target and a dump. A very pure sign-selected high energy ν_μ beam can be created with 20 times the intensity of the previous NuTeV experiment. At the same time, using the beam dump, a flux enriched in ν_τs which are above CC threshold can be produced. This is the only practical source of ν_τs above threshold, since long-baseline experiments, which produce neutrinos through oscillations, must run at low energies. The flux in one year of running will be 150 times that of the previous DoNuT Experiment. The intensity goals, which are challenging, were developed in consultation with the Tevatron Department.

This facility opens new opportunities for physics studies which complement both LHC/ILC and the presently planned neutrino program, and which cannot otherwise be done. Three possible experiments to use this facility are:

- A high-precision ν_τ experiment, with two orders of magnitude more events than DoNuT. The ν_τ sector is essentially unexplored physics territory. Many Beyond-Standard Model theories favor expression in the third family, making this an exciting sector to explore.

- A dedicated search for 10 keV – 5 GeV neutral heavy leptons (also called "neutrissimos") produced by mixing with light neutrinos in meson decays. This facility, with its 800 GeV protons-on-target, allow searches in the GeV range produced via B-decays which are not otherwise possible.

- A high statistics experiment designed to obtain 40 times the world's sample of neutrino-electron scatters. This allows for studies of neutrino universality and unitarity not possible at collider experiments. The design for this experiment, NuSOnG, which could anchor the Tevatron neutrino program, is well underway and was endorsed by the Fermilab Steering Group for further consideration.

3.3 Neutrino Strategy

The neutrino strategy consists of developing a series of world-leading experiments in a phased approach with ever increasing beam intensities and ever increasing detector capabilities. A key element of the strategy is the continuous operation of a neutrino beam facility at Fermilab such that there would be no significant period without running experiments and the acquisition of data with world competitive detectors.

Phase I: Today to 2012

- *Operation of MINOS, MiniBooNE, and SciBooNE;*
- *Construction and operation of MINERVA*
- *Construction of the NOvA detector and the Main Injector upgrades to 700 kW (part of the NOvA project);*
- *Liquid Argon Program: Operation of ArgoNeuT; Construction of MicroBooNE; Design of LAr5 at Soudan; R&D at test stands*
- *Accelerator R&D (Project X)*
- *Conceptual exploration of other neutrino experiments (NuSOnG, HiResNu)*
- *Conceptual design of a second generation long (>1000 km) baseline neutrino program including a beamline, caverns and detectors (LAr and Water Cherenkov detectors) – coordinate efforts with the DUSEL planning process*

The initial phase of the program takes us to the early part of next decade. It is based on the exploitation of the present neutrino beams at Fermilab, the most powerful in the world now and for several years to come. The NuMI beam has been recently upgraded with slip-stacking in the Main Injector to deliver over 300 kW of power, about 40% more than the most recent runs. During this period, MINOS will obtain the most accurate values of oscillation parameters in the "atmospheric" neutrino oscillation region. Also

very importantly, MINOS has sensitivity to θ_{13} that reaches beyond the benchmark limit by CHOOZ. As such, it will provide early input into the search for θ_{13}.

A low energy neutrino beam operating from the Booster will feed MiniBooNE and SciBooNE through the end of their respective runs. The cross sections determined by SciBooNE will be important for the T2K experiment and other long baseline experiments. There remain a lot of physics to be understood in low energy neutrino interactions, including the excess of low energy neutrino events in MiniBooNE, and low energy neutrino cross sections. The MicroBooNE experiment has proposed to study low energy neutrino interactions, in particular, the intriguing low energy excess, while advancing liquid argon TPC R&D, as described below.

While producing physics with existing detectors, we will be building the NOvA detector, including an upgrade of the Main Injector to deliver a total power of 700 kW maintaining Fermilab's leadership in neutrino beam intensity. Both the detector and the upgrades of the Main Injector have been built into the funding profiles provided by the DOE.

During this phase we are building a small detector, MINERvA, to study neutrino cross sections for different materials as well as nuclear scattering models. The construction of this detector has already started and would commence operations towards the end of this period.

The ultimate program in neutrino physics depends on the product of beam intensity, detector mass and detector efficiency. Great gains can be made in all of these. The beam intensity can be increased several fold by upgrades of the Fermilab complex. In particular, during this phase we would complete the design of Project X to greatly increase the neutrino flux, adding flexibility and reliability to the future program.

The second important R&D effort will be the staged program of scalable liquid argon TPC detectors for neutrino physics as described previously. The R&D program scales from small to large detectors, at each step addressing the most pressing R&D questions at the relevant scale, while combining ever more physics with the R&D program.

After the termination of the Tevatron collider run, there will be a possibility to have high energy neutrino beams for other experiments. A proposal to study electro-weak physics with high energy neutrinos could be carried out with the Tevatron in fixed target mode. This would be a unique program with significant discovery potential. During this period we will study what other possibilities in neutrino physics are opened up with the re-use of parts of the Fermilab accelerator complex.

At present we do not know the time scale for the development of the DUSEL laboratory. However, the excavation of a smaller cavern could start early next decade, thus conceptual design for a beam aimed at DUSEL and a detector could begin in this period in coordination with the DUSEL planning process.

Phase II: 2012 – 2016

- *Exploitation of NOvA at 700 kW; continued running of MINERvA with different materials and energies; dismantling of MINOS*
- *Construction of Project X*
- *Liquid Argon program: Continued running of MicroBooNE; construction of LAr5 at Soudan*
- *Design of a second generation very large, longer (> 1000 km) baseline neutrino experiment; coordinate efforts with the DUSEL planning process*
    - *Beamline, caverns and detectors (LAr and Water Cherenkov)*
- *Possible construction of DUSEL smaller caverns and smaller detectors*
- *Scaled-up effort in neutrino factory R&D and design*

Project X could be constructed during this period.

This phase begins with the running of NOvA as soon as about 5 kton of the detector is completed in the Minnesota site. The construction would continue through 2013 when the entire 15 kton would be in place. The beam power of 700 kW together with the long baseline and a totally active detector insures a world leading program. The NOvA detector with the NuMI beam offers quite different sensitivities to the neutrino oscillation parameters than the T2K experiment. The energy of neutrinos is higher and the baseline is longer, both giving greatly enhanced sensitivity to matter effects. During this phase, NOvA is the only experiment which provides information on the mass hierarchy and *CP* violation. Results from the NOvA experiment, along with complimentary results from T2K, will increase our understanding of the neutrino parameters.

The MINERvA detector will begin operation before the start of this period and will continue to operate through the first part of this phase.

The NuMI neutrino physics program could be augmented with the totally active LAr5 at Soudan detector, operating on axis in the Soudan mine, in conjunction with NOvA. LAr5 at Soudan would serve not only to greatly enhance the physics that can be achieved prior to a Phase II program, but would also be a prototype for a large liquid Argon detector at the 100 kton mass scale. We consider it important to build such a detector whether Project X is already under construction or not.

There is considerable interest in Italy to develop 5 kton modules for a massive 20 to 100 kton detector for long base-line experiment from CERN to Grand Sasso. We are currently beginning discussions on how these efforts could be joined with the U.S.'s liquid argon effort.

At present we do not know the time scale for the development of the DUSEL laboratory. We expect that only around the middle of the next decade it will be possible to start the excavation of a large cavern at depth for a detector that would be used for a varied program from neutrino oscillations using a Fermilab beam, to proton decay and supernova neutrinos. We will need to have solid concepts for a beam aimed at a DUSEL

detector, which could be a liquid Argon detector, a water Cherenkov detector, or some combination of the two. There is also a possibility of constructing smaller caverns and smaller detectors during this period.

Depending on the physics results over the next few years it may well be time to seriously develop a neutrino factory. The R&D efforts on a neutrino factory would be enhanced during this period. Project X will be designed with the flexibility to serve as the front end of a neutrino factory and/or a muon collider.

Phase III: 2016 – 2020

In this phase we work toward the goal of precision measurements of the mass and mixing parameters, in particular *CP* violation. This program requires massive detectors, high intensity proton source, and a new world class neutrino beam.

- *Exploitation of Project X with 2.3 MW and combined running of NOvA and LAr5 at Soudan*
- *Design of ultra-massive detectors for the next generation of neutrino and proton decay experiments*
- *Possible construction of DUSEL caverns and construction of neutrino and proton decay detectors*
- *Possible construction start of a new beamline toward DUSEL*
- *Completion of design for a neutrino factory.*

The initial running of Project X would greatly increase the power to NOvA, which will have been running for several years at this time. If prior to this period we have also built a 5 kton LAr detector in the Soudan site, then the program has a remarkable reach on the neutrino oscillation parameter space prior to the investment in a new beamline and massive detectors. Even with only the 700 kW power prior to Project X it would be the program with the greatest reach for $\sin^2 2\theta_{13}$ and the mass hierarchy.

Unless we are very fortunate and the neutrino parameters are measured by this time, it will be important to develop the study of the lepton sector further with the construction a more powerful detector and new beamline to a detector at a long baseline. Our program is designed to develop such a detector and beamline during this period. If the DUSEL project is a part of the national program, the new caverns and detectors located there will enable the commencent of a broad physics program that will last for decades.

If more power and flexibility is required in the world's neutrino program, and greater reach into the neutrino parameters is needed, then a neutrino factory or beta beams could provide a solution in the long term. Coupled with a neutrino factory it will be important to develop detectors that can determine the sign of the final leptons, a great challenge for large detectors. The design of the neutrino factory would be accompanied by the design of a new class of detectors. In any case, Project X would be designed with the flexibility to serve as the front end of a neutrino factory.

3.4 Neutrino Summary

The current Fermilab neutrino program is the best in the world. The MINOS experiment in the NuMI beam will make the most precise measurement of Δm^2_{23} and provide an early glimpse into the search for θ_{13}. Using the Booster neutrino beam, MiniBooNE is probing the possibility that neutrinos quite different from those in the standard paradigm exist, and MiniBooNE and SciBooNE experiments are measuring neutrino cross sections to high precision as well. The MINERvA experiment, which is currently under construction, will use the existing NuMI beam to measure neutrino cross sections to unprecedented precision.

The NOvA experiment, which will be located in Ash River, Minnesota in the NuMI off-axis beam at an 810 km baseline, will be a world class neutrino experiment with the only near-term sensitivity in the world to the mass hierarch. NOvA will also have excellent sensitivity to θ_{13}. The long term vision of building an experiment sensitive to measuring neutrino *CP* violation will evolve by building on what is learned from NOvA and other Phase I experiments.

A liquid Argon detector placed in the NuMI beam will complement and add to the NOvA program, while at the same time advancing this potentially excellent detector technology. The combination of NOvA, a liquid Argon detector and Project X will be a powerful program maximizing the return on the investment that has already been made in the NuMI project, producing physics results from now through the next decade.

Project X could produce the world's most powerful neutrino beam. Developing beam designs and technologies in which those neutrinos are directed towards massive detectors at a very long baseline is an important component of Fermilab's strategic plan. This detector, if located at underground facilities such as the National Science Foundation's DUSEL, would also be a world-class detector for proton decay, addressing the question Do all the forces become one? This detector could also perform high-statistics studies of atmospheric neutrinos and carry out astrophysical searches including detection of relic-supernova neutrinos and neutrino bursts from supernovae in our galaxy and nearby.

In addition to experiments at the long baseline, smaller detectors located in the neutrino beamlines on the Fermilab site can study neutrino interactions over a wide energy range to make precise measurements of neutrino properties and neutrino scattering parameters.

The neutrino strategy that we have outlined will fully exploit the investments that have been made in existing facilities as well as those being planned for the future. This broad based, multi-component neutrino program would ensure that the United States remains a world leader in particle physics throughout the next decade and beyond.

4 Muons

4.1 Introduction

4.1.1 μ → e Conversion in Nuclei

With the discovery of neutrino masses and lepton mixing, the fact that individual lepton-flavor numbers – electron-number, muon-number, and tau-number – are not conserved has been established. All such violating effects to date have been observed in the neutral lepton sector, through the phenomenon of neutrino oscillations. Charged-lepton flavor-violation (CLFV), on the other hand, has been the subject of intense experimental searching since the discovery of the muon but, to this date, no evidence for it has ever been uncovered.

The Standard Model augmented by new physics that leads to the experimentally observed neutrino masses predicts a non-zero rate for CLFV process, but expectations depend dramatically on the mechanism responsible for neutrino mass generation. For example, if the physics responsible for neutrino masses is very heavy (as in the case of a high mass scale seesaw mechanism) or very weakly coupled (as in the case of Dirac neutrinos), expectations for CLFV processes are around forty orders of magnitude smaller than current experimental bounds. The reason for this is that the active neutrino contribution is GIM suppressed, such that the amplitude for CLFV is proportional to the tiny neutrino mass-squared differences. For example, the massive neutrino contribution (Figure 4.1) to $\mu \rightarrow e\gamma$ is

$$Br(\mu \rightarrow e\gamma) = \frac{3\alpha}{32\pi}\left|\sum_{i=2,3} U^*_{\mu i} U_{ei} \frac{\Delta m^2_{1i}}{M^2_W}\right|^2 < 10^{-54}, \qquad (1)$$

Here, $U_{\alpha i}$, $\alpha = e, \mu, \tau$ and i=1,2,3 are the elements of the neutrino mixing matrix and M_W is the W-boson mass.

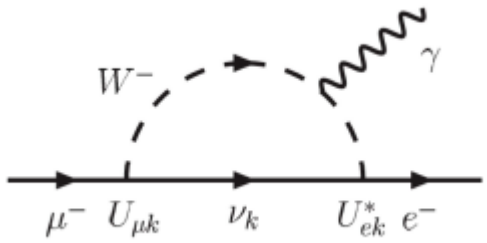

Figure 4.1 Massive neutrino contribution to the charged lepton flavor-violating muon decay μ→eγ. ν_i are neutrino mass eigenstates, while U_α, α=e,μ,τ and k=1,2,3, are the elements of the lepton mixing matrix.

On the other hand, certain neutrino mass generating mechanisms are already disfavored due to the fact that CLFV has yet to be observed. It is fair to say that searches for CLFV are bound to play a key role in uncovering the origin of neutrino masses. Moreover, like

other flavor-changing neutral current processes, searches for CLFV are also among the most powerful and promising probes of new physics at or even above the TeV scale, regardless of its connection to neutrino masses. Concrete examples will be discussed in the next subsection.

Among the different CLFV channels, three rare muon processes stand out, thanks in part to the muon's small mass and long lifetime: $\mu\to e\gamma$, $\mu\to eee$, and $\mu\to e$ conversion in nuclei. Current experiments have been able to rule out, at the 90% confidence level, $\mu\to e\gamma$ with branching ratios above 1.2×10^{-11} and $\mu\to eee$ with branching ratios above 10^{-12}, while the rate for $\mu Ti\to eTi$ normalized to the capture rate $\mu\to\nu$ (conversion in titanium), is constrained to be less than 4.3×10^{-12}. The concurrent exploration of all three rare muon processes is of the utmost importance given that these are all state-of-the-art, extremely challenging experiments and the fact that the three processes "feel" different types of new physics in distinct ways. If CLFV is observed in any of these processes, results from other searches will play a fundamental role in establishing the nature of the lepton-flavor-violating new physics.

Depending on the nature of the CLFV physics, one of the three bounds listed above turns out to be the most significant. For a particular class of models, including several of the standard supersymmetric ones, efforts to observe $\mu\to e\gamma$ prove to be most promising currently and in the immediate future. The MEG experiment, currently taking data at PSI, is aiming to be sensitive to $\mu\to e\gamma$ branching ratios larger than several times 10^{-14}. However, given the existence of very intense future muon sources, $\mu\to e$ conversion will likely serve as the deepest probe of CLFV, superior to $\mu\to e\gamma$ in its new physics reach regardless of the nature of the new physics. Among other factors, it is this feature (which will be discussed in more detail in the next subsection) that drives us to concentrate on the CLFV process where a nuclear-captured muon converts into an electron – $\mu\to e$ conversion in nuclei.

Negatively charged muons that stop in matter are quickly trapped and form muonic atoms, which undergo electromagnetic transitions until the muon is in the 1S orbital. Trapped muons either Michel-decay or convert into neutrinos in the field of the nucleus:

$$\mu^- + (A,Z)\to\nu + (A,Z\text{-}1). \qquad (2)$$

(A,Z) represents a nucleus with mass number A and atomic number Z. Similarly, the $\mu\to e$ conversion process is characterized by

$$\mu^- + (A,Z)\to e^- + (A,Z). \qquad (3)$$

Instead of discussing the rate Γ for this muon and electron number violating process, it is convenient to define the normalized conversion rate:

$$R_{\mu e} \equiv \frac{\Gamma(\mu^- + (A,Z) \to e^- + (A,Z))}{\Gamma(\mu^- + (A,Z) \to \nu_\mu + (A,Z-1))}. \qquad (4)$$

We will often refer to this as the *$\mu\to e$ conversion rate*.

4.1.2 Muon g-2

Flavor-conserving muon properties are also expected to reveal indispensable information concerning physics beyond the standard model. Thanks to the muon small mass and long lifetime, some of these can be measured with great precision. The muon anomalous magnetic moment $(g_\mu\text{-}2)/2 = a_\mu$ is worthy of special attention.

The muon magnetic moment is one of the most precisely measured and calculated quantities in elementary particle physics. A significant effort continues worldwide to improve the precision of the standard-model prediction. Moreover, the current experimental measurement of a_μ shows one of the largest deviations of any observable from the corresponding standard-model prediction, $\Delta a_\mu^{(E821)} = 295(88) \times 10^{-11}$. Owing to this precision, a_μ is not only a sensitive test of all standard model interactions, but also of possible new physics at and above the electroweak scale. If the precision of Δa_μ is improved to 39×10^{-11}, a_μ will be a highly sensitive probe of physics beyond the standard model up to the TeV-scale.

4.2 Comparison to Current HEP Program

It is important to place searches for CLFV in general and $\mu \rightarrow e$ conversion in particular in the larger context of the current and near future developments of the high energy physics program. The same is true for next-generation measurement of a_μ. We will assume that next-generation neutrino oscillation experiments will take place and provide nontrivial information regarding lepton mixing and other new *neutrino physics*. We will also assume that the LHC experiments will have taken enough data to provide a clearer picture of physics at the TeV scale. Finally, we assume that one will either have observed $\mu \rightarrow e\gamma$ or constrained its branching ratio to be less than 10^{-14}. It appears unlikely that a future experiment will be able to significantly improve on this, regardless of whether very intense muon sources are available. This is *not* the case of future searches for $\mu \rightarrow e$ conversion, as will be discussed later.

Model Independent Analysis: a_μ

One can estimate the sensitivity of precision measurements of a_μ to new physics in a model independent way by adding to the standard model effective operators that contribute, at tree level, to the muon magnetic moment. For example,

$$L_{a_\mu} = \frac{m_\mu}{\Lambda^2} \bar{\mu} \sigma_{\mu\nu} \mu F^{\mu\nu}$$

leads to $\Delta a_\mu = 4\, m_\mu^2 / e\Lambda^2$. If the current discrepancy is due to new heavy physics, the current data on the anomalous magnetic moment of the muon translates into a measurement of the new physics scale Λ = 7 TeV. As will be discussed in more detail later, Λ is not necessarily the mass of any new degree of freedom. For example, if one is parameterizing the effect of new heavy degrees of freedom with mass M_{new} that couple to the standard model with a coupling f and contribute to a_μ at the one-loop level

$$\frac{1}{\Lambda^2} = \frac{f^2}{16\pi^2}\frac{1}{M_{\rm new}^2}$$

Model Independent Analysis: μ→e conversion vs. μ→eγ

One can estimate the sensitivity of CLFV processes to new physics in a model independent way by adding to the standard model effective operators that violate lepton flavor. For concreteness, consider the effect of the standard model augmented by the following CLFV effective Lagrangian:

$$L_{CLFV} = \frac{m_\mu}{(\kappa+1)\Lambda^2}\bar{\mu}R\sigma_{\mu\nu}e_L F^{\mu\nu} + \frac{\kappa}{(1+\kappa)\Lambda^2}\bar{\mu}_L\gamma_\mu e_L\left(\sum_{q=u,d}\bar{q}_L\gamma^\mu q_L\right). \qquad (5)$$

Λ is the scale of new physics and κ measures whether the dominant new physics contribution to CLFV comes in the form of a dimension-five, CLFV magnetic moment-type operator ($\kappa << 1$) or from a CLFV four-fermion interaction ($\kappa >> 1$). The effective Lagrangian above will mediate both μ→eγ and μ→e conversion (and, at a less significant level, μ→eee, which will not be discussed). While there is a handful of other effective operators that may also contribute, the ones above contain qualitatively the predictions of most distinct new physics scenarios as far as μ→eγ and μ→e conversion are concerned. The sensitivity of different CLFV probes to Λ as a function κ is depicted in Figure 4.2. Note that, regardless of the value of κ, a μ→e conversion experiment sensitive to capture rates above 10^{-16} probes Λ values smaller than a few thousand TeV!

For $\kappa << 1$, the normalized μ→e conversion is around several times10^{-3} of the branching ratio for μ→eγ, while for $\kappa >> 1$ the normalized capture rate for μ→e conversion is many orders of magnitude larger than the branching ratio for μ→eγ. Hence, a μ→e conversion experiment sensitive to normalized rates above 10^{-16} is at least as sensitive to new physics as a μ→eγ experiment sensitive to branching ratios above a few times 10^{-14}, regardless of the nature of the new physics. It is important to emphasize that while we are using Eq. (5) to make this point, this conclusion is very general and applies to most new physics scenarios that have been explored in the literature to date.

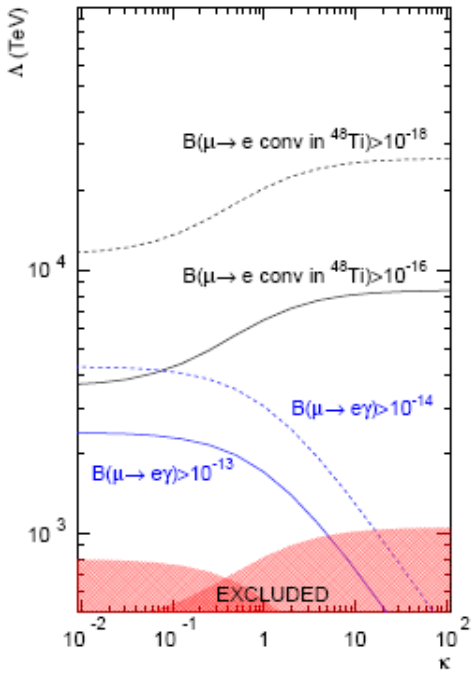

Figure 4.2 Sensitivity of a $\mu \rightarrow e$ conversion in ^{48}Ti experiment that can probe a normalized capture rate of 10^{-16} and 10^{-18}, and of a $\mu \rightarrow e\gamma$ search that is sensitive to a branching ratio of 10^{-13} and 10^{-14}, to the new physics scale Λ as a function of κ, as defined in Eq. (5). The dimensionless parameter κ interpolates between a flavor-violating magnetic moment-type operator (κ <<1) and a flavor-violating four-fermion operator (κ>>1). Also depicted is the currently excluded region of this parameter space.

In the case of a positive CLFV signal in either μ→eγ or μ→e conversion, combined results from different CLFV processes provide detailed information regarding the new physics. For example, should the world be properly described by Eq. (5), a measurement of μ→eγ and μ→e conversion allows one to determine both Λ and κ independently, while a single measurement can only determine a combination of the two new physics parameters. More generally, it is well known that a comparison of $R_{\mu e}$ and the branching fraction for μ→eγ ($B_{\mu e\gamma}$) helps distinguish among models or even measure the value of new physics parameters. A concrete example is depicted in Figure 4.3, where the ratio of branching ratios $C = B_{\mu e\gamma}/R_{\mu e}$ is plotted as a function of tanβ in the case of the MSSM with MSUGRA boundary conditions for the soft SUSY breaking parameters. One can see that a precise measurement of C can determine the sign of the MSSM μ-parameter, especially if tanβ is not too large.

The effective Lagrangian that describes μ→e conversion and μ→eγ contains, in general, several dimension-six operators not included in Eq. (5), including those with different muon and electron chiralities and scalar-scalar four-fermion operators. Information regarding all the different parameters that describe CLFV can be obtained from the CLFV probes themselves. In the advent of a positive signal for μ→e conversion, details of the effective Lagrangian can be obtained by comparing the rate for μ→e conversion in different nuclei, since different nuclei are sensitive to new physics in distinct ways, as

depicted in Figure 4.4. This flexibility is not shared by μ→eγ (where one can only hope to measure, in principle, the final state photon or electron polarizations). In the case of a positive signal in μ→eee, some detailed information regarding the underlying physics can also be obtained by analyzing in detail the kinematics of the three final state leptons.

CLFV and new physics at the TeV scale

By the end of 2008, we expect the LHC experiments to start accumulating data that will reveal the mechanism of electroweak symmetry breaking and explore the physics of the TeV scale. Several theoretically motivated scenarios predict the existence of new degrees of freedom with masses at or below 1 TeV and, if this is the case, one expects some of these new states to be discovered at the LHC.

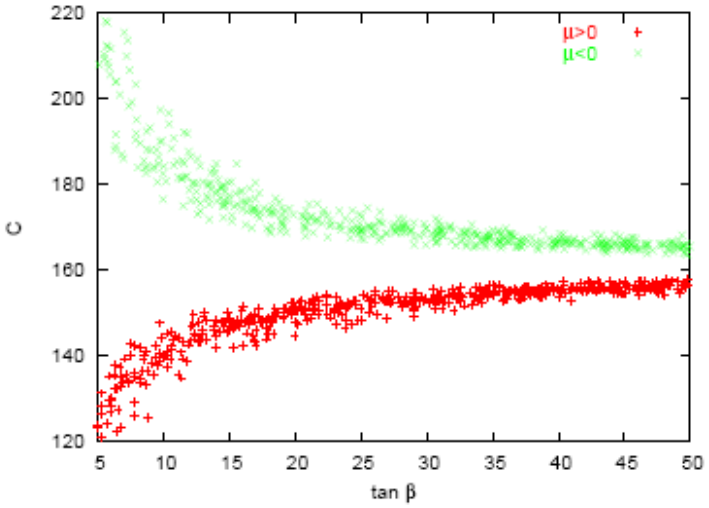

Figure 4.3 $B_{\mu e\gamma}/R_{\mu e}$ in the MSSM with MSUGRA boundary conditions for the soft parameters and neutrino masses induced by the seesaw mechanism, as a function of tanβ for different signs of the μ-parameter. From C. E. Yaguna, Int. J. Mod. Phys. A21, 1283 (2006).

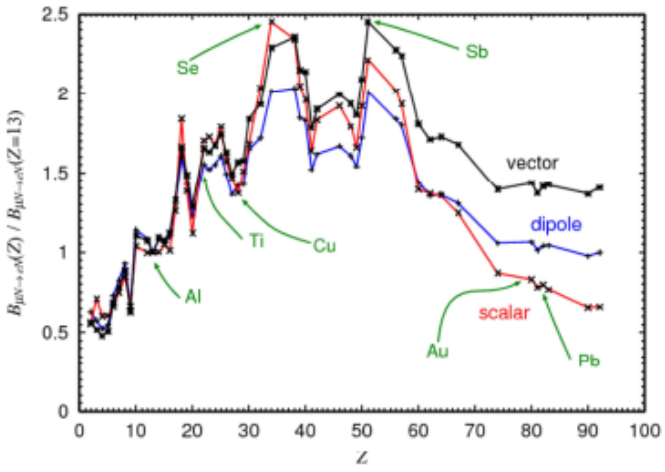

Figure 4.4 μ→e conversion rate for different nuclei, normalized to that for μ→e conversion in aluminum. The different curves represent the contribution of different types of higher dimensional operators. From R. Kitano, M. Koike and Y. Okada, Phys. Rev. D66, 096002 (2002).

New physics at the TeV scale is expected to mediate CLFV processes. Expectations are model-dependent, but detailed computations in specific models lead to CLFV rates very close to current experimental bounds, as will be discussed in more detail shortly. We first conservatively assume that the new physics will predominantly induce flavor-violating magnetic-moment type effective interactions at the one-loop level. A concrete example is depicted in Figure 4.5.

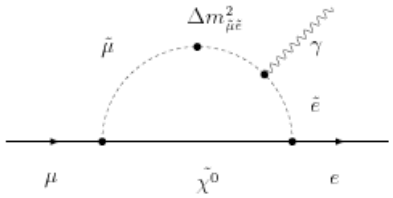

Figure 4.5 MSSM slepton--neutralino contribution to μ→eγ. $\Delta m_{\mu e}^2$ stands for the insertion of an off-diagonal element of the slepton mass-matrix. From Y. Kuno and Y. Okada, Rev. Mod. Phys. 73, 151 (2001).

In this case, CLFV is given by Eq. (6) (potentially augmented by similar operators where the electron and muon chiralities are reversed) with $\kappa \ll 1$ and

$$\frac{1}{\Lambda^2} \sim \frac{eg^2}{16\pi^2} \frac{\theta_{e\mu}}{M_{new}^2}. \qquad (6)$$

M_{new} are the masses of the new states that couple to standard model fields with coupling g and $\theta_{e\mu}$ is a flavor-violating factor, most likely inaccessible to the LHC. If one assumes g (henceforth assumed to be of order one) and M_{new} to be known, failure to observe CLFV translates into bounds on $\theta_{e\mu}$.

As a concrete example, consider the possibility that the currently observed three sigma discrepancy between the standard model prediction and the measurement of the muon anomalous magnetic moment is due to new electroweak scale physics. In this case, the new physics contribution to the anomalous magnetic moment of the muon is capture by a flavor-conserving version of the magnetic moment-type operator that mediates CLFV. Current data on the muon anomalous magnetic moment translates into a measurement of a combination of the new physics scale M_{new} and the new coupling g, in which case currents bounds on CLFV are already quite severe and constrain $\theta_{e\mu} < 10^{-3}$.

Similarly, if the LHC discovers new states with masses M_{new} around 1 TeV, current bounds from CLFV will already translate into $\theta_{e\mu} < 10^{-2}$. In this case, μ→e conversion experiments sensitive to conversion rates greater than 10^{-16} will probe $\theta_{e\mu} > 10^{-4}$.

What are the expected values for $\theta_{e\mu}$? The answer to this is model dependent, but one can identify general categories. Generic new physics models predict $\theta_{e\mu} \sim 1$, in which case searches for CLFV already rule out $M_{new} \sim$ 1TeV. Hence searches for CLFV, along with other flavor observables, already constrain any physics at the TeV scale to be flavor conserving at the leading order. For this reason, one often assumes that the only sources of lepton-flavor violation are the ones already present in the standard model, *e.g.*, the charged-lepton Yukawa couplings and the neutrino mass generating sector. In this case, $\theta_{e\mu}$ values can be computed on a case-by-case basis, and its value may or may not depend on the unknown new physics responsible for neutrino masses and lepton mixing.

Several detailed analyses have been performed for the different independently motivated new physics scenarios, including models with weak scale supersymmetry, models with flat and warped extra-dimensions, and little Higgs models. Some results depend on details of the physics responsible for neutrino masses, about which we will discuss more shortly, but tend to lead to $\theta_{e\mu}$ values such that μ→e conversion is likely to happen with rates above 10^{-17} or so as long as the new physics is observable at the LHC.

Two examples are depicted in Figures 4.6 and 4.7. Figure 4.6 depicts the result of a scan of the MSSM parameter space for different SUSY-GUT scenarios where neutrino masses are generated via the seesaw mechanism. The GUT hypothesis fixes the values of the right-handed neutrino Majorana masses, while there remains the freedom to choose the off-diagonal structure of the neutrino Yukawa couplings. Here two different choices are made: the neutrino Yukawa coupling matrix is PMNS-like with all its mixing angles large as in the physically observable lepton mixing matrix, or it is CKM-like with all its mixing angles small as in the physically observable quark mixing matrix. While the different choices lead to μ→e gamma rates that vary by more than four orders of magnitude, it is clear that a μ→e conversion experiment sensitive to normalized rates above 10^{-17} or so should cover the majority of the LHC accessible parameter space.

Figure 4.7 depicts the result of a scan of the parameter space of the littlest Higgs model with T-parity. The different colored (shaded) points refer to different ansatze for the structure of the mirror lepton mixing sector, not dissimilar from the choice of neutrino Yukawa matrices made in the SUSY example discussed briefly above. Also here, a μ→e conversion experiment sensitive to normalized conversion rates above 10^{-16} should cover the parameter space explored in the figure. This is also true for a handful of points where the branching ratio for μ→eγ is less than 10^{-14}. Note that in this case results do not depend on the mechanism responsible for neutrino masses, but do depend on the unknown mirror fermion mixing matrix.

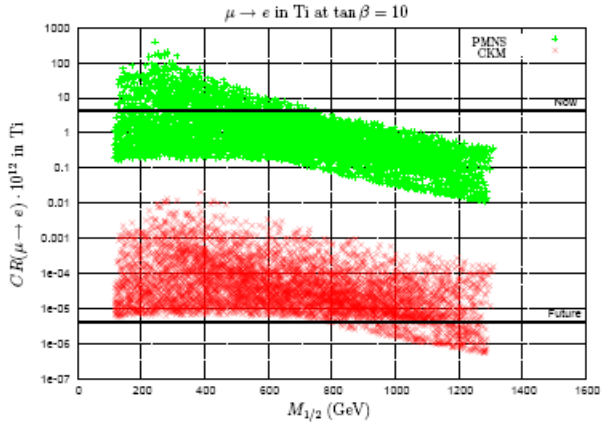

Figure 4.6 μ→e conversion rate in Ti for different SUSY--GUT scenarios. The plots are obtained by scanning the LHC accessible parameter space. The horizontal lines are the present (SINDRUM II) bound and the planned (future) sensitivity to the process both at the proposed PRIME experiment in JPARC and at the proposed mu2e experiment in FNAL. From L. Calibbi, A. Faccia, A. Masiero and S. K. Vempati, Phys. Rev. D74, 116002 (2006).

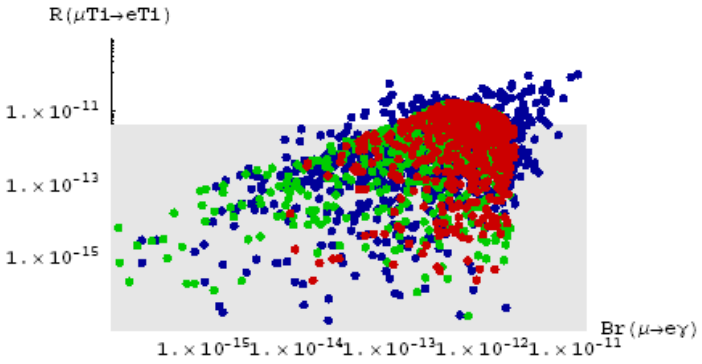

Figure 4.7 μ→e conversion rate in Ti versus μ→eγ branching ratio for different littlest Higgs scenarios. The light grey region is allowed by current searches for CLFV. The different shaded points represent different ansatze for the mirror fermion mixing matrix. From M. Blanke, A. J. Buras, B. Duling, A. Poschenrieder and C. Tarantino, JHEP 0705, 013 (2007).

It is also important to discuss the case where CLFV is generated by new physics at the tree-level, i.e. it is a consequence of the simple exchange of a heavy new physics particle. An example is depicted in Figure 4.8. Other than SUSY with R-parity violation, depicted in Figure 4.8, several well-motivated new physics scenarios lead to similar CLFV effects including the models with lepto-quarks, neutrino mass models with Higgs triplets, and models with extra Z' gauge bosons. In this case, CLFV is described by Eq. (5) (potentially augmented by, say, scalar-scalar four-fermion operators) with κ>>1 and

$$\frac{1}{\Lambda^2} \sim \frac{eg^2}{16\pi^2}\frac{\theta_{e\mu}}{M_{new}^2}, \qquad (7)$$

Here, if M_{new} is measured at the LHC, current bounds from μ→e conversion constrain $g^2\theta_{e\mu}$ to be tiny. In the example depicted in Figure 4.8, $g^2\theta_{e\mu} \sim (\lambda'_{221}/\lambda'_{121})$. Not surprisingly, this parameter is most severely constrained by searches for μ→e conversion in nuclei.

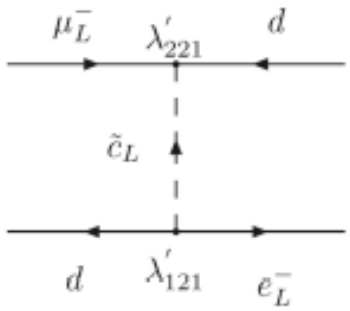

Figure 4.8 MSSM tree-level R-parity violating contribution to μ→e conversion. From A. de Gouvea, S. Lola and K. Tobe, Phys. Rev. D63, 035004 (2001).

To summarize the discussion so far: if the LHC discovers new states at the TeV scale, several distinct new physics scenarios predict CLFV violating process to occur with rates that are close to current experimental bounds. In this case, a positive μ→e conversion

result (which may or may not be accompanied by a positive $\mu \to e\gamma$ or $\mu \to eee$ result) will tell us about the flavor structure of the new physics sector, and may even help distinguish among different new physics scenarios. It is important to emphasize that the information one will extract from the CLFV sector is complementary to the information one can hope to extract from LHC data.

Similarly, in the advent of new physics at the LHC, a negative $\mu \to e$ conversion result will also contribute to our understanding of the new TeV scale physics. It would reveal that (i) the new physics is indeed intrinsically lepton-flavor conserving and (ii) the flavor breaking effects induced by the known sources of flavor violation are smaller than naive expectations. Different physics may explain (ii). For example, in the case of SUSY, low-energy gauge-mediated scenarios usually lead to suppressed flavor-violating effects. Furthermore, as will be discussed in more detail shortly, some of the estimates above depend on the physics responsible for neutrino masses, which may be such that TeV-scale CLFV effects are smaller than naive expectations.

There remains, of course, the possibility that the LHC discovers no new degrees of freedom other than what appears to be a standard model Higgs boson. This will indicate that the new physics beyond the standard model is significantly heavier than the TeV scale. Under these circumstances, searches for CLFV violation remain extremely valuable, especially searches for $\mu \to e$ conversion (and, to a lesser extent, searches for $\mu \to eee$). The reason is that if the LHC fails to discover any beyond-the-standard-model effect, the gauge hierarchy problem will, most likely, prove to be a poor indicator for the new physics scale. In this case, progress in fundamental particle physics, including the answers for the open questions, will have to rely, at least for some time, on indirect new physics probes, i.e. on the intensity frontier. These include precision studies of neutrinos and their properties, precision measurements of well-known standard model quantities (like the anomalous magnetic moment of the muon), and searches for forbidden or extremely suppressed processes, like CLFV muon processes. Under these circumstances, the intensity frontier would be the only game in town. Of the probes listed above, CLFV is the one capable of "directly" reaching out to several thousand TeV, especially in the case of $\mu \to e$ conversion, if new flavor-violating effects are large (in the sense $\theta_{e\mu} \sim 1$) and strongly coupled ($g \sim 1$) and occur at the tree-level (see Eq. (7) and Figure 4.2). While there are, by no means, any guarantees that this is the case, there are reasons to believe in such a scenario. Among other plausibility arguments is the fact that the only palpable evidence for new physics is the existence of non-zero neutrino masses. The tiny neutrino masses are potentially due to new, heavy physics and the large lepton mixing angles seem to indicate that flavor-numbers are not conserved in the neutrino sector. Hence, as long as the neutrino mass scale is not too heavy (above 10^4 TeV), there remains the possibility that $\mu \to e$ conversion will directly teach us about the physics responsible for non-zero neutrino masses.

a_μ and new physics at the TeV scale

If there are new degrees of freedom at the TeV scale, it is widely expected that the new physics that governs these new states and how they interact with the standard model

fields will help address many fundamental questions and lead to qualitative progress in our understanding of fundamental physics. Due to the expected importance and complexity of physics at the TeV-scale, we need to combine and cross-check information from the LHC with information from as many complementary experiments as possible. The measurement of the muon magnetic moment a_μ is indispensable in this respect.

As an example, we discuss in more detail the example of supersymmetric extensions of the standard model. A simple model with equal masses gives

$$a_\mu^{(\mathrm{SUSY})} \simeq \frac{\alpha(M_Z)}{8\pi \sin^2\theta_W}\frac{m_\mu^2}{\tilde{m}^2}\tan\beta\left(1-\frac{4\alpha}{\pi}\ln\frac{\tilde{m}}{m_\mu}\right); \simeq (\mathrm{sgn}\mu)\,13\times10^{-10}\,\tan\beta\left(\frac{100\ \mathrm{GeV}}{\tilde{m}}\right)^2$$

where tanβ is the ratio of the vacuum expectation values of the two Higgs boson fields. In order to discuss the relative sensitivity of LHC and a_μ to tanβ, we reconsider the situation discussed in R. Lafaye, T. Plehn and D. Zerwas, hep-ph/0404282. In this reference it has been assumed that the MSSM reference point SPS1a is realized, and the potential of the LHC to determine MSSM parameters has been worked out. By performing a global fit of the MSSM to all available LHC data, a large set of MSSM parameters can be determined to a precision of a few percent. Apart from the sign of the μ parameter, which has been assumed to be positive, tanβ could be determined only poorly: tanβ = 10.22 +/- 9.1. In such a situation, an improved a_μ measurement will be the perfect complement of the LHC. One can simply study the MSSM-prediction for Δa_μ as a function of tanβ (all other parameters are known from the global fit to LHC data) and compare it to the measured value. One can display the result in a "blue band" plot, similar to the case of the LEP precision data, which can be compared to the standard model predictions as a function of the standard-model Higgs boson mass. The resulting possible future "blue band" plot for tanβ determined by the measurement of the muon anomalous magnetic moment is shown in Figure 4.9 (Left). As can be seen from the plot, the improvement of the determination of tanβ from the a_μ measurement is excellent.

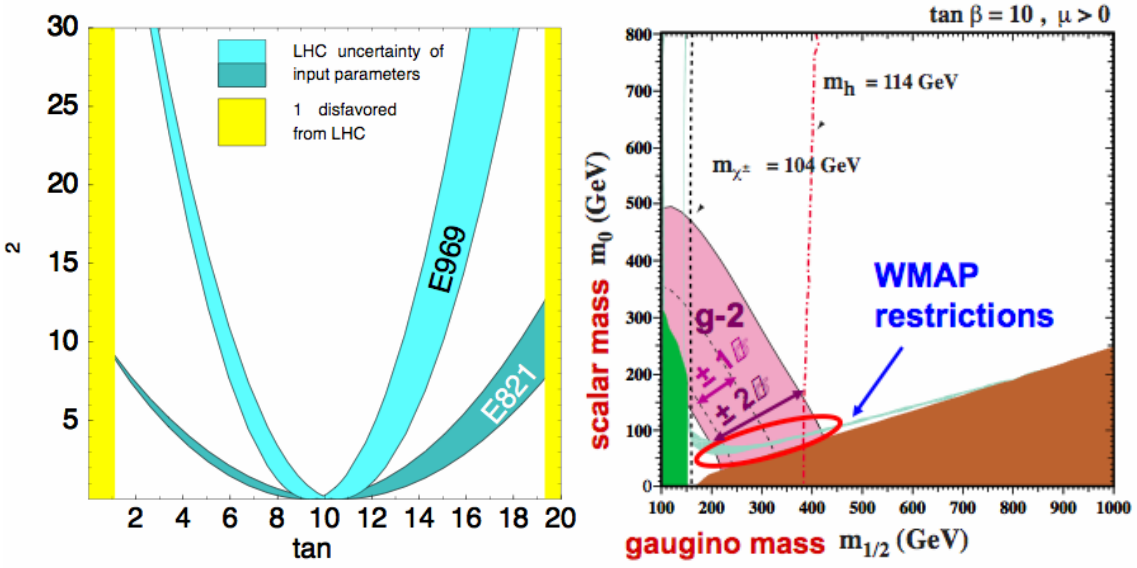

Figure 4.9 Left: A possible future ``blue band'' plot, where tanβ is determined from the measurement of a_μ. The white region between the yellow vertical bars indicates the plus/minus one sigma region from the LHC-determination of tanβ^{LHC}= 10.22 +/- 9.1. The darker blue band is with the present E821 restrictions. The lighter blue band corresponds to $\Delta a_\mu = 295(39) \times 10^{-11}$. It

is assumed that the MSSM reference point SPS1a is realized and that the MSSM parameters have been determined by a global fit to the values given in hep-ph/0404282, Table 5, and that the measured value a_μ^{exp} coincides with the actual value of the SPS1a point. The plot shows $\Delta\chi^2$ as a function of tanβ. All MSSM parameters except for tanβ have been set to the values determined at the LHC. The width of the blue curves results from the uncertainty on these parameters. The plot indicates that the precision for tanβ that can be obtained using a_μ is limited by the precision of the other input parameters, but is still better than 20% and thus much better than the determination using LHC data alone. Right: The $m_0 - m_{1/2}$ plane of the CMSSM parameter space for tanβ=10, A_0=0, sign(μ)=+1. The $\Delta a_\mu = 295(39) \times 10^{-11}$ between experiment and standard-model theory is from J.P. Miller, E. de Rafael and B.L. Roberts, hep-ph/0703049, and Rep. Prog. Phys. 70, 795-881 (2007), see text. The brown wedge on the lower right is excluded by the requirement the dark matter be neutral. Direct limits on the Higgs and chargino masses are indicated by vertical lines. Restrictions from the WMAP satellite data are shown as a light-blue line. The *g*-2 1 and 2-standard deviation boundaries are shown in purple. The region ``allowed'' by WMAP and *g*-2 is indicated by the ellipse, which is further restricted by the limit on M_h. (Figure courtesy of K. Olive).

A second example concerns the restriction of special, highly constrained models of new physics such as the constrained MSSM (CMSSM). The CMSSM has only four free continuous parameters. One precise measurement such as the future determination of Δa_μ effectively fixes one parameter as a function of the others and thus reduces the number of free parameters by one. In fact, the CMSSM is very sensitive not only to a_μ but also to the dark matter (assumed to consist of neutralinos) relic density. As shown in Figure 4.9 (Right), both observables lead to orthogonal constraints in CMSSM parameter space, and therefore imposing both constraints leaves only two free parameters and thus allows for very stringent tests of the CMSSM at the LHC.

A third example is the distinction between two different, well-motivated scenarios of supersymmetry breaking such as anomaly-mediated and gravity-mediated supersymmetry breaking. The two scenarios lead to different values of superpartner masses, but a major qualitative difference is the different sign for the MSSM-parameter μ preferred in both scenarios (if the current experimental constraint on $B(b \rightarrow s\gamma)$ is imposed). The LHC is not particularly sensitive to the sign of μ, and thus cannot test this fundamental difference. However, the sign of μ determines the sign of the supersymmetry contributions to a_μ. The current discrepancy between the standard model and experiment already favors a positive μ parameter, but the magnitude of the uncertainty does not allow a definite conclusion. An improved measurement with uncertainty 39×10^{-11} has the potential to unambiguously determine the sign of μ and thus one of the central supersymmetry parameters. Depending on the future central value of a_μ, either anomaly- or gravity-mediated supersymmetry breaking could be ruled out or at least seriously constrained.

A new more precise measurement of a_μ will be highly valuable in this respect since it will provide a benchmark and stringent selection criterion that can be imposed on any model that is tested at the LHC. For example, if Δa_μ persists to be as large as it is today, many non-supersymmetric models will be ruled out. If Δa_μ turns out to be rather small, supersymmetric models will be seriously constrained.

Finally, we invite the question of the usefulness of next-generation precision measurements of the muon anomalous magnetic moment in the advent that the LHC does not discover any new degrees of freedom other than a standard model Higgs boson. Under these circumstances, new physics contributions to a_μ are widely expected to be smaller than the foreseeable theoretical error on the standard model prediction of a_μ, such that the current three sigma discrepancy is expected to go away. Nonetheless, there is no

guarantee that Δa_μ should be unobservably small. Indeed, under these circumstances a non-zero Δa_μ would indicate that there is new physics at the TeV scale, but that it escaped the scrutiny of the LHC experiments. Under these circumstances, only an energy-frontier leptonic collider would provide valuable complementary information to discover the new physics exposed by Δa_μ.

CLFV, neutrino masses, and the matter--antimatter asymmetry of the Universe

As discussed in the introduction, massive neutrinos and lepton mixing imply that CLFV *must* occur at some level. While the active neutrino contribution to CLFV is known, as already discussed, to be tiny there remains the likely possibility that the new physics responsible for neutrino masses will induce CLFV at observable levels. Several examples of this have been mentioned in passing above.

Here we will discuss in detail the MSSM case in order to underline the potential importance of CLFV to understanding neutrino masses and other related phenomena, including leptogenesis. In the MSSM with MSUGRA boundary conditions large CLFV are generated if neutrino masses are a consequence of the seesaw mechanism. In more detail, a non-zero off-diagonal slepton mass-squared (see Figure 4.5)

$$\Delta m^2_{\tilde{l}\tilde{e}} \simeq \sum_k \frac{M^2_{SUSY}}{16\pi^2} y^*_{\mu k} y_{ek} \log\left(\frac{M_{GUT}}{M_k}\right), \qquad (8)$$

is generated where $y_{\alpha k}$, $\alpha = e, \mu, \tau$ and k=1,2,3 are the neutrino Yukawa couplings, M_k are the right-handed neutrino Majorana masses, M_{SUSY} is a typical supersymmetric mass and M_{GUT} is a typical ultraviolet cut-off, often equated with the GUT scale. In this case, the rate for muon CLFV is proportional to $(\Delta m^2_{\mu e})^2 (\theta_{\mu e} \Delta m^2_{\mu e} / M^2_{SUSY})$, such that it probes some combination of the neutrino Yukawa couplings and hence provides non-trivial information regarding the neutrino mass sector; this statement is very dependent on the physics of SUSY breaking, which we are assuming is well known.

Knowledge of the neutrino Yukawa couplings is also fundamental when it comes to determining whether leptogenesis is the mechanism responsible for the matter--antimatter asymmetry of the Universe. The amount of baryon number generated depends on a linear combination of neutrino Yukawa couplings and right-handed Majorana neutrino masses different from the one above (proportional to $\propto \mathrm{Im}[(y^\dagger y)^2_{j1}]$ in the case of thermal leptogenesis), while a third linear combination determines the observed active neutrino masses:

$$m_{\alpha\beta} = \sum_k y_{\alpha k} \frac{v^2}{M_k} y_{\beta k}. \qquad (9)$$

It has been shown that, given the right circumstances, neutrino oscillation measurements combined with positive results from CLFV, positive results from searches for neutrinoless double-beta decay, and information regarding the low-energy SUSY and SUSY breaking, can provide enough information in order to test leptogenesis. Hence, if

thermal leptogenesis is ever to be tested experimentally, CLFV will certainly play a fundamental role.

It is important to emphasize that negative results from CLFV, combined with the discovery of SUSY at the LHC, may prove as important positive results. The reason is as follows. In the MSSM, standard thermal leptogenesis requires the lightest right-handed neutrino Majorana mass to be larger than 10^{-9} GeV or so. This translates into a rough lower bound on the neutrino Yukawa couplings, using Eq. (9): $y^2 \geq 10^{-5}$. This, in turn, implies that $\theta_{e\mu} > 10^{-6}$. Hence, if CLFV experiments can rule out $\theta_{e\mu} > 10^{-6}$, standard thermal leptogenesis would be severely disfavored. Such sensitivity could only be obtained, if at all, in searches for $\mu \rightarrow e$ conversion fed by very intense muon sources.

4.3 Experimental Program

4.3.1 Muon Conversion Measurements

Muon conversion in nuclei is unique in the sense that extremely intense muon beams can be used to extend the experimental sensitivity orders of magnitude beyond current limits. This is a consequence of the fact that the detected final state consists of a single particle of fixed energy, in contrast with other processes (e.g. $\mu \rightarrow e\gamma$, $\mu \rightarrow eee$). At the high rates necessary to reach the desired sensitivity, processes with multi-particle final states are limited by backgrounds from accidental coincidences of particles from multiple decays; these increase linearly with rate and are absent in the conversion experiment. Further, the fact that the energy of the final state particle is significantly higher than the majority of most particles resulting from decay or capture (again in contrast with the case of $\mu \rightarrow e\gamma$, $\mu \rightarrow eee$) vastly simplifies the complexities of dealing with very high instantaneous decay rates.

The only current experiment in CLFV is the MEG ($\mu \rightarrow e\gamma$) experiment at the Paul Scherrer Institute in Switzerland. It uses a surface muon beam (muons originating from the decay of pions at rest near the surface of a production target). The antimuons are stopped in a thin target and the monochromatic positrons and photons are detected and their momenta and time of origin are determined. The experiment is limited in sensitivity to a branching fraction of $\sim 10^{-13}$ by a combination of reasonable running time and maximum allowed instantaneous rates in the photon detector, and by backgrounds. Backgrounds are dominated by accidental coincidences of positrons from one muon decay (which peak at the kinematic maximum) and photons from either radiative decay or annihilation in flight of a positron from a second muon. Reducing the background to one event at a sensitivity of 10^{-13} requires measurements at the precision of the state-of-the-art detector technology for the photon and positron times, the photon energy and position, and the positron momentum. This experiment may be upgraded to handle higher rates that could allow a measurement with a sensitivity of 10^{-14} in a few years of running, but backgrounds will then likely be sufficiently high that the sensitivity for a discovery will increase only with the square root of the running time. If the branching fraction is

near the current upper limit of 2 x 10^{-11}, a measurement of $R_{\mu e}$ with a precision approaching 10% could be made.

Interest in improved CLFV experiments now focuses on μ→e conversion. All approaches use a low energy muon beam to stop muons in a thin target, where they are Coulomb captured. The monochromatic electron resulting from the muon conversion is detected and its energy measured with high precision to eliminate backgrounds. To improve significantly on the sensitivity of previous searches, substantial improvements in all aspects of these experiments must be made.

Two approaches have been explored. The Mu2e Collaboration, consisting of 50 scientists from 11 institutes, has recently submitted an LOI to Fermilab to measure muon conversion with an apparatus and muon beam based on the MECO experiment. The MECO experiment would have used a proton beam pulsed at about 1 MHz to allow conversion electrons to be detected between pulses when many sources of backgrounds associated with electrons and pions in the muon beam are reduced. This proposal was developed in great detail and was optimized to use an 8 GeV proton beam of up to 100 kW of instantaneous power at 50% duty cycle. The proposed sensitivity was approximately 1 detected event for a value of $R_{\mu e}$ = 2 x 10^{-17}, with an expected background of about 1 event.

The MECO design (see Figure 4.10) was optimized for this intensity and the performance was limited by the potential for radiation damage to the solenoid magnet surrounding the

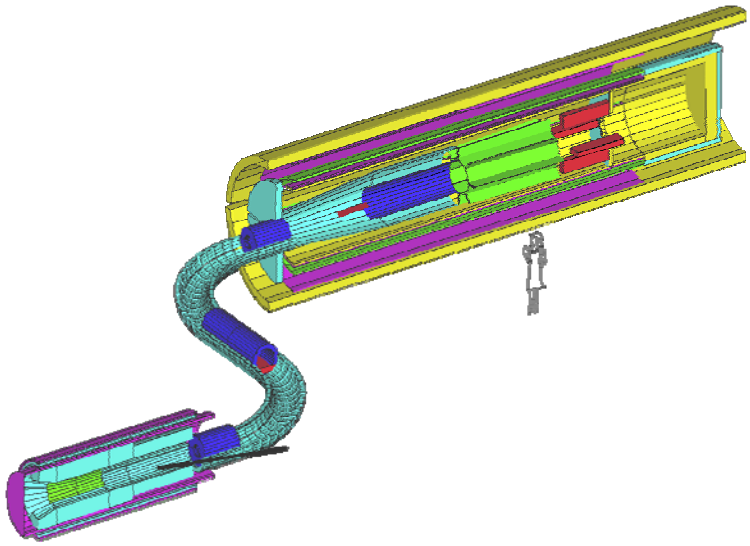

Figure 4.10 The muon beamline and detector apparatus proposed for the MECO μ→e conversion experiment, which has been taken as the baseline design for the Mu2e exeriment. The elements comprise a production solenoid at the left surrounding a production target on which a proton beam from the right impinges, a curved transport solenoid with momentum and sign selection collimators, and a detector solenoid with muon stopping target, proton shield (blue), tracking chambers (light green) and calorimetric electron calorimeter.

muon production target, by cooling for the small muon production target, and by instantaneous intensity in the tracking chambers. With one final-state particle, accidental backgrounds of the type that limit μ→eγ experiments are not present, and increased instantaneous intensity would cause increased background only to the extent that electron

momentum resolution is degraded by effects of higher tracking chamber rates. The dominant background is from muons that decay in a Coulomb bound orbit (DIO electrons) and hence can have energy as large as that of conversion electrons. This background is intrinsic to the process and is reduced only by better electron energy resolution. In the case of MECO, the resolution is derived in roughly equal parts from energy loss dispersion as the electron exited the stopping target and traversed the detectors, and from scattering within the spectrometer. The MECO design was developed to the level of a technical proposal with a validated cost.

The Mu2e experiment at Fermilab would run simultaneously with a neutrino program and, depending on the development of the complex, which is discussed below, could also run in parallel with other experiments that would use an intense 8 GeV source.

A second approach has been proposed by the PRISM/PRIME collaboration. It would use the much higher power (2-4 MW) that could be available in a beam from the JPARC 30 GeV synchrotron that is currently under construction. The proton beam would be pulsed at relatively low frequency (perhaps 100 Hz) and a relatively pure and monochromatic muon beam would be made using a beam channel and fixed focus, alternating gradient (FFAG) storage ring to exchange the initial narrow time and large momentum spread of the muon beam to produce a narrow momentum spread. The instantaneous stopping rate would be very high (~10^5 times that of the MECO proposal) and a different detection technique was proposed. It was proposed to use a large aperture, high field curved solenoid channel to select and transport high momentum particles (e.g. conversion electrons) to a detector region and to suppress lower momentum particles from muon decay and capture. The beamline and apparatus are shown in Figure 4.11. Backgrounds from DIO electrons would be reduced by virtue of a thinner stopping target and reduced material in the electron flight path. This approach has not yet been developed to the level of a technical proposal and validated cost. The sensitivity that could be achieved in this approach was estimated at ~10^{-18}.

Recently, the PRISM/PRIME collaboration proposed the COMET experiment. It would use a pion capture and muon transport similar to that of Mu2e / MECO, and use the PRISM/PRIME approach for the electron detection. It is proposed to run at the JPARC facility using a 56 kW 8 GeV beam, and would reach a sensitivity of below 10^{-16}. Both COMET and PRISM/PRIME would use the full resources of the JPARC synchrotron, and could not run simultaneously with the neutrino program at JPARC.

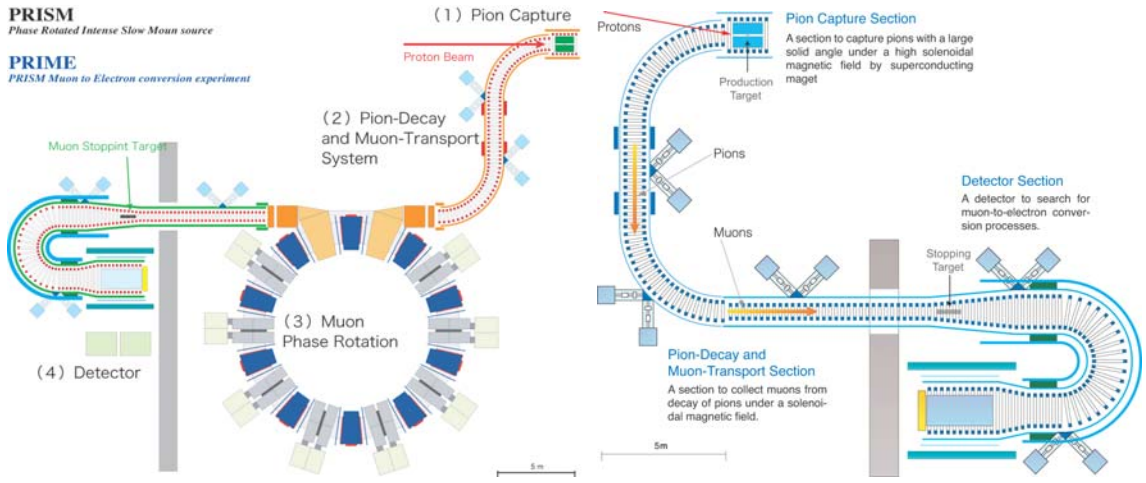

Figure 4.11 Left: the PRISM/PRIME proposed muon beamline and μ→e conversion experiment. It comprises a muon production solenoid, transport solenoid, FFAG ring, further transport solenoid, muon stopping target solenoid, electron momentum selection solenoid, and detector solenoid with electron detectors. Right: the COMET muon beamline and experiment, comprising pion capture solenoid, muon transport, stopping region, electron transport, and detector solenoid with electron detectors.

In principle, one or both of these approaches could be implemented at Fermilab. The Project X implementation being discussed could provide as much as 200 kW of 8 GeV protons (2.5×10^{14} Hz) with > 90% duty cycle, corresponding to about 2.5 instantaneous and 5 times the average intensities for which MECO was designed. Upgrades to the MECO approach are being studied by the Mu2e collaboration, Fermilab accelerator physicists, and others in order to take advantage of these higher rates.

On the accelerator side, current studies at Fermilab are focused on reusing the accumulator and debuncher rings to stack protons and re-bunch them to provide the necessary time structure. This would be done by coalescing the stored beam into a single bunch that would then be resonantly extracted over a period of ~1 second. Figure 4.12 shows the accelerator complex with modifications to use protons from either the Booster or Project X to produce an appropriately pulsed proton beam. Based on the potential for instabilities in these rings, from electron cloud effects for example, it is now believed that a new ring based on either the recycler or Tevatron tunnel may be needed to handle more than 50 kW beam power. Instantaneous intensity considerations also affect the muon beamline. Some could be ameliorated simply, for example by increasing the bore of the superconducting magnet surrounding the production target and increasing the shielding around the target. Others require more study and possibly a significant change in approach, for example the need for a 5-fold increase in target cooling.

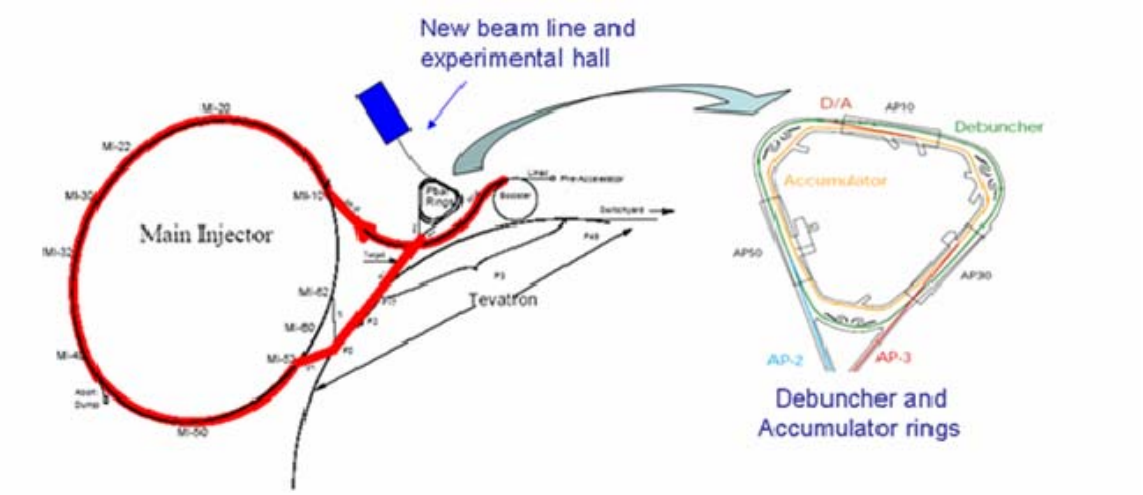

Figure 4.12 The Fermilab accelerator complex with provisions for a pulsed, slow extracted 8 GeV proton beam driven from either the Booster or Project X. Alternatives for using either the recycler or a ring in the Tevatron tunnel to replace the debuncher/accumulator rings to rebunch the proton beam are being studied, as are scenarios for injecting from the Project X linac into the accumulator/debuncher complex.

Modifications to the MECO/Mu2e approach would also be required to deal with increased rates, which would be above 2.5 MHz per channel. The spectrometer design was optimized to minimize multiple scattering and resulted in a configuration that did not have highly redundant tracking and that would be susceptible to tracking errors at these high rates. Most of the rate is due to products of muon capture (protons, neutrons, and photons), and these could be reduced by increasing the length of the solenoid surrounding the detectors, allowing the detectors themselves to be placed farther from the stopping target and reduce their subtended solid angle for neutral particles. Protons from muon capture typically have momentum about 100 MeV/c and their flux at the detectors is reduced with thin absorbers (they are very heavily ionizing) and by self absorption in the stopping target. More complicated geometries that exploit the opposite helicity of the trajectories of protons and electrons could reduce the proton flux with some loss in electron detection efficiency.

An upgraded Mu2e experiment could reach a sensitivity of 1 event for $R_{\mu e} = 10^{-18}$ in a few years (5×10^7 seconds) data collection. If $R_{\mu e}$ is near the current limit of 6×10^{-13} (or the limit of $\sim 10^{-13}$ implied by limits on $B_{\mu e \gamma}$ in photon mediated mechanisms) it would be measured with a statistical precision below 1%. With a large data sample, background from muon decay in orbit and other sources would not significantly increase the uncertainty in this measurement. Different nuclei (at least aluminum and titanium) could be studied, and the value of $R_{\mu e}$ compared with $B_{\mu e \gamma}$. If $R_{\mu e}$ is small ($<10^{-17}$), this approach would likely not be background free without additional improvements that will require significant study to implement. The stopping target thickness could be re-optimized to reduce energy loss of the outgoing electron, with some loss in muon stop rate. Re-optimized selection criteria and analysis strategies could also be directed to increase background rejection at the cost of reduced sensitivity.

This approach could be phased, with the first phase using the booster as the proton source and the second phase using the Project X linac. The first phase could reach a sensitivity of a few times 10^{-17} in 2-3 years of running simultaneous with a neutrino program. Depending on results of the first phase, the second phase, also run in parallel with a neutrino program and possibly other experiments, would either measure $R_{\mu e}$ with precision and for different nuclei or extend the search sensitivity by 1-2 orders of magnitude. Provisions for running at the highest Project X intensity would be incorporated. For example sufficient production solenoid bore to accommodate increased shielding and a detector solenoid long enough to reduce detector rates would be incorporated in the experiment.

4.3.2 Muon g-2 Measurements

All currently discussed experiments to improve the measurement of g-2 would use the existing precision superconducting muon storage ring that was built for E821 at BNL. The experimental concept would also be essentially unchanged. It is based on injecting highly polarized muons at the magic momentum of 3.094 GeV/c; at this momentum, the electric field used for weak focusing does not affect the muon spin precession. The muons circle the storage ring and their spins advance with a "precession frequency" proportional to g-2. The decay positrons times and energies are measured by calorimeters placed on the inside of edge of the storage ring (see Figure 4.13). Decay positrons from the stored muons are collected over an interval of 700 μs, ~11 time-dilated muon lifetimes.

Muons were produced using twelve 50 ns wide pulses of 24 GeV protons per 2.7 s AGS acceleration cycle delivered to a pion production target. Pions were momentum selected (0.5% $\Delta p/p$) and near-forward muons from the approximately 40% of the pions that decayed were collected. A final beamline bend, tuned to pass particles at the magic momentum, was used to separate muons from the pions entering the storage ring. Once in the ring, three fast kickers were fired to deflect the muons (~15,000 per spill) onto stable orbits. E821 was limited by the high instantaneous rate of stored muons and by the background *flash* that originated from pions that entered the ring during the injection.

E821 achieved an overall uncertainty of 0.54 ppm on the muon anomaly, a precision deduced from three high-statistics runs with approximately equal contributions of ~0.7 ppm from positive and negative muon samples. The final error included a 0.46 ppm statistical contribution, 0.21 ppm precession frequency systematic, and 0.17 ppm event-averaged magnetic field systematic.

A next-generation experiment would use at least 20 times more stored muons with a goal of improving the precision by a factor of 5 or more. More highly segmented detectors and faster electronics aimed at reducing systematic uncertainties for the same instantaneous muon intensity are envisaged. Significant improvement in the g-2 measurement also requires increasing the frequency of muon stores and reducing pion-induced background. Ways to increase the number of stored muons have been well documented in Proposal E969 to BNL. They include improvements to the muon decay beam lattice design, the

inflector magnet, and the kicker. Required additional improvements would use a much longer decay beamline and significantly greater pulse frequency. The longer decay line would allow nearly all pions to decay, eliminating the pion flash and increasing the muon/pion yield. Also, the ratio of the central pion to final muon momentum could be set to the optimal value of 1.005, increasing the figure-of-merit, NA^2. To achieve the long decay beam, a muon accumulator ring to store the pion / muon burst for up to 10 turns is being studied at BNL. At FNAL, a very long (0.5 – 1.0 km) decay beamline is envisioned. At BNL, the pulse frequency might be increased to 36 per 2.7 s cycle time. At Fermilab, schemes to extract as many as 84 pulses per 1.33 s cycle are being studied. The latter would be an increase of about 14 and 5 with respect to E821 and an upgraded experiment at BNL.

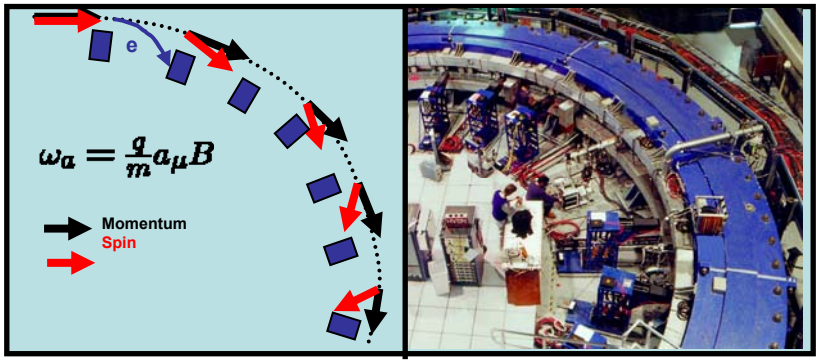

Figure 4.13 Left: Muon spin and momentum vectors with exaggerated spin motion as the muon circles the ring. The difference between the spin and momentum directions is the precession frequency, which is directly proportional to the muon anomaly, a_m. Right: Photo of the same arc of the storage ring with partial installation of detectors.

The cross section for 3.1 GeV/c positive pion production is 3 times smaller using the 8.9 GeV/c protons compared with 24 GeV/c protons. This reduction is contrasted by the combined effect of many storage improvements from upgrades and the forward decay long beamline to yield an overall *increase* in muons per proton of at least tenfold. In such a plan, more muons are delivered per second but at a lower instantaneous rate compared to BNL, a distinct advantage both for statistics and for systematic error control.

Reductions in the systematic uncertainties will also be required. Upgrades to the measurement design will reduce the uncertainty on the precession measurement and improvements in the shimming and monitoring of the magnetic field will reduce the uncertainty on the magnetic field systematic. The aim is to keep all systematic uncertainties below the statistical errors. Of the total running time, roughly 25% would be devoted to the study of systematic errors.

At Fermilab, it is estimated that ~4(6) x 10^{20} protons will give a 0.1 ppm measurement using positive (negative) muons. This corresponds to 8x10^7 s, a number of operational years, running at 16kW beam power or proportionately less if greater beam power (up to 50 kW?) with a Project X beam.

Both theory and experiment have now reached similar sub-ppm precision and a plan is seen to get to 0.1 ppm. The g-2 experimental team has also considered plans for efforts

beyond 0.1 ppm in precision. One idea, which would require an extremely powerful accelerator, such as the Project X linac, is an "all-integrating" experiment where very intense muon fills in a storage ring are measured by calorimeters in current mode. The g-2 asymmetry is carried by the flow of energy vs. time. Monte Carlo studies show that even with a reduced asymmetry due to integrating over the full decay spectrum, the statistical precision suffers by only about 10% compared with the conventional method. There is no pileup effect in this method; it is quite similar to high-rate, parity-violating electron scattering asymmetry measurements. Perhaps in the Project X era, this type of measurement can be realized. This concept could be tested parallel with conventional event analysis in the early phases of a Fermilab experiment.

4.4 Muon Summary

Both an experiment to search for muon to electron conversion at a sensitivity starting below 10^{-16} and extending to ~10^{-18} and an experiment to improve the measurement of the muon's anomalous magnetic moment (g-2) are highly motivated and should be part of a strong program in flavor physics at Fermilab. For both experiments, a phased approach is proposed.

The design for a conversion experiment (MECO) is rather mature and could be implemented relatively quickly (the Mu2e proposal), probably limited by the time for funding approval. It could be running within 5 years of initial funding. Even with 16-20 kW of beam power, it would be a powerful probe of new physics. The strategy would be to incorporate the possibility of modifying the beam and detectors to take advantage of the significant flux increase that could be provided by Project X. Again, the MECO design has the advantage that it could run at 100 kW of instantaneous power, within a factor of two of the 200 kW from a 100% duty cycle storage ring. The advantages of the extra power are clear, particularly in the case that a signal is seen and studies of target dependence and precise comparison with the decay rates for muon to positron and photon are possible. Better understanding of how the experiment could handle the full 200 kW from a Project X beam should be a priority.

In the context of experiments outside the U.S., the situation is not clear. A proposal for a rather different concept (PRISM/PRIME), to reach sensitivity about what might be done at Project X, is proposed for JPARC, also with an earlier phase at lesser sensitivity. It is likely to be a number of years before the PRISM/PRIME proposal is definitively acted on. The earlier phase (COMET) could be done on a timescale comparable to the first phase of mu2e.

A g-2 experiment with precision a factor of 5 better than the current precision could also be implemented relatively quickly, assuming that a way of ejecting >50 pulses per second from a storage ring can be found. Achieving this improvement with only the 16 kW booster source would require extended running and a somewhat increased flux from the Project X linac would reduce this. The advantages of Fermilab vs. another site (e.g. BNL or JPARC) are not so clear. Decreased pion production at 8 GeV vs 24 or 30 GeV could

be offset by more efficient pion production or muon capture. The choice of an optimal site would likely depend more on facility availability and total cost than on technical considerations. An even more ambitious plan that would utilize a large fraction of the available Project X intensity requires extensive study and testing; the latter could be done during the first phase of running.

5 Kaons

5.1 Introduction

The rare decays $K^+ \to \pi^+ \nu\bar{\nu}$ and $K_L^0 \to \pi^0 \nu\bar{\nu}$ play an important role in the search for the underlying mechanism of flavor mixing and *CP* violation. As such they are among the most incisive probes of physics beyond the Standard Model (SM). Of the many rare *K*- and *B*-decays, the $K^+ \to \pi^+ \nu\bar{\nu}$ and $K_L^0 \to \pi^0 \nu\bar{\nu}$ modes are unique since their SM branching ratios can be computed to an exceptionally high degree of precision, not matched by any other flavor-changing neutral current (FCNC) process involving quarks, and they have exquisite sensitivity to new physics contributions.

The exceptional theoretical cleanness of $K \to \pi\nu\bar{\nu}$ decays is a consequence of the severe suppression of non-perturbative effects in these processes: a powerful suppression which is not present in meson decays receiving contributions gluon-penguin and/or photon-penguin amplitudes. A related important virtue, following from their peculiar electroweak structure, is the fact that $K \to \pi\nu\bar{\nu}$ amplitudes can be described in terms of a single effective operator, namely

$$Q_{sd}^{\nu\bar{\nu}} = (\bar{s}_L \gamma^\mu d_L)\,(\bar{\nu}_L \gamma_\mu \nu_L)\ . \qquad (1)$$

The hadronic matrix elements of $Q_{sd}{}^{\nu\nu}$ relevant for $K \to \pi\nu\bar{\nu}$ amplitudes can be extracted directly from the well-measured $K \to \pi e \nu$ decay rates, taking into account small Isospin Breaking (IB) corrections. The latter have recently been estimated beyond the leading order and turn out to be a negligible source of uncertainty.

In the case of $K_L^0 \to \pi^0 \nu\bar{\nu}$, which is *CP*-violating and dominated by the top-quark contribution, the SM Short-Distance (SD) dynamics is encoded in a perturbatively calculable real function X that multiplies the CKM factor $\lambda_t = V_{ts}^* V_{td}$. In the $K^+ \to \pi^+ \nu\bar{\nu}$ case a charm quark contribution proportional to $\lambda_c = V_{cs}^* V_{cd}$ also has to be taken into account, but the recent NNLO QCD calculation of the dimension-six charm quark corrections (A.J. Buras et al., Phys. Rev. Lett. 95, 261805) and the progress in the evaluation of the residual Long-Distance (LD) effects (G. Isidori et al., Nucl. Phys. B 718, 319 (2005)) elevated the theoretical cleanness of $K^+ \to \pi^+ \nu\bar{\nu}$ almost to the level of $K_L^0 \to \pi^0 \nu\bar{\nu}$. More details will be given in the following.

An striking feature of $K \to \pi\nu\bar{\nu}$ decays is that their clean theoretical character remains valid in essentially all extensions of the SM and that $Q_{sd}{}^{\nu\nu}$, due to the special properties of the neutrinos, remains the only relevant operator. Consequently, in most SM extensions the New Physics (NP) contributions to $K^+ \to \pi^+ \nu\bar{\nu}$ and $K_L^0 \to \pi^0 \nu\bar{\nu}$ can be parametrized in a model-independent manner by just two parameters, the magnitude and the phase of the function

$$X = |X|\ exp(i\theta_X), \qquad (2)$$

that multiplies λ_t in the relevant effective Hamiltonian. In the SM, $|X| = X_{SM}$ and $\theta_X = 0$. The parameters $|X|$ and θ_X can be extracted from $B(K_L^0 \to \pi^0 \nu\bar{\nu})$ and $B(K^+ \to \pi^+ \nu\bar{\nu})$ with small, controllable uncertainties, while the function X can be calculated in any extension of the SM within perturbation theory. Of particular interest is the ratio

$$B(K_L^0 \to \pi^0 \nu\bar{\nu}) / B(K_L^0 \to \pi^0 \nu\bar{\nu})_{SM} = |X / X_{SM}|^2 \, [\sin(\beta - \theta_X) / \sin\beta]^2 \qquad (3)$$

Bearing in mind that $\beta \sim 21.4^o$, this equation shows that $K_L^0 \to \pi^0 \nu\bar{\nu}$ is a very sensitive function of the new phase θ_X, or of new sources of *CP* violation. The pattern of the two $K \to \pi\nu\bar{\nu}$ branching ratios as a function of θ_X is illustrated in Figure 5.1 (left). We note that the ratio of the two modes shown in Figure 5.1 (right) depends very mildly on $|X|$ and therefore provides an excellent tool to extract the non-standard *CP*-violating phase θ_X.

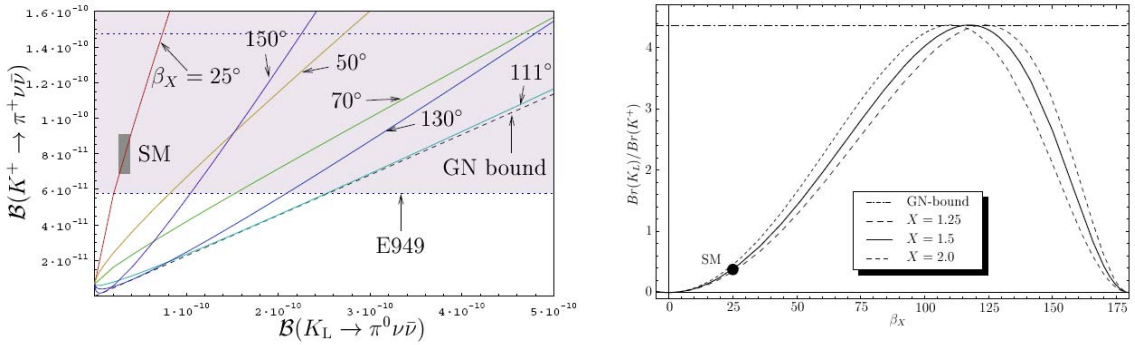

Figure 5.1 Left: $B(K^+ \to \pi^+ \nu\nu)$ vs. $B(K_L \to \pi^0 \nu\nu)$ for various values of $\beta_X = \beta - \theta_X$ (including E949 data) characterizing new physics as discussed in the text. The dotted horizontal lines indicate the lower part of the experimental range and the grey area the SM prediction. We also show the Grossman-Nir (GN) bound. Right: The ratio of the $K \to \pi\nu\nu$ branching ratios as a function of β_X for $|X|$=1.25, 1.5, 2.0. The horizontal line is again the GN bound (from A. J. Buras,et al., Nucl. Phys. B 697, 133 (2004)).

The exceptional cleanness of the two decays, and their strong suppression within the SM, implies a sensitivity to new particles well above the TeV scale in several realistic scenarios such as supersymmetry or little-Higgs models (see below). As stressed in a series of recent works, sizable non-standard effects could show up in these rare decays without significant signals in B physics and, in specific scenarios, even without new particles within the LHC reach. On the other hand, if LHC finds new physics in the TeV range, then the energy scale of the new degrees of freedom will be known and the measurements of the two $K \to \pi\nu\bar{\nu}$ rates will be essential in determining the flavor structure of the new theory. An updated discussion about the impact of rare K decays in the LHC era can be found in the recent review by G. Buchalla *et al.* (arXiv:0801.1833) on which the present discussion on $K \to \pi\nu\bar{\nu}$ is largely based.

5.1.1 $K^+ \to \pi^+ \nu\bar{\nu}$ and $K_L^0 \to \pi^0 \nu\bar{\nu}$ in the SM

After summation over the three lepton families, the SM branching ratios for the $K \to \pi\nu\bar{\nu}$ decays can be written as

$$\mathcal{B}(K^+ \to \pi^+ \nu\bar{\nu})_{\rm SM} = \kappa_+ \left[\left(\frac{{\rm Im}\,\lambda_t}{\lambda^5} X_{\rm SM} \right)^2 + \left(\frac{{\rm Re}\,\lambda_t}{\lambda^5} X_{\rm SM} + \frac{{\rm Re}\,\lambda_c}{\lambda} \left(P_c + \delta P_{c,u} \right) \right)^2 \right], \quad (4)$$

$$\mathcal{B}(K_L \to \pi^0 \nu\bar{\nu})_{\rm SM} = \kappa_L \left(\frac{{\rm Im}\,\lambda_t}{\lambda^5} X_{\rm SM} \right)^2, \quad (5)$$

where $\lambda = |V_{us}|$, while $\kappa_+ = (5.165 \pm 0.025) \times 10^{-11}\ (\lambda/0.225)^8$ and $\kappa_L = (2.231 \pm 0.013) \times 10^{-10}\ (\lambda/0.225)^8$ include the IB corrections in relating $K \to \pi\nu\bar{\nu}$ to the $K \to \pi e \nu$ rates (Mescia and Smith, Phys. Rev. D 76 (2007) 034017). The dimension-six top quark contribution, $X_{SM} = 1.464 \pm 0.041$, accounts for 63% and almost 100% of the total rates in the charged and neutral decay, respectively. The top-quark contribution is known at the NLO accuracy, with a scale uncertainty of slightly below 1%. In the charged decay, dimension-six charm-quark corrections and sub-leading dimension-eight charm and up-quark effects, characterized by $P_c = 0.38 \pm 0.04$ and $\delta P_{cu} = 0.04 \pm 0.02$, amount to moderate 33% and a mere 4%. Light quark contributions are negligible in the case of the $K_L^0 \to \pi^0 \nu\bar{\nu}$ decay.

Taking into account all the indirect constraints from the latest global Unitarity Triangle (UT) fit, the SM predictions of the two $K \to \pi\nu\bar{\nu}$ rates are

$$B(K^+ \to \pi^+ \nu\bar{\nu})_{SM} = (8.22 \pm 0.84) \times 10^{-11}$$
$$B(K_L^0 \to \pi^0 \nu\bar{\nu})_{SM} = (2.76 \pm 0.40) \times 10^{-11} \quad (6)$$

with an uncertainty which is mainly of parametric nature (top- and charm-quark masses, and CKM factors as discussed below).

While the determination of $|V_{td}|$, $\sin 2\beta$, and γ from the $K \to \pi\nu\bar{\nu}$ system is without doubt still of interest, with the slow progress in measuring the relevant branching ratios and much faster progress in the extraction of the angle γ from the $B_s \to DK$ system to be expected at the LHC, the role of the $K \to \pi\nu\bar{\nu}$ system will shift towards the search for NP rather than the determination of the CKM parameters.

In fact, determining the UT from tree-level dominated *K*- and *B*-decays and thus independently of NP will allow determination of the true values of the CKM parameters. Inserting these values in Eqs. (4) and (5) yields very precise SM predictions for the rates of both rare *K*-decays. A comparison with future data on $K \to \pi\nu\bar{\nu}$ may then give a clear signal of potential NP contributions in a theoretically clean environment. In the $K_L^0 \to \pi^0 \nu\bar{\nu}$ case, even deviations by 15% from the SM expectations could be considered as signals of NP, while such a conclusion cannot be drawn in most other decays in which the theoretical errors are typically of order 10%.

5.1.2 $K^+ \to \pi^+ \nu\bar{\nu}$ and $K_L^0 \to \pi^0 \nu\bar{\nu}$ beyond the SM

Minimal Flavor Violation

In models with Minimal Flavor Violation (MFV) both decays are, as in the SM, governed by a single real function X that can take a different value than in the SM due to new particle exchange in the relevant Z-penguin and box diagrams. First restricting our discussion to the so-called constrained MFV (CMFV), in which strong correlations between K- and B-decays exist, one finds that the branching ratios for $K^+ \to \pi^+ \nu\bar{\nu}$ and $K_L^0 \to \pi^0 \nu\bar{\nu}$ cannot be much larger than their SM values given in Eq. (6). The 95% probability bounds are (Bobeth et al. Nucl. Phys. B726, 252 (2005)):

$$B(K^+ \to \pi^+ \nu\bar{\nu})_{CMFV} < 11.9 \times 10^{-11},\ B(K_L^0 \to \pi^0 \nu\bar{\nu})_{CMFV} < 4.6 \times 10^{-11} \qquad (7)$$

Explicit calculations in a model with one Universal Extra Dimension (UED) and in the littlest Higgs model without T-parity give explicit examples of this scenario with the branching ratios within 20% of the SM expectations. Effects of similar size are also found in the MFV version of the Minimal Supersymmetric of the SM (MSSM).

Probably the most interesting property of this class of models is a theoretically clean determination of the angle β of the standard UT, which utilizes both branching ratios and is independent of the value of X. Consequently, this determination is universal within the class of MFV models and any departure of the resulting value of β from the corresponding one measured in B-decays would signal non-MFV interactions.

Littlest Higgs Model with T-parity

The structure of $K \to \pi\nu\bar{\nu}$ decays in the Littlest Higgs model with T-parity (LHT) differs notably from the one found in MFV models due to the presence of mirror quarks and leptons that interact with the light fermions through the exchange of heavy charged (W_H) and neutral (Z_H, A_H) gauge bosons. The mixing matrix V_{Hd} that governs these interactions can differ from V_{CKM}, which implies the presence of non-MFV interactions. Instead of a single real function X that is universal within the K-, B_d- and B_s-systems in MFV models, one now has three functions

$$X_K = |X_K|\, exp(i\theta_K),\ X_d = |X_d|\, exp(i\theta_d),\ X_s = |X_s|\, exp(i\theta_s) \qquad (8)$$

that, due to the presence of mirror fermions, can have different phases and magnitudes. This possibility can have a major impact on the $K \to \pi\nu\bar{\nu}$ system, since the correlations between K- and B-decays are partly lost and the presence of a large phase θ_K can change the pattern of these decays from the one observed in MFV. A detailed analysis shows that both branching ratios can depart significantly from their SM values, and can be as high as 5.0×10^{-10}. As shown in Figure 5.2 (left), there are two branches of allowed values with strong correlations between both branching ratios within a given branch. In the lower branch only $B(K^+ \to \pi^+ \nu\bar{\nu})$ can differ substantially from the SM expectations reaching

values well above the present central experimental value. In the second branch $B(K_L^0 \to \pi^0 \nu\bar{\nu})$ and $B(K^+ \to \pi^+ \nu\bar{\nu})$ can be as high as 5.0 x 10^{-10} and 2.3 x 10^{-10}, respectively. Moreover, $B(K_L^0 \to \pi^0 \nu\bar{\nu})$ can be larger than $B(K^+ \to \pi^+ \nu\bar{\nu})$ which is excluded within MFV models. Other features distinguishing this model from MFV are thoroughly discussed in arXiv:hep-ph/0610298 (M. Blanke et al).

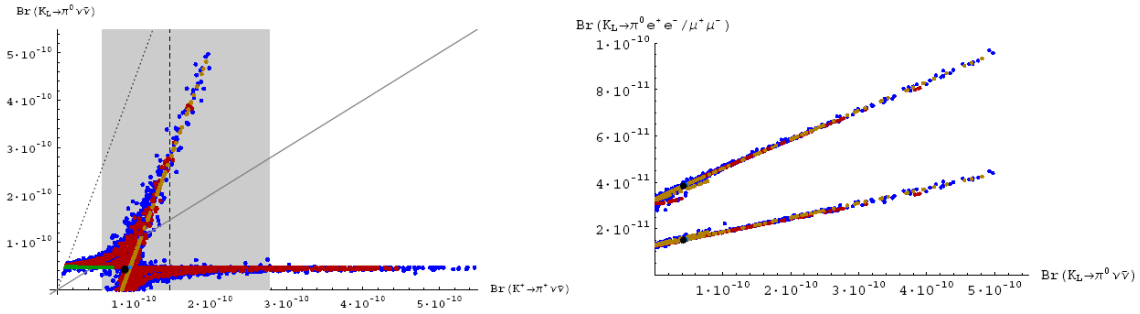

Figure 5.2 Left: $B(K_L \to \pi^0 \nu\nu)$ vs. $B(K^+ \to \pi^+ \nu\nu)$ in the LHT model. The shaded area represents the experimental 1σ-range for $B(K^+ \to \pi^+ \nu\nu)$. The GN bound is displayed by the dotted line, while the solid line separates the two areas where $B(K_L \to \pi^0 \nu\nu)$ is larger or smaller than $B(K^+ \to \pi^+ \nu\nu)$. Right: $B(K_L \to \pi^0 e+e-)$ (upper curve) and $B(K_L \to \pi^0 \mu\mu)$ (lower curve) as functions of $B(K_L \to \pi^0 \nu\nu)$ in the LHT model.

Supersymmetry

Within the MSSM with *R*-parity conservation, sizable non-standard contributions to $K \to \pi\nu\bar{\nu}$ decays can be generated if the soft-breaking terms have a non-MFV structure. The leading amplitudes giving rise to large effects are induced by: (i) chargino/up-squark loops (ii) charged Higgs/top quark loops. In the first case, large effects are generated if the left-right mixing (*A* term) of the up-squarks has a non-MFV structure. In the second case, deviations from the SM are induced by non-MFV terms in the right-right down sector, provided the ratio of the two Higgs vacuum expectation values ($tan\beta = v_u/v_d$) is large ($tan\beta \sim$ 30-50).

The effective Hamiltonian encoding SD contributions in the general MSSM has the following structure:

$$\mathcal{H}_{\rm eff}^{\rm (SD)} \propto \sum_{l=e,\mu,\tau} V_{ts}^* V_{td} \left[X_L (\bar{s}_L \gamma^\mu d_L)(\bar{\nu}_{lL} \gamma_\mu \nu_{lL}) + X_R (\bar{s}_R \gamma^\mu d_R)(\bar{\nu}_{lL} \gamma_\mu \nu_{lL}) \right] , \qquad (9)$$

where the SM case is recovered for $X_R = 0$ and $X_L = X_{SM}$. In general, both X_R and X_L are non-vanishing, and the misalignment between quark and squark flavor structures implies that they are both complex quantities. Since the $K \to \pi$ matrix elements of ($s_L \gamma^\mu d_L$) and ($s_R \gamma^\mu d_R$) are equal, the combination $X_L + X_R$ allows us to describe all the SD contributions to $K \to \pi\nu\bar{\nu}$ decays. More precisely, we can simply use the SM expressions for the branching ratios in Eqs. (4) to (5) with the following replacement

$$X_{SM} \to X_{SM} + X^{SUSY}{}_L + X^{SUSY}{}_R \, . \qquad (10)$$

In the limit of almost degenerate superpartners, the leading chargino/up-squarks contribution is:

$$X_L^{\chi^\pm} \approx \frac{1}{96}\left[\frac{(\delta^u_{LR})_{23}(\delta^u_{RL})_{31}}{\lambda_t}\right] = \frac{1}{96\lambda_t}\frac{(\tilde{M}_u^2)_{2_L 3_R}(\tilde{M}_u^2)_{3_R 1_L}}{(\tilde{M}_u^2)_{LL}(\tilde{M}_u^2)_{RR}}\,. \qquad (11)$$

As pointed out by Colangelo and Isidori (JHEP 9809, 009 (1998)) a remarkable feature of the above result is that no extra $O(M_W/M_{SUSY})$ suppression and no explicit CKM suppression is present (as it happens in the chargino/up-squarks contributions to other processes). Furthermore, the (δ^u_{LR})-type mass insertions are not strongly constrained by other *B*- and *K*-observables. This implies that large departures from the SM expectations in $K \to \pi\nu\bar{\nu}$ decays are allowed. As illustrated in Figure 5.3 (left), $K \to \pi\nu\bar{\nu}$ are the best observables to determine/constrain from experimental data the size of the off-diagonal (δ^u_{LR}) mass insertions or, equivalently, the up-type trilinear terms A_{i3} $[(\tilde{M}_u^2)_{i_L 3_R} \approx m_t A_{i3}]$. Their measurement is therefore extremely interesting in the LHC era.

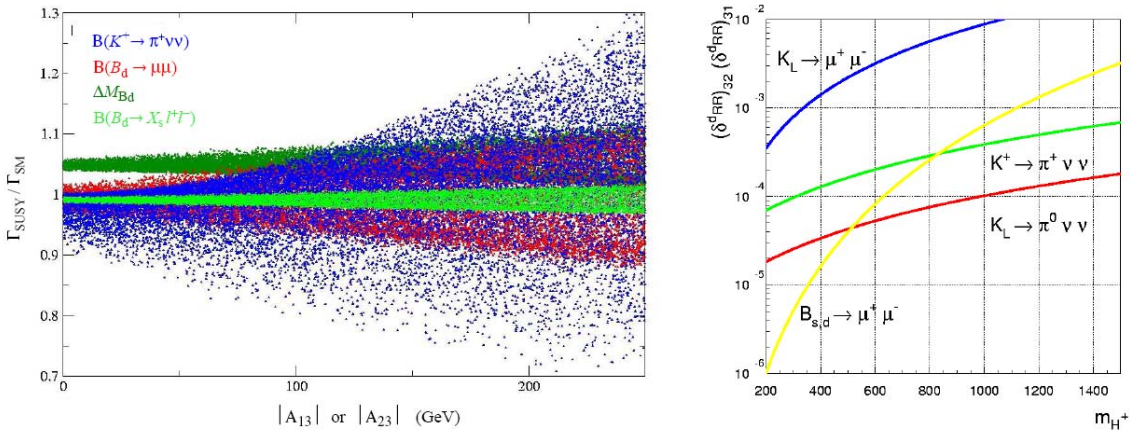

Figure 5.3 Supersymmetric contributions to $K \to \pi\nu\nu$ (from Isidori et al. JHEP 0608, 064 (2006), Phys. Rev. D73 (2006), 055017). Left: Dependence of various FCNC observables (normalized to their SM value) on the up-type trilinear terms A_{13} and A_{23}, for $A_{ij} < \lambda A_0$ and $\tan\beta$=2-4 (other key parameters in GeV: μ = 500 ± 10, M_2 = 300 ± 10, $M_{uR\ tilde}$ = 600 ± 20, $M_{qL\ tilde}$ = 800 ± 20, A_0=1000). Right: Sensitivity to $(\delta^d_{RR})_{23}(\delta^d_{RR})_{31}$ of various rare *K*- and *B*-decays as a function of M_{H^+}, setting $\tan\beta$ = 50, $\mu < 0$ and assuming almost degenerate superparteners (the bounds from the two $K \to \pi\nu\nu$ modes are obtained assuming a 10 % measurements of their branching ratios while the $B_{s,d} \to \mu^+ \mu^-$ bounds refer to the present experimental limits).

In the large $\tan\beta$ limit, the charged Higgs/top-quark exchange leads to:

$$X_R^{H^\pm} \approx \left[\left(\frac{m_s m_d\, t_\beta^2}{2M_W^2}\right) + \frac{(\delta^d_{RR})_{31}(\delta^d_R)_{32}}{\lambda_t}\left(\frac{m_b^2\, t_\beta^2}{2M_W^2}\right)\frac{\epsilon_{RR}^2 t_\beta^2}{(1+\epsilon_i t_\beta)^4}\right] f_H(y_{tH})\,. \qquad (12)$$

where $y_{tH} = m_t^2/M_H^2$, $f_H(x) = x\,/\,4(1\text{-}x) + x \log x\,/\,4(x\text{-}1)^2$ and $\varepsilon_{i,RR}\ t_\beta = O(1)$ for $t_\beta = \tan\beta \sim 50$. The first term of Eq. (12) arises from MFV effects and its potential $\tan\beta$ enhancement is more than compensated by the smallness of $m_{d,s}$. The second term on the r.h.s. of Eq. (12), which would appear only at the three-loop level in a standard loop expansion can be largely enhanced by the $\tan^4\beta$ factor and does not contain any suppression due to light quark masses. Similarly to the double mass-insertion mechanism of Eq. (11), in this case the potentially leading effect is the one generated when two off-diagonal squark mixing terms replace the two CKM factors V_{ts} and V_{td}.

The coupling of the $(s_R\ \gamma^\mu\ d_R)\ (\nu_L\ \gamma^\mu\ \nu_L)$ effective FCNC operator generated by charged-Higgs/top-quark loops is phenomenologically relevant only at large tanβ and with non-MFV right-right soft-breaking terms: a specific but well-motivated scenario within grand-unified theories. These non-standard effects do not vanish in the limit of heavy squarks and gauginos, and have a slow decoupling with respect to the charged-Higgs boson mass. Moreover, the *B*-physics constraints still allow large room for non-standard effects in $K \rightarrow \pi\nu\nu$ even for flavor-mixing terms of CKM size (see Figure 5.3 right).

5.1.3 Theoretical Uncertainties

In the following sections on experimental prospects at Fermilab for $K^+ \to \pi^+\nu\bar{\nu}$ and $K_L^0 \to \pi^0\nu\bar{\nu}$, we outline a series of measurements culminating with O(1000) events, in each channel, at the rates predicted by the Standard Model. Here we outline the main sources of theoretical uncertainty in the SM predictions and discuss prospects for reducing them over the coming decade.

We expect that the measurements will remain statistics limited, so the target for the theoretical uncertainty on the rate is 3%. The present status, Eqs. (6), of the SM calculations yield total "theoretical" uncertainties of 14% (K_L) and 10% (K^+). In both cases, the dominant error comes from the determination of the CKM matrix, which in Eqs. (6) is taken from the global UT fit. Other important uncertainties stem from the experimental error in m_t, experimental and theoretical errors in α_s, theoretical errors in m_c (for K^+ only), higher-order electroweak and QCD corrections, higher-dimension contribution with a charmed quark (for K^+ only), and long-distance effects (for K^+ only).

Let us start with the neutral mode. It is convenient to summarize the theoretical calculation in a way that shows the origin of the uncertainties:

$$\mathcal{B}(K_L \to \pi^0\nu\bar{\nu}) \propto r_{K_L}\mathcal{B}(K^+ \to \pi^0 e^+\nu) \times \frac{\alpha^2}{\sin^4\theta_W} \times \left[\frac{\mathrm{Im}\, V_{ts}^* V_{td}}{|V_{us}|}\right]^2 \times [X(m_t, \alpha_s)]^2, \qquad (13)$$

where $r_{K_L} = 0.944$ summarizes corrections to isospin symmetry, necessary to extract the semileptonic form factor from $K^+ \rightarrow \pi^0 e^+ \nu$. Higher-order corrections would improve the short-distance factor *X*, which is where the m_t and α_s dependence enter. In the region of interest $X(m_t) \sim m_t^{1.15}$; if, as seems likely, the Tevatron and LHC experiments bring the error in the top mass down to 0.5%, then the error from this source in Eq. (13) from m_t fits within the error desired budget. A more subtle concern, when m_t is so precise, is how to connect the experimental definition of m_t with a clear field-theoretical concept necessary for compatibility with perturbative QCD corrections to *X*. Similarly, it seems likely that the precision of α, $\sin\theta_W$, and α_s are good enough, but care is needed to make sure that all factors in Eq. (13) are in the same scheme.

The most challenging uncertainties are in the CKM factors. At the amplitude level one has

$$\frac{\mathrm{Im}\, V_{ts}^* V_{td}}{|V_{us}|} = \frac{|V_{cb}|\,\mathrm{Im}\, V_{ub}}{|V_{us}|} = \frac{|V_{cb}||V_{ub}|\sin\delta_{KM}}{|V_{us}|} = \frac{(A\lambda^2)(A\lambda^3\eta)}{\lambda}, \qquad (14)$$

where the first relation exploits three-generation unitarity, and the last form uses the Wolfenstein parametrization. If one is confident that new physics does not alter the rate, then the rate prescribes a precise constraint on the CKM combination $(A^2\lambda^4)^2$. At the percent level of precision, however, it is more likely that (and more interesting if) new TeV-scale physics interferes with the SM. Then, to obtain a precise test of the SM, the CKM parameters must be improved by other means.

Two general strategies may be envisioned, either determining individual CKM elements directly, or constraining the four free parameters of the CKM matrix through a global fit. In the context of searches for percent-level deviations from the SM, these strategies may be not so different: processes that occur at the tree level of the electroweak interactions will be used to determine CKM, with SM loop processes used for searches. A global fit based on SM-dominated processes could, then, leverage several quantities to improve the overall precision.

For this document we will focus on the direct approach. The current error on $|V_{us}|$ is close to 1%, with K_{l3} and K_{l2} decays giving similar accuracy and good agreement. Within the next decade improvements in lattice QCD will reduce the error further, and better computing resources will enable lattice calculations with several formulations of the computationally demanding sea quarks. As long as one does not propagate errors in $B(K_L^0 \to \pi^0 \nu\bar{\nu})$ as λ^8, the error from $|V_{us}| = \lambda$ is not an obstacle.

The current error on $|V_{cb}|$ is also close to 1% from inclusive semileptonic decays of B mesons. With a recent unquenched lattice calculation for the exclusive decay $B \to D^* l \nu$, however, the inclusive and exclusive determinations disagree. (The error on the exclusive method is 2-3% and the discrepancy is 8%.) Nevertheless, this discrepancy will very likely be resolved before a 1000-event experiment taken place because it has repercussions throughout flavor physics.

The real challenges come from V_{ub}. The magnitude comes from semileptonic decays, inclusive or exclusive, and the phase from *CP* asymmetries. At present the theoretical uncertainties on $|V_{ub}|$ are 5-10%, for both inclusive and exclusive approaches. One will probably have to tame higher-dimension corrections to the inclusive rate, to attain percent-level accuracy. This may not be feasible. For the exclusive decays, one must focus on $B \to \pi l \nu$, and compute the decay form factor with lattice QCD. The current error budget contains several few-percent contributors, so it will be challenging, albeit feasible, to control all of them at the sub-percent level. The LHCb experiment forecasts an uncertainty in the UT angle $\gamma = \delta_{KM}$ of 5^o (2.5^o) in 2 fb^{-1} (10 fb^{-1}). For $\gamma \sim 80^o$, this corresponds to a 1% (0.6%) error in $\sin\delta_{KM}$.

In summary, reducing the parametric and theoretical uncertainties in $B(K_L^0 \to \pi^0 \nu\bar{\nu})_{\rm SM}$ to the 3-5% level seems feasible, but challenging both for theory (particularly lattice QCD) and experimental (for $\sin\delta_{KM}$).

For the charged mode, the analog of Eq. (13) reads

$$\mathcal{B}(K^+ \to \pi^+ \nu\bar{\nu}) \;\propto\; r_{K^+}\mathcal{B}(K^+ \to \pi^0 e^+ \nu) \times \frac{\alpha^2}{\sin^4\theta_W} \times \frac{1}{|V_{us}|^2} \times \sum_l |V_{ts}^* V_{td} X(m_{\rm t}, \alpha_s) + V_{cs}^* V_{cd} X_{\rm NL}(m_{\rm c}, m_l, \alpha_s)|^2, \qquad (15)$$

where $r_{K^+} = 0.901$ summarizes corrections to isospin asymmetry, similarly to r_{K_L}. The short-distance contribution of the charmed quark, $X_{NL}(m_c, m_t, \alpha_s)$, sums large logarithms $\ln(m_c/M_W)$ and depends on the lepton mass m_l. The contribution $X_{NL}(m_c, m_t, \alpha_s)$ is GIM-suppressed relative to $X(m_t, \alpha_s)$ by $(m_c/m_t)^2$, so only the O(l) real part of $V_{cs}^* V_{cd}$ plays a significant role, even at the percent level. In addition to CKM uncertainties, an important uncertainty comes from the charmed-quark mass, taken in Eqs. (6) to be $m_c = 1.30 \pm 0.05$, leading to a 5% uncertainty in $B(K^+ \to \pi^+ \nu\bar{\nu})$. Unquenched lattice QCD calculations with a non-perturbative mass renormalization could cut this in half, bringing us close to the target. An additional complication for the charged mode, when the target is 3% precision, is the contribution from the up quark in the loop. Here one can have long-distance effects of the form $K^+ \to \pi^0 l^+ \nu \to \pi^+ \nu\nu$. A combination of ChPT and lattice QCD should be able to control this contribution at the needed level.

In the charged mode, the combined error from CKM uncertainties and the charmed-quark mass may make it difficult to reduce the theoretical error to 3%. Much of the CKM error cancels, however, in the ratio $B(K^+ \to \pi^+ \nu\bar{\nu}) / B(K_L^0 \to \pi^0 \nu\bar{\nu})$. If we can observe 1000 events of each, it may be most incisive to confront the ratio and $B(K_L^0 \to \pi^0 \nu\bar{\nu})$ with the SM. In both cases the theoretical and experimental errors would be comparable.

5.1.4 Conclusions

The rare $K \to \pi\nu\bar{\nu}$ decays are excellent probes of new physics. Firstly, their exceptional cleanness allows access to very high energy scales. As stressed in a series of recent works, new physics could be seen in rare K decays without significant signals in $B_{d,s}$-decays and, in specific scenarios, even without new particles within the LHC reach. Secondly, if LHC finds new physics, its energy scale will be fixed. Then, the measurements of the two $K \to \pi\nu\bar{\nu}$ rates would be very helpful in discriminating among models.

The sensitivity to the scale of new physics from precise measurements of these modes grows like $1/\sigma^{1/2}$, where σ is the relative experimental error. This growth is valid up to the level where the theory errors start to dominate (i.e. up to $\sigma \sim 3\%$ measurements). The normalization of this law depends on the flavor structure of the model. In pessimistic scenarios (such as MFV models), new particle masses in the (few) x (100 GeV) range can be accessed with $\sigma \sim 3\%$, while with the same precision new particles well above the TeV

(even up to 10^4 TeV) are probed in new physics models with a non-minimal flavor structure.

It is worth stressing that if a deviation from the SM is seen in one of the two $K \to \pi\nu\bar{\nu}$ channels, key independent information about the nature of new physics can be obtained also from the two $K_L \to \pi^0 l^+ l^-$ *(l=e,μ)* modes. The latter are not as clean as the neutrino modes, but are still dominated by SD dynamics and very sensitive to new physics. Different correlations among these four channels are expected in different models (see e.g. Figure 5.2). These correlations can be used as powerful tests to shed light on the nature of new effects. In all cases where visible effects are found, the information extracted from the four modes is essential to establish the new flavor structure in the *s* → *d* sector. Rare *K* decays are thus an integral part, along with B-physics and collider observables, of the grand project of reconstructing the best model from data.

5.2 Prospects for Measuring $K_L^0 \to \pi^0\nu\bar{\nu}$ at Fermilab

5.2.1 General Considerations and the KOPIO Experiment at BNL

Definitively measuring $K_L^0 \to \pi^0\nu\bar{\nu}$ decay at the few × 10^{-11} branching ratio level represents a significant experimental challenge. The poorly defined signal consists of a neutral kaon followed by a neutral pion, $K_L \to \pi^0$, with the pion immediately decaying into two γ's with no other observed particles. Potential backgrounds, from other *K* decays, at branching ratios many orders of magnitude higher, have similar signatures. In addition, neutrons, which are inevitably present in a neutral beam, can create π^0s from material in or near the beam. Therefore, the experimental strategy involves proving that candidate events have low probabilities of being due to background. The principal intrinsic source of background is $K_L \to \pi^0\pi^0$ with branching ratio 8.64×10^{-4}. This can fake signal either when one of the two π^0s is missed entirely by the detector, or when one γ from each of the π^0s is missed and the two odd γ's happen to reconstruct to a π^0 to within the resolution of the detector. Another kaon-induced background comes from $K_L \to 3\pi^0$ which is much less likely to be mistaken for the signal but which has a much higher branching ratio. Other backgrounds can be induced by $K_L \to \pi^+\pi^-\pi^0$ to the extent that charged particle vetoing is imperfect, and $K_L \to \pi^- e^+ \nu$ if charged particle vetoing fails and the two charged particles manage to make or appear to be γ's. There are many other possible background processes.

Any attempt to detect $K_L^0 \to \pi^0\nu\bar{\nu}$ must rely on extremely efficient charged and neutral particle vetoing and very good resolution for γ's. There have been two approaches suggested, basically a high and a low energy approach. The former relies on a small, intense forward beam of kaons, high resolution γ detection and the highly efficient neutral and charged vetoing possible at high energies. The dedicated $K_L^0 \to \pi^0\nu\bar{\nu}$ experiment, KEK-391a, has taken this approach (although the KEK-PS was limited to

medium energies), and recently released a new 90% CL upper limit, $B(K_L^0 \to \pi^0 \nu\bar{\nu}) < 6.7 \times 10^{-8}$. This experiment will be upgraded and moved to JPARC where a future second phase (presently not defined) will seek a clear measurement. The low energy approach was epitomized by the KOPIO experiment proposed for the Brookhaven AGS which aimed at accumulating several hundred events. [2]

The low energy technique is illustrated in Figure 5.4. It focuses upon obtaining the maximum possible information about each event, i.e. the direction, energy, production time and decay position of the K_L, and the directions, energies and times of the γ's. In addition, it requires highly efficient hermetic rejection of events (vetoing) with extra particles. A low energy neutral beam is created by protons tightly bunched in time, so that the production time of the kaons is known, modulo the 25 MHz period of the proton μ-bunches. Combined with direction and timing measurements on the final state γ's, this gives the time-of-flight (TOF) and therefore the energy of the incident kaon. The directional measurement of the γ's also gives the kaon decay position, assuring that the photons originated in a $\pi^0 \to \gamma\gamma$ decay. Finally, energy measurement of the γ's allows powerful kinematic constraints to be imposed on candidate events in the K_L^0 center-of-mass system.

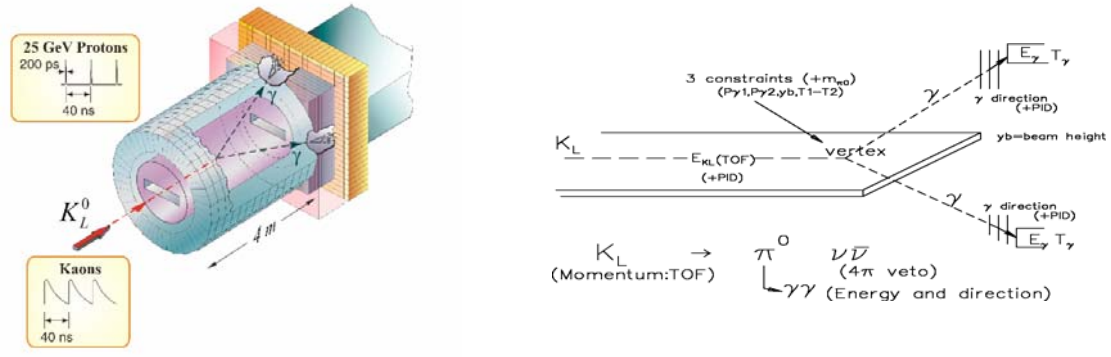

Figure 5.4 Left: The principles of the low energy approach to measuring $K_L^0 \to \pi^0 \nu\bar{\nu}$. Right: Kinematic measurements.

In order to optimize the low energy beam to enable the TOF technique (with usable K_L's between 0.4 and 1.4 GeV/c), it is necessary to go to a very large production angle. To obtain the high flux necessary for a measurement at the 10^{-12}/event level, KOPIO was forced to use a rather large beam solid angle; to maintain at least one beam kinematic constraint the beam profile was made very asymmetric, (narrow in the vertical and extremely wide in the horizontal). Figure 5.5 shows the result of a simulation of a 6000-hr KOPIO run. Figure 5.6 shows the results of a maximum likelihood analysis developed

[2] KOPIO passed all technical reviews and had progressed to a baseline review commissioned by the NSF in May of 2005. The RSVP program (KOPIO and MECO) was canceled for financial reasons relating to NSF and DOE funding issues.

to use events of varying signal to background resulting in the precision of a measurement at the Standard Model level ~11%.

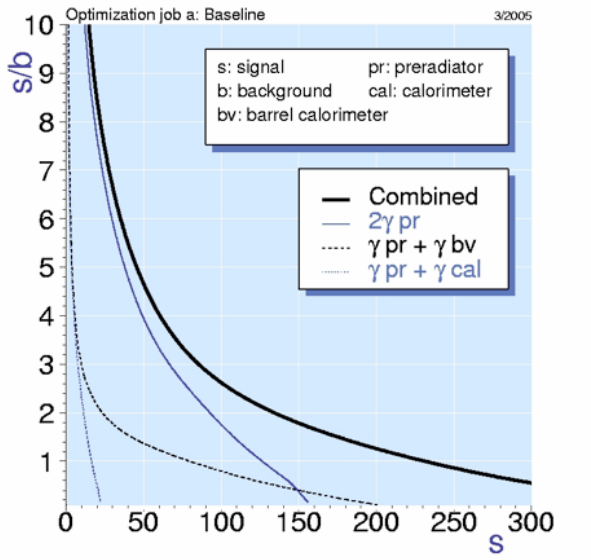

Figure 5.5 Signal/background vs number of signal events for 6000-hr run of KOPIO at the BNL AGS. Beyond S:B of ~1:2, the gain in precision is very slow, and the requirements on knowledge of the background become more and more difficult to meet.

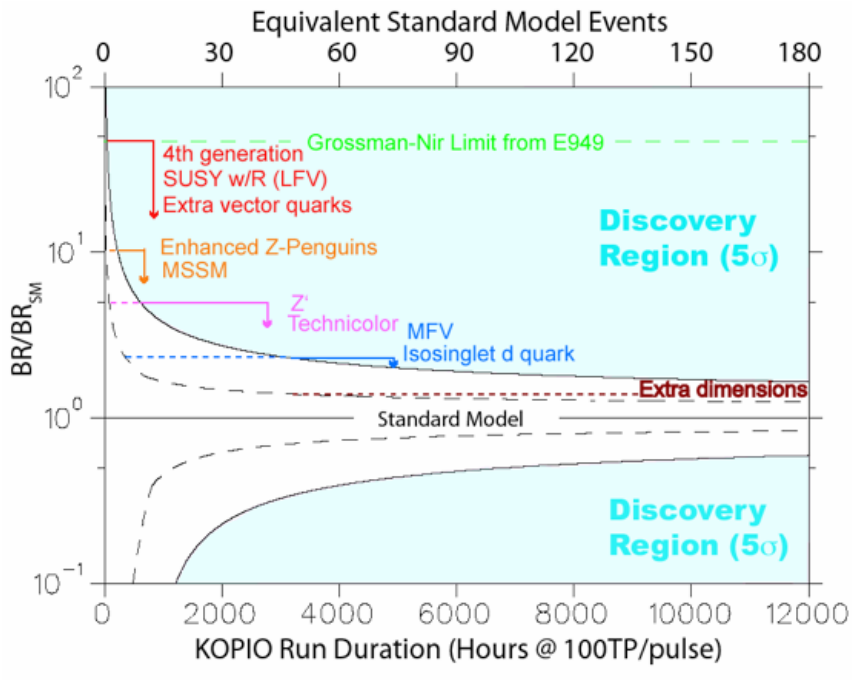

Figure 5.6 Reach of KOPIO experiment (as of 2005) as a function of running time. Solid lines show the 5σ limits in terms of branching ratio relative to that of the Standard Model (SM). Dashed lines show the corresponding 3σ limits. "Equivalent Standard Model Events" means the number of SM events with no background that would have equivalent reach.

5.2.2. $K_L^0 \to \pi^0 \nu \bar{\nu}$ at Fermilab

Given the possible progression of 8 GeV intensity at Fermilab from the existing Booster complex to Project X beams, a low-energy $K_L^0 \to \pi^0 \nu \bar{\nu}$ experiment is a very appealing possibility. As will be discussed below, an experiment at the SM-level precision ~3% (7-10%) appears feasible for Project X (Booster intensity) beams. Perhaps the most attractive approach is a version of the low energy experiment in which the beam aperture is substantially reduced compared to KOPIO. This would allow the experiment to benefit greatly from any increase in the available proton flux. Moreover it would be much easier to mount, and more robust than KOPIO. The large beam aperture was a factor that made KOPIO as technically challenging as it was due to the very large, very thin vacuum chamber required.

To make estimates of the sensitivity achievable at Fermilab, we assume based on simulations that the effective cross section at 8 GeV is half of that at 21 GeV and compare with projections for the experiment proposed at BNL. In terms of available protons, we also assume Booster performance of 22.5 x 10^{12} every 1.4 second where the average proton flux per second is 16.1 x 10^{12} which is 60% that assumed at BNL; when factors relating to accidental losses are taken into account the ratio of effective kaons per second is 0.93. When Project X beams are available at 10 times the intensity of the Booster, significant further progress in precision can be made although the technique is eventually limited by instantaneous rates of various types (accidental spoiling of events by other kaon decays in the same microbunch, accidentals due to stopped muons, accidentals due to neutron interactions in the beam veto, etc.). Figure 5.7 shows the effective yield relative to that for the Booster, as a function of the relative proton intensity available for the KOPIO beam geometry. Using three times Booster intensity provides the maximum gain. Based on parameter variations studies, one could benefit significantly by improving on the resolutions.

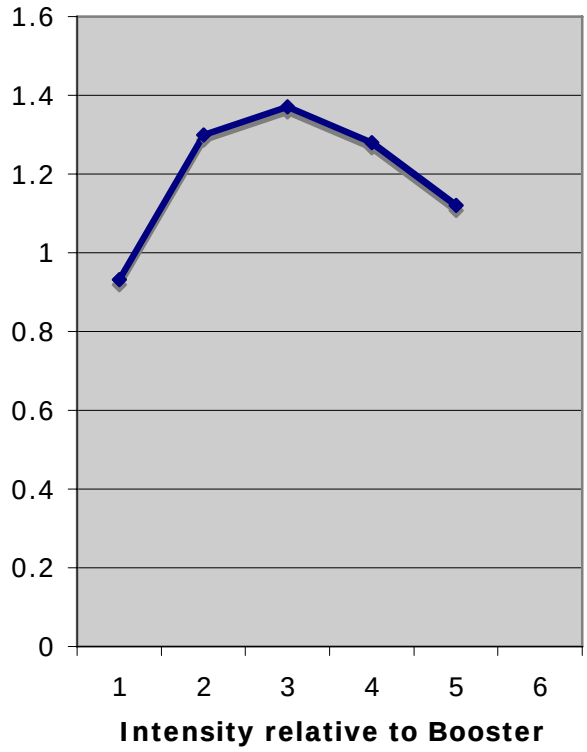

Figure 5.7 Relative effective yield of a KOPIO-type experiment at Project X, as a function of the ratio of the proton intensity relative to that available at the Booster.

A possible approach for a Fermilab $K_L^0 \to \pi^0 \nu\bar{\nu}$ is to put the entire experiment in vacuum and to use a small symmetric beam aperture. Placing all detectors in vacuum would remove the difficult thin vacuum vessel but would require vacuum operation of the preradiator photon tracking chambers. Reducing the size of the beam would make the experiment much less difficult. Many mechanical issues would be made easier and the experiment could be reconfigured to have a considerably higher acceptance. Moreover, many types of background would be diminished or eliminated. As mentioned above, the spoiling of event candidates by additional decays in the same μ-bunch would be much reduced. The loss in effective statistics due to the small beam acceptance would be somewhat mitigated because of the reduction in accidentals, and in spoilage by additional events in a μ-bunch. However, the reconfiguration of the experiment that this geometry allows could result in an increase in geometric acceptance of a factor 2 or even more. Assuming improvements up to a factor 4.3 for the best events (S/B ~ 8) and 1.7 for medium quality events (S/B ~ 2) a statistical precision of 10% may be reached at the Booster intensity level in a 5 year run. At initial Project X intensity (10 x Booster intensity), 300 equivalent events would be observed per year which allows a 3% measurement to be made for $K_L^0 \to \pi^0 \nu\bar{\nu}$. The sensitivity of the experiment would continue to increase if more proton intensity were available. At 60 times the Booster intensity there would be ~900 equivalent events per year. As shown in Figure 5.8, this is

the peak sensitivity that could be reached given the above assumptions although optimization promises to provide further gains.[3]

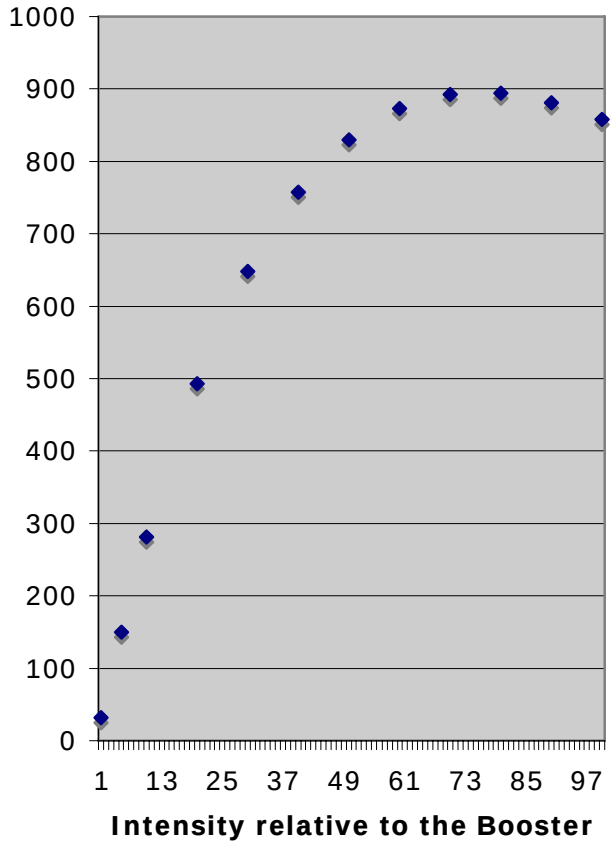

Figure 5.8 Equivalent events per year for a small aperture, low energy experiment as a function of the proton intensity.

5.3 Prospects for Measuring $K^+ \to \pi^+ \nu\bar{\nu}$ at Fermilab

Definitively measuring $K^+ \to \pi^+ \nu\bar{\nu}$ decay at the 10^{-10} branching ratio level represents a significant experimental challenge. The poorly defined signal consists of a charged kaon followed by a charged pion, $K^+ \to \pi^+$, with no other observed particles. Potential

[3] Note that the potential of such a detector has not been fully explored. The reduction of beam aperture has profound effects on many aspects of the experiment. To give an example, KOPIO's acceptance was reduced by randoms in the beam "catcher" veto, and by the fact that the initial "flash" of photons from the μ-bunch tended to blind the veto for a few ns. To achieve this recovery speed, it was necessary to insert a 7 cm Pb absorber in the upstream beam. Simulation indicated that the beam veto could be made redundant at the cost of tightening the kinematic cuts to the point where 20% of the acceptance was lost. This cost would clearly be very much smaller for a twenty-fold smaller beam. If the beam veto were removed, there would be no need for the photon absorber, increasing the kaon flux by nearly a factor 2, and eliminating a major source of scattering of beam neutrons. This in turn reduces random veto effects and allows the detection elements to be moved closer to the beam, thus increasing the geometric acceptance. This is only one example among many of the advantages of this configuration.

backgrounds, primarily from other K decays at branching ratios 10 orders of magnitude higher, have similar signatures. Therefore, the experimental strategy involves proving that candidate events have low probabilities of being due to background. The principal sources of background are shown in Figure 5.9. To be successful at detecting $K^+ \to \pi^+ \nu\bar{\nu}$ and separating it from background, the detector must have powerful π^+ identification so that $K^+ \to \mu^+ \nu \left(K_{\mu 2}\right)$ and $K^+ \to \mu^+ \nu\gamma \left(K_{\mu 2\gamma}\right)$ decays can be rejected, highly efficient 4π solid angle photon detection coverage for vetoing $K^+ \to \pi^+ \pi^0 \left(K_{\pi 2}\right)$ events and other decays, and an efficient K^+ identification system for eliminating beam-related backgrounds.

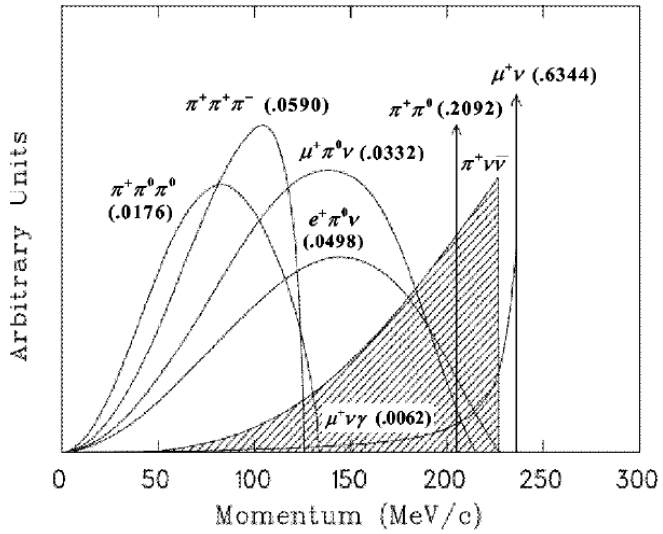

Figure 5.9 Momentum spectra (in MeV/c) of charged particles from K^+ decays in the rest frame. The values in the parentheses represent the branching ratios of the decay modes. The hatched spectrum shows the π^+ momentum from $K^+ \to \pi^+ \nu\bar{\nu}$ decay assuming the V − A interaction.

BNL E949 (which was upgraded from E787) was the culmination of long series of stopped kaon experiments searching for $K^+ \to \pi^+ \nu\bar{\nu}$ spanning 50 years. Like its predecessors, it employed a low momentum beam of stopping kaons. E949 used a 710 MeV/c K^+ beam which was slowed in a degrader and stopped in a scintillating fiber detector. Measurement of the $K^+ \to \pi^+ \nu\bar{\nu}$ decay involved observation of the daughter π^+ in the absence of other coincident activity. The π^+ was identified by its kinematic features obtained from energy in scintillator calorimeter, momentum, and range measurements. In addition, E949 used high-speed digitizers on all fast detectors to make precise observations of the complete $K^+ \to \pi^+ \to \mu^+ \to e^+$ decay sequence. The entire E949 spectrometer was surrounded by a 1 T solenoidal magnetic field along the beam direction. In addition to the use of scintillating fibers and the large systems of 500 MHz digitizers, the challenges of E949 spurred the development of the world's most efficient detector of radiation and the invention and development of a version of blind analysis methodology to avoid bias in background predictions and analysis of data. The numerous sources of potential background were extensively studied in E787 and E949 resulting in reliable and testable background predictions and a likelihood analysis method for evaluating potential

candidate events for probability of being due to $K^+ \to \pi^+ \nu\bar{\nu}$ or background. For the entire data sets from the E787/E949 experiments the number of background events expected was considerably less than 1 event.

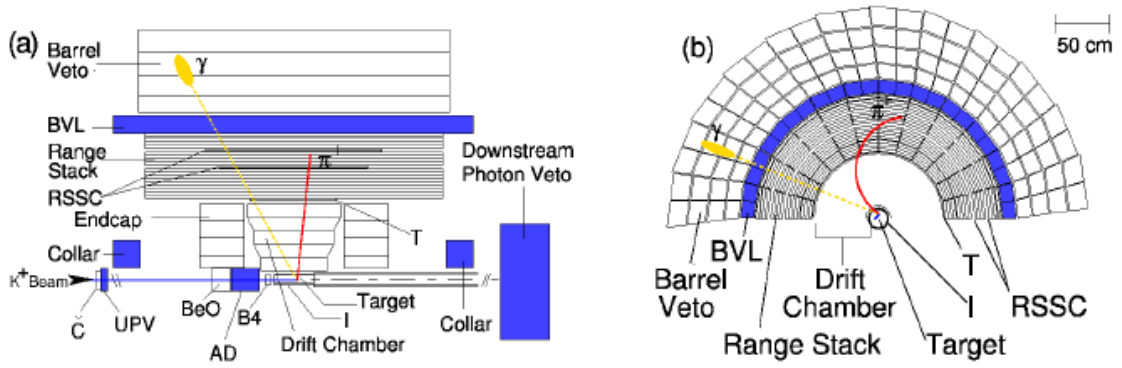

Figure 5.10 Schematic side (a) and end (b) views of the upper half of the E949 detector. Illustrated in this figure, an incoming K+ that traverses all the beam instruments, stops in the target and undergoes the decay $K^+ \to \pi^0\pi^+$. The outgoing π+ and one photon from $\pi^0 \to \gamma\gamma$ are also shown.

Three events consistent with $K^+ \to \pi^+ \nu\bar{\nu}$ decay were observed by E787 and E949 in the momentum region $211 \le P \le 229$ MeV/c as shown below in Figure 5.11. The branching ratio observed was $\mathrm{B}(K^+ \to \pi^+ \nu\bar{\nu}) = (1.47^{+1.30}_{-0.89}) x 10^{-10}$. The estimated probability that all the $K^+ \to \pi^+ \nu\bar{\nu}$ candidates observed by E787 and E949 were due to background was 0.001. The measured branching ratio was twice as large as the SM prediction of $\mathrm{B}(K^+ \to \pi^+ \nu\bar{\nu}) = (0.74 \pm 0.20) x 10^{-10}$ but was consistent within the uncertainty. Limits were obtained from E787 data for the phase space region below the $K_{\pi 2}$ peak, and E949 data are still under analysis. E787 and E949 also studied many other rare K decay processes and provided the most sensitive searches for several non-Standard Model processes such as $K^+ \to \pi^+ a$ where a is an axion.

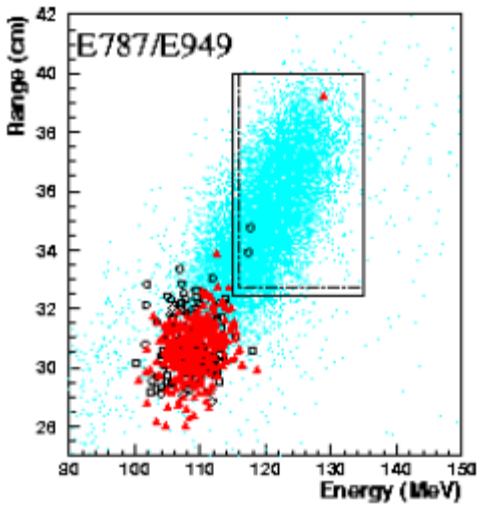

Figure 5.11 Range vs kinetic energy of the events satisfying all of the cuts, except for the phase space cuts on both the range and energy. The plot shown combines E787 and E949 data. The inner rectangle represents the signal region defined in E787 (dashed lines) and E949 (solid lines). Events near *E* = 108 MeV were due to $K_{\pi 2}$ decays which were not removed by the photon veto cuts. The light points represent the expected distribution of $K^+ \to \pi^+ \nu \bar{\nu}$ events from simulation.

The CERN NA62 experiment proposes to take the next step in sensitivity of up to 80 SM events with a promising high energy in-flight decay experiment. Other ultra-rare in-flight decay experiments such as the search for $K_L \to \mu e$ have obtained very high sensitivities, but the new techniques proposed for the high sensitivity $K^+ \to \pi^+ \nu \bar{\nu}$ in-flight experiment have yet to be demonstrated.

In order to evaluate the potential of a new stopping kaon experiment driven by 8 GeV beams potentially available at the Fermilab Booster (16 kW) and upgraded to Project X (205 kW), we will extrapolate from the experience of E949 taking advantage of the potential for incremental improvements in a well-established technique. All estimates are made relative to the expectations for E949 at the BNL AGS.[4] For the Fermilab experiments, it is assumed that kaon beams of lower momentum, e.g. 450-400 MeV/c will be used instead of the 710 MeV/c used by E949, in order to improve the kaon stopping efficiency to approximately 70% from 20% in E949. In addition, the following assumptions were made:

- **Project X primary beam properties.** It is assumed there will be $2.25\ 10^{14}$ p/1.4s (10 x higher than for the existing Booster complex) available at 8 GeV for 5000 hrs./yr. with a 100% duty factor.

- **K Production Cross Sections at 8 GeV.** *K* production cross sections at 0 degrees for 8 GeV protons relative to 21.5 GeV protons were estimated using several codes. The values for 8 GeV yields at 450 and 400 MeV/c relative to those for 21.5 GeV at 710 MeV/c were estimated to be 0.16 and 0.11.

[4] See E949 proposal. Actual operation of E949 was prematurely stopped by DOE after one short run.

- **Kaon beam line:** A separated beam of 13 m length with acceptance of 25 msr was assumed for operation at 450 MeV/c $\pm 7\%$. This would be a gain of a factor of about 2 in solid angle acceptance and 1.2 in momentum acceptance relative to LESB3 at the AGS used by E949.

- **Detector Improvements.** For the Fermilab experiments, a momentum spectrometer with a 2-3 T magnetic field will be assumed allowing the detector to be considerably smaller in diameter than the E949 detector; the detector can also be made longer to increase the momentum acceptance. A detector of reduced radius will facilitate many improvements in performance: 1) The small overall acceptance attained by E949, approximately 0.002, was due in part to the necessity for tight cuts suppressing muon backgrounds; isolated accidentals in the range stack (RS) counter where the pion stopped could fake the second pulse in the $\pi \to \mu \to e$ decay sequence. Using much finer segmentation of the RS (e.g. 5 mm x 5 mm elements instead of the 20 mm x 200 mm counters of E949) this background source would be suppressed by a factor of 100 allowing a significant improvement in acceptance. Fine segmentation of the RS will also facilitate improvements in π^+ tracking; 2) It will be assumed that 2x better momentum resolution can be obtained due to the higher field. This will make 2-body background rejection easier and result in acceptance gains; 3) The smaller detector will allow use of a higher quality non-sampling photon veto detector such liquid xenon with more radiation lengths than in E949. This will also result in better background rejection and higher acceptance. Overall, an acceptance gain of 2.5 will be assumed.

- A**ccidental losses.** Accidental losses (killing of valid events) due to extraneous hits in the photon veto system were substantial in E949. These accidental losses appeared to scale with the incident flux, or kaon energy E_k lost by beam kaons which did not stop in the E949 target; although there was some accidental spoiling from old $\mu \to e$ decays it appears that most of the losses were due to kaons which interacted in the E949 absorber producing neutral particles interacting in the RS. Applying this model to the Fermilab experiments which would be run at much lower momenta with consequently much higher stopping efficiency, accidental spoiling would be much less of a problem resulting in only small acceptance losses.

Based on the assumptions above and five years of operation, the number of events to be expected for Fermilab experiments using the 8 GeV Booster intensity and the projected Project X (206 kW) beams would be approximately 200 and 1300, corresponding to an anticipated precision, including projected background subtraction, of approximately 10% and 3% respectively. Further improvements in precision could be anticipated if the beam power were to increase.

5.4 Kaon Strategy

The kaon experimental strategy consists of developing a set of world-class experiments that evolve into world-leading experiments in a phased approach with ever increasing beam intensities and relatively modest detector upgrades. The physics reach of this program compared to other world-wide programs is tabulated below. The world-class experiments can be driven with an 8 GeV Booster beam, followed by world-leading experiments driven by Project X beam. This evolution is illustrated in the road-map. The road-map and table below includes the possibility of 120 GeV Main Injector beam driving higher energy kaon experiments that are not discussed here, but could play an important role if the schedule for Project X is substantially delayed.

Facility	Duty Factor	Clock hours	Beam hours	Projected # of K → πνν per year
CERN-SPS (450 GeV)	30%	1420	405	40 (charged)
FNAL: Booster Stretcher (8GeV, 17kW)	90%	5550	5000	40 (charged)
FNAL: Main Injector-Tev-Stretcher (120 GeV)	90%	5550	5000	200 (charged)
FNAL: Project X Stretcher (8GeV, 200kW)	90%	5550	5000	250 (charged)
JPARC-I (30 GeV)	21%	2780	580	*~1 (neutral)
BNL AGS (24 GeV)	50%	1200	600	20 (neutral)
JPARC-II (30 GeV)	21%	2780	580	*30 (neutral)
FNAL: Booster Stretcher (8GeV, 17kW)	90%	5550	5000	30 (neutral)
FNAL: Project X Stretcher (8GeV, 200kW)	90%	5550	5000	300 (neutral)

*For JPARC, we assume that neutrino and kaon programs share the beam (50% - 50%).

Developing a Common Platform

The charged and neutral kaon experiments driven by an 8 GeV beam could likely share a common target station, possibly without compromising flux for either experiment, thereby easing proton economics. These experiments share experimental and theory proponents, beam and detector technology issues, design and analysis techniques. The proponents could naturally self-organize into a common collaboration that would be best suited to develop the details of the Fermilab kaon roadmap matched to various resource profiles. (This collaboration would be robust against variations in the relative schedule between the charged and neutral programs that could arise through limited-resource staging pressures or the state of world-wide competition.) A plausible scenario is the relatively early start of the $K^+ \to \pi^+ \nu\bar{\nu}$ experiment that benefits from the BNL E787/E949 recent experience, followed by a start for the $K_L^0 \to \pi^0 \nu\bar{\nu}$ experiment which ultimately may be more incisive but may benefit from additional R&D. The resources required for construction and early start of the charged program are likely less than the

neutral program, and the $K^+ \to \pi^+ \nu\bar{\nu}$ experiment does not require the micro-bunching RF beam structure necessary for the neutral experiment.

A cohesive approach also leverages the usefulness of these modes to understanding new short-distance physics. Although each mode is interesting in its own right, the combination of both measurements provides an incisive test of flavor violation mediated by new particles, such as those that may be observed at the LHC.

The R&D Phase Today through 2010:

The next generation $K^+ \to \pi^+ \nu\bar{\nu}$ experiment will benefit from the past decade of HEP detector R&D that has made major strides in very low-mass tracking, calorimetry and data acquisition. One year of design effort will be necessary to transfer these R&D dividends to the next generation experiment based on the stopped kaon technique. For the $K_L^0 \to \pi^0 \nu\bar{\nu}$ experiment new detector technologies have emerged recently, in particular, charged particle tracking in vacuum, which may substantially improve the performance of the experiment. R&D will be necessary to exploit these recent developments and to design the $K_L^0 \to \pi^0 \nu\bar{\nu}$ experiment so that it can take full advantage of the Project X intensity. In parallel with development of the detector projects, the 8 GeV slow-spill source, RF structure, target station and beamlines must be developed.

The Phase-I Construction and Operation Phase, 2011-2018:

Both the $K^+ \to \pi^+ \nu\bar{\nu}$ and $K_L^0 \to \pi^0 \nu\bar{\nu}$ experiments will be multi-year construction efforts. As previously noted, construction of the $K^+ \to \pi^+ \nu\bar{\nu}$ experiment could plausibly start earlier and be shorter in duration. Early results from either the JPARC neutral experiment or the CERN charged experiments, if they take place, could inform staging, particularly if an anomalous signal is seen. New physics seen at the LHC in this time-frame may also influence the sequence of events leading to these experiments.

Transitioning to Project X intensity 2018-2020:

Both experiments will be designed at the outset to exploit the intensity upgrade of Project X. It is likely however that some upgrades to the detectors and beamlines will be necessary for this step. After this transition the $K^+ \to \pi^+ \nu\bar{\nu}$ and $K_L^0 \to \pi^0 \nu\bar{\nu}$ experiments will lead the field and will be in a position to deliver very high sensitivity. During this phase, both experiments will detect O(1000) events (at the Standard Model rate). The resulting 3% precision is well matched to the theoretical and parametric uncertainties expected at this time. These measurements, with their well-understood theoretical description, will be needed to help distinguish between competing models that accommodate the TeV-scale discoveries of the LHC.

5.5 Kaon Summary

Precise measurements of the rare decays $K^+ \to \pi^+ \nu\bar{\nu}$ and $K_L^0 \to \pi^0 \nu\bar{\nu}$ are essential for a deeper understanding of the mechanism of flavor mixing and *CP* violation. Among the many rare *K*- and *B*-decays, the $K \to \pi\nu\bar{\nu}$ modes are unique: they are highly sensitive to new physics at mass scales up to *O*(1000) TeV, and their Standard Model rates can be computed to exceptionally high degrees of precision, not matched by any other flavor-changing neutral current process involving quarks. Fortunately, precise measurements of $K^+ \to \pi^+ \nu\bar{\nu}$ and $K_L^0 \to \pi^0 \nu\bar{\nu}$ at the few per cent precision (at the SM levels) appear to be feasible at Fermilab beginning with the 8 GeV Booster level intensity and progressing to the use of the intense beams of Project X. The charged mode $K^+ \to \pi^+ \nu\bar{\nu}$ has already been observed at BNL and an evolution of the well established technique would confidently yield a high statistics result. Observation of the more challenging neutral mode would be pursued using a carefully studied proposed method involving neutral *K* time-of-flight for suppression of backgrounds; beginning at the Booster intensity level and progressing to Project X would also yield a clean high sensitivity result. The combination of these high precision measurements on $K \to \pi\nu\bar{\nu}$ and decays, in conjunction with complementary proposed efforts at CERN and JPARC, would result in a powerful contribution to the interpretation of possible new physics appearing at the LHC or at much higher mass scales.

6 Charm Mixing and *CP* Violation Program at the Tevatron

Over the past year the Belle and Babar experiments have published evidence for mixing in the D^0 system (Belle Collaboration, Phys. Rev. Lett. 98, 211803, 2007, and Babar Collaboration, Phys. Rev. Lett. 98, 211802, 2007). The CDF experiment has also presented evidence for this effect (CDF Collaboration, arXiv:0712.1567; submitted to Phys. Rev. Lett.). These measurements indicate a relatively large value for the mixing parameter y of ~1%; for $x = \Delta M/\Gamma$, a statistically significant nonzero value is obtained from a fit combining all measurements of D^0 mixing parameters (http://www.slac.stanford.edu/xorg/hfag/charm/Beijing07/results_mix+cpv.html). If the values of x and y turned out to be larger than SM predictions, or if $x >> y$, new physics would be indicated. To search for *CP*-violating effects, x and y can be measured separately for D^0 and antiD^0 decays. *CP* violation is parameterized by the ratio of the complex coefficients relating flavor eigenstates to mass eigenstates, $|q/p|$, and by a possible weak phase $\phi = \mathrm{Arg}(q/p)$. Differences in $|q/p|$ and ϕ from 1 and 0, respectively, would indicate new physics. Figure 3.4.1 (left) shows the current Heavy Flavors Averaging Group (HFAG) confidence contours for $|q/p|$ and ϕ (http://www.slac.stanford.edu/xorg/hfag/charm/Beijing07/results_mix+cpv.html). The central value is one standard deviation away from the no-*CP*-violation point.

There has been a series of fixed-target charm experiments performed at Fermilab using both photon and hadron beams. Technological advances that have occurred since those experiments ran (*e.g.*, in radiation-hard tracking, triggering, and computing) could greatly increase the sensitivity of such experiments. It is now feasible to trigger on decay vertices at the first or second level. The latter was realized by the HERA-B experiment at DESY, and the former was planned for the BTeV experiment at the Tevatron. Such a trigger would allow an experiment to run at much higher interaction rates than previously, and thus greatly increase the number of recorded charm decays. Recently, some work has begun to study the feasibility of a fixed-target-geometry experiment running at the Tevatron. The goal would be to measure the mixing parameters x and y and *CP*-violating parameters $|q/p|$ and ϕ with very high statistics. Below we estimate the expected sensitivity and compare it to that expected for e^+e^- experiments Belle and Babar. We also briefly discuss prospects for LHCb.

6.1 Expected Sensitivity

We scale our sensitivity estimate from that of HERA-B. This experiment reconstructed 61.3 +/– 13 "D^*-tagged" Cabibbo-favored $D^0 \rightarrow K^-\pi^+$ decays in 182 x 10^6 hadronic interactions (HERA-B Collaboration, Eur. Phys. Jour. C 52, 531, 2007). Multiplying this yield by the ratio of partial widths $\Gamma(D^0 \rightarrow K^+\pi^-) / \Gamma(D^0 \rightarrow K^-\pi^+) = 0.377\%$ gives a $D^0 \rightarrow K^+\pi^-$ fractional yield (including trigger and reconstruction efficiencies) of 1.3 x10^{-9}. If we assume a future fixed-target experiment runs at a 5 MHz interaction rate (as achieved by HERA-B), then in one year of running the experiment could potentially reconstruct (5 MHz)(2 x 10^7 s)(1.3 x 10^{-9})(0.5) = 64,000 tagged $D^0 \rightarrow K^+\pi^-$ decays, where we have assumed a trigger efficiency of 50% relative to that of HERA-B. We can also scale from the E791 experiment, which reconstructed ~35 D^*-tagged $D^0 \rightarrow$

$K^+\pi^-$ decays in ~5 x 10^{10} hadronic interactions (E791 Collaboration, Phys. Rev. D 57, 13, 1998). These values imply a fractional yield of 7 x 10^{-10}, and thus an absolute yield of 35,000 events per year. Here we have assumed a trigger and selection cut efficiency of 50% relative to that of E791. This assumption is conservative, as E791 had a deadened region in the center of the drift chambers where the 500 GeV π^- beam passed through. If we assume a reconstruction efficiency similar to that of the FOCUS photoproduction experiment, we obtain a yield of ~70,000 events per year.

To compare with the *B* factories, we note that Belle has reconstructed 4024 D^*-tagged $D^0 \rightarrow K^+\pi^-$ candidates in 400 fb^{-1} of data (Belle Collaboration, Phys. Rev. Lett. 96, 151801, 2006). If the *B* factories were to run until an aggregate sample of 1500 fb^{-1} were collected, they would have a total of 15,000 $D^0 \rightarrow K^+\pi^-$ decays, only 1/4 to 1/2 of our estimate for a fixed-target experiment after one year of running. Three years of fixed-target running could provide more than an order-of-magnitude more decays, substantially increasing the sensitivity to *x* and *y*. This is just one example of the mixing and *CP* measurements possible. It should also be noted that a fixed-target experiment would have much better lifetime resolution than that of the *B*-factory experiments. This would reduce backgrounds and also systematic errors in time-dependent measurements.

To compare to LHCb, we use numbers from a Monte Carlo study of the sensitivity of LHCb to $D^{*+} \rightarrow D^0\pi^+_{tag} \rightarrow K^+\pi^-\pi^+_{tag}$ decays (LHCb public note LHCb-2007-049, July 10, 2007). Assuming σ_{bb} = 500 μb, and estimating various trigger and reconstruction efficiencies, this study concludes that 58,000 "wrong-sign" signal decays would be reconstructed in one year of running (2 fb^{-1}). This yield is similar to our estimate above for a Tevatron experiment. However, there are important differences between LHCb and a Tevatron experiment:

- LHCb would use D^*'s produced in *B* decays rather than prompt D^*'s, as the trigger is efficient only for the former. However, there will be a substantial number of prompt D^*'s selected that will affect the decay time distribution and thus must be accounted for; this may not be straightforward. A Tevatron fixed-target experiment would produce (essentially) only prompt D^*'s.

- To reconstruct the D^* decay vertex position (which is the D^0 birth position), LHCb must partially reconstruct a $B \rightarrow D^*X$ decay. The efficiency for this is estimated from MC simulation to be 51% (Table 15 of LHCb public note LHCb-2007-049, July 10, 2007), but this factor is not known and may be smaller. At a fixed-target experiment, the D^* vertex position is at the target (and known with high precision).

- The trigger electronics for a future Tevatron experiment would be at least one generation more advanced than that of LHCb.

To estimate the sensitivity of a Tevatron experiment, we use the fact that the expected signal yield, background level, and decay time resolution are similar to those assumed for LHCb. The LHCb study found that the statistical errors on mixing parameters x'^2 and y'

for 232,500 reconstructed signal decays would be 8.1 x 10^{-5} and 1.1 x 10^{-3}, respectively (assuming a signal-to-background ratio of 0.20). This yield corresponds to 3.6 years of running of a Tevatron experiment. Using these statistical errors in a global fit to present measured values of observables (and also correspondingly reducing the statistical error on y_{CP}, which a Tevatron experiment would also measure), we obtain the contour plot shown in Figure 3.4.1(right). This plot has much smaller allowed regions for $|q/p|$ and ϕ than does the current world average plot (Figure 3.4.1, left).

6.2 Experimental Strategy

A Tevatron charm mixing + *CP* violation experiment could play an important and unique role in future flavor physics measurements. If a Super-*B* factory were not built, then the only other experiment able to make these measurements would be LHCb, and, as discussed above, it is uncertain what their sensitivity to mixing will be. The BES-III experiment at IHEP has sensitivity to $R_M = x^2+y^2$ and y via correlated D branching fractions measured in $\psi(3770) \rightarrow DD$ decays (D. M. Asner and W. M. Sun, Phys. Rev. D 73, 034024, 2006; hep-ph/0507238,v4), but the D's are essentially at rest, so time-dependent measurements are not possible. A Tevatron fixed-target experiment could provide an order-of-magnitude more sensitivity than will result from the current generation of *B*-factory experiments. This region is of particular interest for physics beyond the SM that could be discovered at the Tevatron Collider or at the LHC.

Following the shutdown of the Tevatron collider program, it would be opportune to proceed with a diverse Tevatron fixed-target program of neutrino experiments and slow-spill experiments. In such a scenario, a major component of the slow-spill program could be a very high statistics charm mixing + *CP* violation experiment. We believe it would be timely to begin studying and designing such an experiment now, such that an experimental program could follow the shutdown of the collider program in an efficient manner.

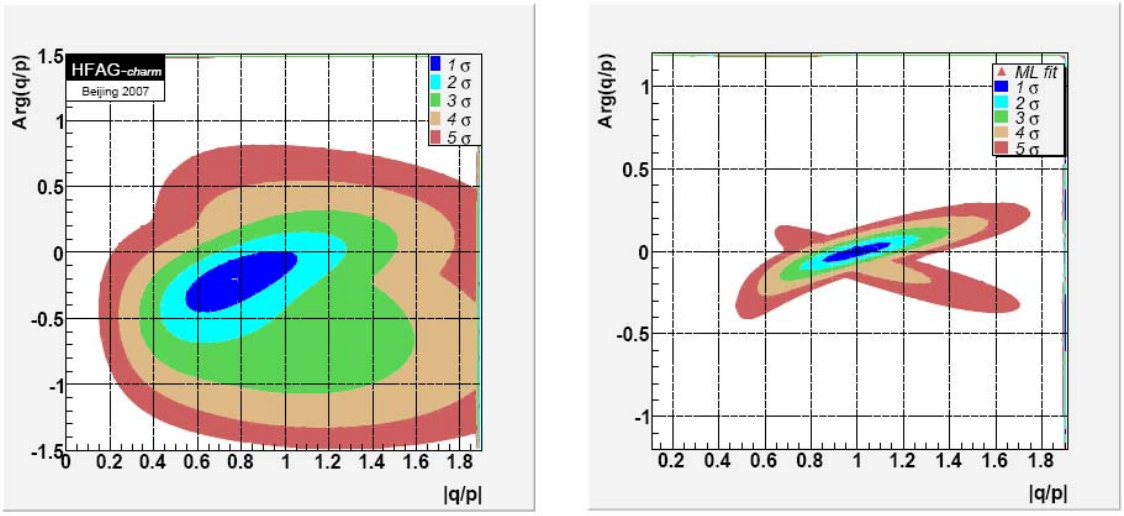

Figure 3.4.1 Contour plots for *CP*-violating parameters $|q/p|$ and ϕ. Left: using current measured values and errors. Right: reducing the error bars for y_{CP} and the Belle $D^0 \rightarrow K^+\pi^-$ result for x'^2 and y' according to the LHCb MC study.

7 Physics with Antiprotons

With its intense cooled antiproton beam, Fermilab can explore issues in QCD, search for new physics using hyperons and charmed mesons, and pursue unique investigations of the properties of antihydrogen. Project X will improve Fermilab's "proton economics," enhancing the ability for this physics to be pursued in parallel with the initiatives described elsewhere in this report.

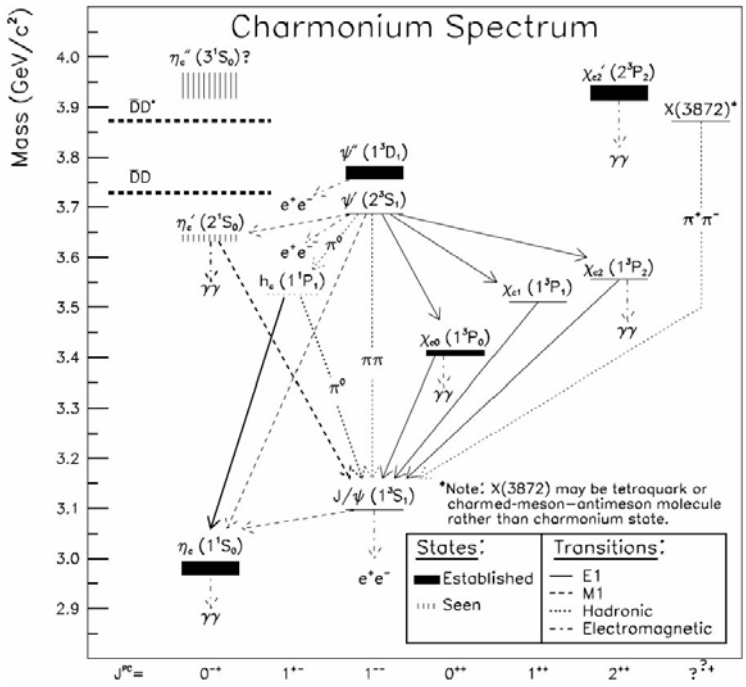

The theory of the strong interaction plays an important role in allowing us to infer the flavor physics of quarks and extract the quark mixing matrix from observations made on hadrons. Heavy-quark–antiquark bound states ("quarkonia") offer a unique testing ground for QCD. Both potential-model and lattice-gauge Monte Carlo techniques have had success in predicting aspects of heavy-quark systems. Quenched-approximation lattice-QCD predictions of the masses of low-lying charmonium states are already in qualitative agreement with the experimental values, and agreement at the few-percent level is now becoming possible using dynamical quarks on the lattice. The charmonium system (depicted in the figure) is an important proving ground for QCD calculations in that the bound c and $\bar{c}$ quarks are moving slowly enough that relativistic effects are significant but not dominant, and are sufficiently massive that non-perturbative effects are well understood. After certification by comparison with experiment, these techniques can then be confidently applied in interpreting such physics results as *CP* asymmetries in the beauty system.

Physics topics that can be addressed with an antiproton facility include

- precision $\bar{p}p \rightarrow$ charmonium studies;
- elucidation of several "mystery states" in the charmonium region;
- studies of open charm, including measurements of $D^0 / \bar{D}^0$ mixing and searches for *CP* violation;
- hyperons, including searches for hyperon *CP* violation and studies of rare decays;
- the search for glueballs and gluonic hybrid states predicted by QCD; and
- trapped-$\bar{p}$ and antihydrogen studies.

The anticipated shutdown of the Tevatron in 2009 presents the opportunity for a world-leading antiproton physics program. To maximize the Tevatron Collider luminosity, Fermilab has developed the world's most intense (as well as highest-energy) antiproton source. At CERN, the LEAR antiproton storage ring was decommissioned in 1996 to make way for the LHC. Its successor facility, the Antiproton Decelerator (AD), provides antiproton beams at momenta of 100 and 300 MeV/c, at intensities up to $\approx 2 \times 10^7$ per minute. Of the topics listed above, the CERN AD is pursuing the last one. Germany's ≈billion-Euro upgrade plan for the GSI-Darmstadt nuclear-physics laboratory includes construction of 30 and 90 GeV rapid-cycling synchrotrons for protons and radioactive beams as well as low- and medium-energy antiproton storage rings, which are planned to start operating in 2016. Even after this Facility for Antiproton and Ion Research (FAIR) comes on line, the antiproton production capability of the Fermilab Antiproton Source will remain unequalled. All of the listed topics have been discussed as components of the physics program of the GSI-FAIR project with many covered by its general-purpose PANDA detector. Many of them are within the energy range of the Accumulator (see table) and can be pursued more rapidly at Fermilab.

Process	Threshold $\sqrt{s}$ (GeV)	Threshold $p_{\bar{p}}$ (GeV/c)
$\bar{p}p \to \bar{\Lambda}\Lambda$	2.231	1.437
$\bar{p}p \to \bar{\Sigma}^-\Sigma^+$	2.379	1.854
$\bar{p}p \to \bar{\Xi}^+\Xi^-$	2.642	2.620
$\bar{p}p \to \bar{\Omega}^+\Omega^-$	3.345	4.938
$\bar{p}p \to \eta_c$	2.980	3.678
$\bar{p}p \to \psi(3770)$	3.771	6.572
$\bar{p}p \to X(3872)$	3.871	6.991
$\bar{p}p \to X \text{ or } Y(3940)$	3.940	7.277
$\bar{p}p \to X \text{ or } Y(4260)$	4.260	8.685

In the charmonium region, the list includes a number of intriguing recent discoveries: the states provisionally named $X(3872)$, $X(3940)$, $Y(3940)$, $Y(4260)$, and $Z(3930)$. In addition, the h_c, η_c, and η_c' masses and widths, χ_c radiative-decay angular distributions, and η_c' $(2S)$ radiative widths, important parameters of the charmonium system that remain to be precisely determined, are well suited to the $\bar{p}p$ technique. As discussed later, the recent observation of apparent flavor-changing neutral currents in hyperon decay can also be investigated; indeed, high sensitivity can be achieved to rare and symmetry-violating hyperon decays generally.

Fermilab experiments E760 and E835 made the world's most precise ($\lesssim 100$ keV) measurements of charmonium masses and widths. This was possible thanks to the extra-ordinarily narrow energy spread of the stochastically cooled antiproton beam and the absence of Fermi motion and negligible energy loss in the hydrogen cluster-jet target. The other key advantage of the antiproton-proton annihilation technique is its ability to produce charmonium states of all quantum numbers, in contrast to e^+e^- machines, which produce primarily 1^- states and the few states that couple directly to them, and (with relatively low statistics) states accessible in B decay or in 2γ production.

We propose an experimental program aimed at those measurements for which the Fermilab Antiproton Source is best suited: (1) precision studies of states in the charmonium region, (2) the search for new physics in hyperon decay, (3) the search for new physics in charm mixing and CP violation, and (4) precision studies of antihydrogen.

Many of these measurements can be performed with a common apparatus using existing, well-developed experimental technologies. Depending on the resources that will be available, existing detector components might be recycled for these purposes; alternatively, modest expenditures for new equipment could yield improved performance.

7.1 Capabilities of the Fermilab Antiproton Source

The Antiproton Source now cools and accumulates antiprotons at a stacking rate of $\approx 2 \times 10^{11}$ antiprotons/hr. Given the 60 mb annihilation cross section, it could thus support in principle a luminosity up to about 5×10^{32} cm^{-2} s^{-1}, with antiproton stacking $\approx 50\%$ of the time and collisions during the remaining $\approx 50\%$. However, we anticipate operating at $\lesssim 2 \times 10^{32}$ cm^{-2} s^{-1}, which allows $\gtrsim 80\%$ duty cycle, poses less of a challenge to detectors and triggers, and requires a smaller fraction of the protons from the Main Injector. An order of magnitude above the typical E835 luminosity of 2×10^{31} cm^{-2} s^{-1}, this assumes increased target density, possible via various approaches: an improved cluster jet, a wire or pellet of plastic or metal in the beam halo, a solid-hydrogen target on the tip of a cold finger, or a stream of solid-hydrogen pellets.

Comparison of running conditions and antiproton yields for FNAL after the Tevatron program and possible new facilities at FNAL and GSI are presented in the table below.

Facility	Stacking Rate (10^{10}/hr)	Stacking duty factor	Clock hours	Yearly antiprotons produced (10^{13})
FNAL Accumulator Experiment	20	15%	5550	17
FNAL New Ring Experiment	20	90%	5550	100
GSI FAIR	3.5	90%	2780	9

7.2 Physics Goals

To clarify the issues for a future low-energy antiproton facility, we next consider a few representative physics examples: studying the mysterious $X(3872)$ state, improved measurement of the parameters of the h_c, searching for hyperon *CP* violation, and studying a recently discovered rare hyperon-decay mode. (This is of course far from an exhaustive list of the topics to be studied.)

7.2.1 X (3872)

The $X(3872)$ was discovered in 2003 by the Belle Collaboration via the decay sequence $B^{\pm} \rightarrow K^{\pm} X(3872)$, $X(3872) \rightarrow \pi^{+}\pi^{-} J/\psi$. Its

Experiment	Year	Mode	Events
Belle	2003	$\pi^{+}\pi^{-}J/\psi$	35.7 ± 6.8
CDF	2004	$\pi^{+}\pi^{-}J/\psi$	730 ± 90
D0	2004	$\pi^{+}\pi^{-}J/\psi$	522 ± 100
Belle	2004	$\omega(\pi^{+}\pi^{-}\pi^{0})J/\psi$	10.6 ± 3.6
BaBar	2005	$\pi^{+}\pi^{-}J/\psi$	25.4 ± 8.7
Belle	2005	$\gamma J/\psi$	13.6 ± 4.4
Belle	2006	$D^{0}\overline{D}^{*0}$	23.4 ± 5.6

existence was quickly confirmed by CDF, DØ, and BaBar. It has now been seen in a variety of modes as shown in the table above; taken together, these results imply $J^{PC} = 1^{++}$. A state at this mass with these quantum numbers does not appear to fit within the charmonium spectrum.

Inspired by the coincidence of the $X(3872)$ mass and the $\bar{D}^0 D^{*0}$ threshold, a number of ingenious solutions to this puzzle have been proposed, including an *S*-wave cusp or a tetraquark state. Perhaps the most intriguing possibility is that the $X(3872)$ represents the first clear-cut observation of a meson-antimeson molecule: specifically, a bound state of $D^0\bar{D}^{*0} + \bar{D}^0 D^{*0}$. A key measurement is then the precise mass difference between the X and that threshold; if the molecule interpretation is correct, it should be very slightly negative, in accord with the small molecular binding energy:

$$0 < E_X = (m_{D^0} + m_{D^{*0}} - m_X)c^2 = 10 \text{ MeV}.$$

With the latest CLEO measurement $m_{D^0} = 1864.847 \pm 0.150 \pm 0.095$ MeV/c^2, we have $E_X = 0.6 \pm 0.6$ MeV/c^2, with the uncertainty dominated by our knowledge of m_X. A measurement of the width is also highly desirable. According to the Particle Data Group (2007), the width is expected to be less than 2.3 MeV. The systematic uncertainties in the width measurements of χ_{c1} and $\psi(2S)$ of the FNAL experiment E835 can serve as guidance here, allowing us to project to a width measurement better than 30 keV. Additional important measurements include $B[X(3872) \to \pi^0\pi^0 J/\psi]$ and $B[X(3872) \to \gamma J/\psi]$, to confirm the quantum-number assignment and further exclude identification as a charmonium state. The recent report from the Belle Collaboration of a near-threshold enhancement in $B \to D^0\bar{D}^0\pi^0 K$ decays tends to support the $D^0\bar{D}^{*0}$ -molecule interpretation. Interestingly, the enhancement is observed at a mass of $3875.2 \pm 0.7^{+0.3}_{-1.6} \pm 0.8$ MeV/c^2, 2.0σ higher than the world-average value of m_X. With the fine resolution available in $\bar{p}p$ formation the line shape of the X(3872) can be measured and the "single" or "double" peak issue can be resolved. It is clear that the additional avenue that $\bar{p}p$ formation provides to the study of this state could be extremely valuable in deciphering the nature of the $X(3872)$.

The production cross section for $X(3872)$ in $\bar{p}p$ annihilation has not been measured, but it has been estimated by Braaten to be similar in magnitude to that of the χ_c states. Additionally, the observed rate and kinematic distributions of $\bar{p}p \to X(3872)$ + anything at the Tevatron and of $B^{\pm} \to K^{\pm} X(3872)$ suggest that the production rate of $X(3872)$ in $\bar{p}p$ formation (at $\sqrt{s}$ = 3871.2 ± 0.5 MeV/c^2) should not differ greatly from that for charmonium states. By scaling from E760, at 10^{32} cm^{-2} s^{-1} we could then expect to produce ~ 0.1 $X(3872)$ event per second. The lower limit $B[X(3872) \to \pi^+\pi^- J/\psi] > 0.042$ at 90% C.L. then implies a signal of $\gtrsim 4 \times 10^{-3}$ detected events per second in the experiment we propose, or $\gtrsim 4 \times 10^3$ events in that mode per nominal month (1.0×10^6 s) of running. By way of comparison, the table above shows current sample sizes, which are likely to increase by not much more than an order of magnitude as the experiments complete during the current decade. (Although CDF and D0 could amass samples of order 10^4 $X(3872)$ decays, the large backgrounds in the CDF and D0 observations, reflected in the uncertainties on the numbers of events observed, limit their incisiveness.)

Given the uncertainties in the cross section and branching ratios, the above may well be an under- or overestimate of the $\bar{p}p$ formation and observation rates, perhaps by as much as an order of magnitude. Nevertheless, it appears that a new experiment at the Antiproton Accumulator could obtain the world's largest clean samples of $X(3872)$, in perhaps as little as a month of running. The high statistics, event cleanliness, and unique precision available via $\bar{p}p$ formation could enable the world's smallest systematics. Such an experiment could thus provide a definitive test of the nature of the $X(3872)$.

7.2.2 h_c

Observing the h_c ($1\ ^1P_1$) charmonium state and measuring its parameters were high-priority goals of both E760 and E835, as well as of their predecessor experiment, CERN R704. Being very narrow and having suppressed couplings both to e^+e^- and to the states that are easily produced in e^+e^- annihilation, the h_c is difficult to study experimentally.

A key prediction of QCD and perturbation theory is that the charmonium spin-zero hyperfine splitting, as measured by the mass difference Δm_{hf} between the h_c and the spin-weighted average of the χ_c states, should be close to zero. Using the current PDG-average values, $\langle m(^3P_J)\rangle = 3525.36 \pm 0.06$ MeV and $m(h_c) = 3525.93 \pm 0.27$ MeV, we find $\Delta m_{hf} = -0.57 \pm 0.28$ MeV, non-zero at the 2σ level but within the range expected from QCD. The PDG error on $m(h_c)$ includes a scale factor of 1.5 due to the tension among the four most precise measurements. Moreover, the most precise measurements (from E760 and E835) are based on signals that are statistically marginal, and whether the E760 observation was in fact a signal has been called into question by E835. The R704 result is on even weaker ground: a $\bar{p}p \rightarrow h_c \rightarrow J/\psi\ X$ decay at the level implied by Baglin et al. is most likely ruled out by both E760 and E835. Thus of the four results used by the PDG, only one is clearly reliable, and the claimed precision on $m(h_c)$ is far from established. This motivates an improved measurement. Also of interest are the width and branching ratios of the h_c, for which QCD makes clear predictions; the decay modes also bear on the question of isospin conservation in such decays.

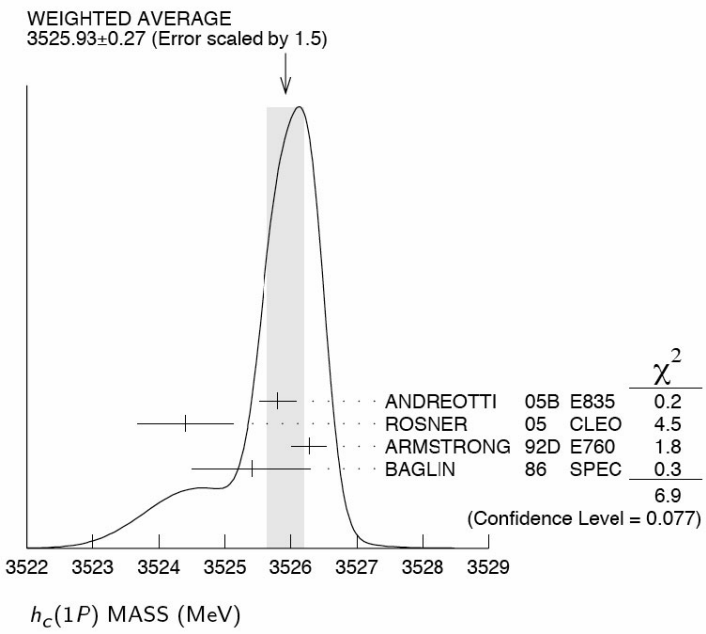

Ideogram of h_c mass measurements (from Particle Data Group, Review of Particle Physics, 2006)

E835 sensitivity in the $h_c \rightarrow \eta_c\, \gamma \rightarrow (\gamma\gamma)\gamma$ mode was limited by the $\eta_c \rightarrow \gamma\gamma$ branching ratio of only $(2.8 \pm 0.9) \times 10^{-4}$. Moreover, the acceptance times efficiency was reduced to only ≈ 3% by cuts needed to eliminate the substantial background from π^0 decays. Given a magnetic spectrometer, favorable modes in which to observe η_c include (among others) $\varphi\varphi$, φK^+K^-, K^*K^*, and $\eta'\pi^+\pi^-$. These have branching ratios up to two orders of magnitude larger, as well as more-distinctive decay kinematics, than $\eta_c \rightarrow \gamma\gamma$, probably allowing looser cuts to be used and higher efficiency to be achieved. For example, the $K^+K^-K^+K^-$ final state which would be a signature of $\eta_c \rightarrow \varphi\varphi$ has no quarks in common with the initial $\bar{p}p$ state and so should contain very little background. The $\eta_c \rightarrow \varphi\varphi$ mode was searched for in E835 but without a magnet its detection was barely feasible. Reliably assessing the improvement in performance for these modes with a magnetic spectrometer will require detailed simulation work, but at least an order of magnitude in statistics seems likely. Additional improvement in sensitivity will come from increased luminosity.

Provided detailed simulation studies bear out these ideas, we will soon have the opportunity to resolve this 20-year-old experimental controversy.

7.2.3 Hyperon CP violation

In addition to the well-known *CP* violation in kaon and *B*-meson mixing and decay, the standard model predicts slight *CP* asymmetries in decays of hyperons. In the kaon and beauty systems, such effects appear to be dominated by standard model processes. It thus behooves us to study other systems as well (such as hyperons), in which the signatures of new physics might stand out more sharply.

Hyperon *CP* violation would be of the direct type, since hyperon/antihyperon mixing would violate conservation of baryon number. The hyperon *CP* asymmetries heretofore considered most accessible involve comparison of the angular distributions of the decay products of polarized hyperons with those of the corresponding antihyperons; however, partial-rate asymmetries are also expected and may be detectable. More than one hyperon *CP* asymmetry may be measurable in medium-energy $\bar{p}p$ annihilation to hyperon-antihyperon pairs. To be competitive with previous Ξ and Λ angular-distribution asymmetry measurements would require higher luminosity (≈ 10^{33}) than is likely to be available, as well as a very substantial upgrade relative to the E835 apparatus. While summarizing the state of hyperon *CP* asymmetries generally, we here emphasize in particular $\Omega^- / \bar{\Omega}^+$ partial-rate asymmetries, for which there is no previous measurement.

By angular-momentum conservation, in the decay of a spin-1/2 hyperon to a spin-1/2 baryon plus a pion, the final state must be either *S*-wave or *P*-wave (or in the case of the Ω^-, *P*- or *D*-wave). The interference term between the two amplitudes gives rise to parity violation, described by Lee and Yang in terms of two independent parameters α and β: α is proportional to the real and β to the imaginary part of this interference term. *CP* violation can be sought as a difference in $|\alpha|$ or $|\beta|$ between a hyperon decay and its *CP*-conjugate antihyperon decay or as a particle–antiparticle difference in the partial widths for such decays. For a precision angular-distribution asymmetry measurement, it is

Exp't	Facility	Year	Modes	${}^{*}A_\Lambda$ / ${}^{\dagger}A_{\Xi\Lambda}$ / ${}^{\ddagger}A_{\Omega\Lambda}$
R608	ISR	1985	$pp \to \Lambda X, pp \to \overline{\Lambda} X$	$-0.02 \pm 0.14^{*}$
DM2	Orsay	1988	$e^+e^- \to J/\psi \to \Lambda\overline{\Lambda}$	$0.01 \pm 0.10^{*}$
PS185	LEAR	1997	$\overline{p}p \to \overline{\Lambda}\Lambda$	$0.006 \pm 0.015^{*}$
CLEO	CESR	2000	$e^+e^- \to \Xi^- X, \Xi^- \to \Lambda\pi^-$, $e^+e^- \to \overline{\Xi}^+ X, \overline{\Xi}^+ \to \overline{\Lambda}\pi^+$	$-0.057 \pm 0.064 \pm 0.039^{\dagger}$
E756	FNAL	2000	$pN \to \Xi^- X, \Xi^- \to \Lambda\pi^-$, $pN \to \overline{\Xi}^+ X, \overline{\Xi}^+ \to \overline{\Lambda}\pi^+$	$0.012 \pm 0.014^{\dagger}$
HyperCP	FNAL	2004	$pN \to \Xi^- X, \Xi^- \to \Lambda\pi^-$, $pN \to \overline{\Xi}^+ X, \overline{\Xi}^+ \to \overline{\Lambda}\pi^+$	$(0.0 \pm 6.7) \times 10^{-4\,\dagger}$
HyperCP	FNAL	2006	$pN \to \Omega^- X, \Omega^- \to \Lambda K^-$, $pN \to \overline{\Omega}^+ X, \overline{\Omega}^+ \to \overline{\Lambda} K^+$	$-0.004 \pm 0.12^{\ddagger}$

necessary to know the relative polarizations of the initial hyperons and antihyperons to high accuracy.

The table below summarizes the experimental situation. The first three experiments cited studied Λ decay only, setting limits on the *CP*-asymmetry parameter

$$A_\Lambda \equiv \frac{\alpha_\Lambda + \bar{\alpha}_\Lambda}{\alpha_\Lambda - \bar{\alpha}_\Lambda},$$

where α_Λ ($\bar{\alpha}_\Lambda$) characterizes the Λ ($\overline{\Lambda}$) decay to (anti)proton plus charged pion. If *CP* is a good symmetry in hyperon decay, $\alpha_\Lambda = -\bar{\alpha}_\Lambda$.
Fermilab E756, E871 ("Hyper*CP*"), and CLEO used the cascade decay of charged Ξ hyperons to produce polarized Λ's, in whose subsequent decay the slope of the (anti)proton angular distribution (in the "helicity" frame) measures the product of α_Ξ and α_Λ. If *CP* symmetry is obeyed in hyperon decay this product should be identical for Ξ^- and $\overline{\Xi}^+$ events. The asymmetry parameter is thus

$$A_{\Xi\Lambda} \equiv \frac{\alpha_\Xi\alpha_\Lambda - \bar{\alpha}_\Xi\bar{\alpha}_\Lambda}{\alpha_\Xi\alpha_\Lambda + \bar{\alpha}_\Xi\bar{\alpha}_\Lambda}$$

The power of this technique derives from the relatively large |α| value for the $\Xi^- \to \Lambda\pi^-$ decay, $\alpha_\Xi = -0.458 \pm 0.012$. Hyper*CP* recorded the world's largest samples of hyperon and antihyperon decays, including 2.0×10^9 and 0.46×10^9 Ξ^- and $\overline{\Xi}^+$ events. When the full analysis is complete, it should determine $A_{\Xi\Lambda}$ with a statistical uncertainty $\delta A \approx 2 \times 10^{-4}$. The standard model predicts this asymmetry to be of order 10^{-5}. Thus if the Hyper*CP* full analysis reveals a significant effect, it will be evidence for a new source of *CP* violation in the baryon sector. (Various standard model extensions predict effects as large as $O(10^{-3})$). Such an observation could be of relevance to the mysterious mechanism that gave rise to the cosmic baryon asymmetry. Hyper*CP* has also set the world's first limit on *CP* violation in Ω decay, using a sample of 5.5×10^6 $\Omega^- \to \Lambda K^-$ and 1.9×10^6 $\overline{\Omega}^+ \to \Lambda K^+$ events: $A_{\Omega\Lambda} = [-0.4 \pm 9.1\ (\text{stat}) \pm 8.5\ (\text{syst})] \times 10^{-2}$. This asymmetry is predicted to be $\leq 4 \times 10^{-5}$ in the standard model but can be as large as 8×10^{-3} if new physics contributes.

While *CPT* symmetry requires the lifetimes of a particle and its antiparticle to be identical, partial-rate asymmetries violate only *CP*. For most hyperon decays, partial-rate asymmetries are expected to be undetectably small. However, this need not be the case for the decays $\Omega^- \to \Lambda K^-$ and $\Omega^- \to \Xi^0\pi^-$, for which the particle/antiparticle partial-rate asymmetries could be as large as 2×10^{-5} in the standard model and one to two orders of magnitude larger if non-SM contributions are appreciable. The quantities to be measured are

$$\Delta_{\Lambda K} \equiv \frac{\Gamma(\Omega^- \to \Lambda K^-) - \Gamma(\bar{\Omega}^+ \to \bar{\Lambda} K^+)}{\Gamma(\Omega^- \to \Lambda K^-) + \Gamma(\bar{\Omega}^+ \to \bar{\Lambda} K^+)}, \quad \Delta_{\Xi\pi} \equiv \frac{\Gamma(\Omega^- \to \Xi^0\pi^-) - \Gamma(\bar{\Omega}^+ \to \bar{\Xi}^0\pi^+)}{\Gamma(\Omega^- \to \Xi^0\pi^-) + \Gamma(\bar{\Omega}^+ \to \bar{\Xi}^0\pi^+)}$$
$$\approx \frac{1}{2\Gamma}(\Gamma - \bar{\Gamma}) = 0.5(1 - \Gamma/\bar{\Gamma})$$
$$\approx 0.5(1 - N/\bar{N}),$$

where in the last step we have assumed nearly equal numbers (N) of Ω and ($\bar{N}$) of $\bar{\Omega}$ events, as would be the case here. Sensitivity at the 10^{-4} level then requires $O(10^7)$ reconstructed events. Measuring such a small branching-ratio difference reliably will require the clean exclusive $\bar{\Omega}^+\Omega^-$ event sample produced less than a π^0 mass above threshold, or $4.94 < p_{\bar{p}} < 5.44$ GeV/c.

Hyperon-production cross sections in low- and medium-energy $\bar{p}p$ annihilation are known for Λ, Σ, and Ξ. The inclusive hyperon-production cross section at $p_{\bar{p}} = 5.4$ GeV/c ($\sqrt{s} = 3.5$ GeV) is about 1 mb. At 2×10^{32} cm^{-2} s^{-1} this amounts to some 2×10^5 hyperon events produced per second, or 2×10^{12} per year.[5] The exclusive $\bar{p}p \to \bar{\Omega}\Omega$ cross section can be estimated by extrapolation, giving ~ 60 nb at 5.4 GeV/c. At luminosity of 2.0×10^{32} cm^{-2} s^{-1}, some 1.2×10^8 $\bar{p}p \to \bar{\Omega}\Omega$ events are then produced in a nominal 1-year run (1.0×10^7 s). Assuming the typical detector acceptance times efficiency of 50% and given the various branching ratios, an estimated 1.4×10^7 events each in $\Omega^- \to \Xi^0\pi^-$ and $\bar{\Omega}^+ \to \bar{\Xi}^0\pi^+$ are observed, and 4.1×10^7 events each in $\Omega^- \to \Lambda K^-$ and $\bar{\Omega}^+ \to \bar{\Lambda} K^+$, giving the following statistical sensitivities for partial-rate asymmetries:

$$\delta\Delta_{\Xi\pi} \approx 0.5/\sqrt{N_{\Xi\pi}} \approx 1.3 \times 10^{-4},$$
$$\delta\Delta_{\Lambda K} \approx 0.5/\sqrt{N_{\Lambda K}} \approx 7.8 \times 10^{-5}.$$

Tandean and Valencia have estimated $\Delta_{\Xi\pi} \approx 2 \times 10^{-5}$ in the standard model but possibly an order of magnitude larger with new-physics contributions. Tandean has estimated $\Delta_{\Lambda K}$ to be $\leq 1 \times 10^{-5}$ in the standard model but possibly as large as 1×10^{-3} if new physics

Asymm.	Mode	SM	NP
A_Λ	$\Lambda \to p\pi$	$\lesssim 10^{-5}$	$\lesssim 6 \times 10^{-4}$
$A_{\Xi\Lambda}$	$\Xi^\mp \to \Lambda\pi$, $\Lambda \to p\pi$	$\lesssim 0.5 \times 10^{-4}$	$\leq 1.9 \times 10^{-3}$
$A_{\Omega\Lambda}$	$\Omega \to \Lambda K$, $\Lambda \to p\pi$	$\leq 4 \times 10^{-5}$	$\leq 8 \times 10^{-3}$
$\Delta_{\Xi\pi}$	$\Omega \to \Xi^0\pi$	2×10^{-5}	$\leq 2 \times 10^{-4}$
$\Delta_{\Lambda K}$	$\Omega \to \Lambda K$	$\leq 1 \times 10^{-5}$	$\leq 1 \times 10^{-3}$

[5] Experience suggests that a data-acquisition system that can cope with such a high event rate is both feasible and reasonable in cost.

contributes.[6] It is worth noting that these potentially large asymmetries arise from parity-conserving interactions and hence are limited by constraints from ε_K; they are independent of A_Λ and A_Ξ, which arise from the interference of parity-violating and parity-conserving processes. The table summarizes predicted hyperon *CP* asymmetries.

Of course, experimental sensitivities will include systematic components whose estimation will require careful and detailed simulation studies, beyond the scope of this report. Nevertheless, the potential power of the technique is apparent: the experiment discussed here may be capable of observing the effects of new physics in Omega *CP* violation via partial-rate asymmetries, and it will represent a substantial improvement over current sensitivity to Omega angular-distribution asymmetries.

7.2.4 FCNC hyperon decays

Among recent Hyper*CP* results is the observation of the rarest hyperon decay ever, $\Sigma^+ \to p\mu^+\mu^-$. Surprisingly, based on the 3 observed events, the decay is consistent with being two-body: $\Sigma^+ \to p\ X_0,\ X_0 \to \mu^+\mu^-$, with $m(X_0) = 214.3 \pm 0.5$ MeV/c^2. With current statistics this interpretation is of course not definitive: the estimated probability that the 3 events are consistent with the SM form-factor decay spectrum is 0.8%. The measured branching ratio is $[3.1 \pm 2.4\ (\text{stat}) \pm 1.5\ (\text{syst})] \times 10^{-8}$ assuming intermediate two-body decay, or $[\ 8.6^{+6.6}_{-5.4}\ (\text{stat}) \pm 5.5\ (\text{syst})] \times 10^{-8}$ assuming three-body Σ^+ decay.

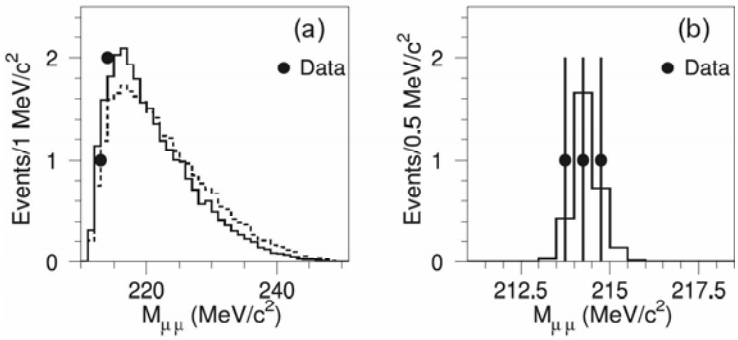

Dimuon mass distribution of the Hyper*CP* $\Sigma^+ \to p\mu^+\mu^-$ events (Phys. Rev. Lett. **94**, 021801 (2005).

If real, the X_0 cannot be an ordinary hadron: at that mass it would certainly have been observed in previous experiments. The Hyper*CP* result has notably been interpreted in the context of non-minimal supersymmetry by D. S. Gorbunov and co-workers and by He, Tandean, and Valencia: the X_0 might be an "sgoldstino" (the supersymmetric partner of a Goldstone fermion) or a light pseudoscalar Higgs boson.

Confirming or refuting the existence of the X_0 should be a high priority for a new hyperon experiment. While it might be desirable to use clean, exclusive $\bar{p}p \to \bar{\Sigma}^+\Sigma^-$ events just above threshold, this would require a $\bar{p}$ momentum well below what has been accomplished in the past by deceleration in the Antiproton Accumulator, as well as very high luminosity to access the $O(10^{-8})$ branching ratio. An experimentally less challenging

[6] The large sensitivity of $\Delta_{\Lambda K}$ to new physics in this analysis arises from chromomagnetic penguin operators and final-state interactions via $\Omega \to \Xi\pi \to \Lambda K$. (Large final-state interactions of this sort should also affect $\Delta_{\Xi\pi}$ but were not included in that prediction.)

but equally interesting objective is the corresponding FCNC decay of the Ω^-, with predicted branching ratio of $O(10^{-6})$ if the X_0 is real. (This large increase over that for $\Sigma^+ \rightarrow p\mu^+\mu^-$ reflects the additional phase space available; the standard model prediction is $B(\Omega^- \rightarrow \Xi^-\mu^+\mu^-) = 6.6 \times 10^{-8}$.) Again assuming a 60 nb cross section, 2×10^{32} luminosity, and 50% acceptance times efficiency, 120 or 40 observed events are predicted in the two cases (pseudoscalar or axial-vector X_0) that appear to be viable.

In addition, given the large inclusive hyperon rates at $\sqrt{s} \approx 3.5$ GeV, sufficient sensitivity might be available at that setting to test the Hyper*CP* $\Sigma^+ \rightarrow p\mu^+\mu^-$ result directly. Alternatively, it is possible that a dedicated run just above $\bar{\Sigma}^+\Sigma^-$ threshold may have competitive sensitivity; evaluating this will require a detailed simulation study.

7.2.5 Charm

A recent calculation by Braaten implies competitive sensitivity for open charm, with *D*-pair production rate about 100/s at $\sqrt{s} \approx 4$ GeV ($\sigma \approx 1$ μb). This could lead to a sample of $O(10^9)$ events/year produced and more than 10^8/year reconstructed, an order of magnitude beyond the statistics accumulated by the *B* Factories. Whether this sensitivity can be realized in practice will depend on details of trigger and analysis efficiency whose estimation will require detailed simulation studies. Nevertheless, there appears to be the potential for competitive measurements, e.g., of D^0 mixing and possible *CP* violation in charm decay.

7.2.6 Antihydrogen CPT tests

There is also interest in the possibility of decelerating antiprotons sufficiently to carry out trapped-antiproton and antihydrogen experiments. This capability could make Fermilab the world's premiere facility for this kind of research, and could attract a new community of physicists, including some now working at CERN's AD. Such experiments are already possible at low (~1%) efficiency using existing equipment at Fermilab, via antiproton deceleration in the Main Injector followed by energy degradation in a block of suitable material (e.g., steel). The efficiency could be somewhat improved by the addition of a small decelerating linac and concomitant reduction in degrader thickness. Ultimately, with the addition of a new, wider-energy-range antiproton ring (which might be built for a variety of applications as mentioned below), the rate of antiprotons deliverable to traps could substantially exceed that available at the AD.

A complementary approach is the study of antihydrogen atoms in flight, which may overcome some of the difficulties encountered in the trapping experiments at CERN. The first steps in this direction were taken by Fermilab E862, in which the formation of antihydrogen in flight was observed during 1996–7. Methods to measure in flight the antihydrogen Lamb shift and fine structure (the $2s_{1/2} - 2p_{1/2}$ and $2p_{1/2} - 2p_{3/2}$ energy differences) were subsequently worked out. Additional progress on this program of measurements may be compatible with normal Tevatron Collider operations — a possibility that is currently under investigation. In any case, if the feasibility of the

approach is borne out by future work, the program is likely to continue into the post-Tevatron era.

7.2.7 Antimatter gravitation measurement

The intensity of the Fermilab antiproton beam appears sufficient to allow the gravitational force on antimatter to be measured for the first time. Such a measurement will allow us to test our understanding of gravity in new ways. General Relativity (GR) makes a strong prediction that gravity does not distinguish between matter and antimatter. A direct measurement will thus allow some fundamental assumptions of GR to be tested experimentally (for example, the equivalence principle has never been tested with antimatter). While we have some very good experimental evidence that supports GR, we also know that there are serious fundamental inconsistencies between GR and quantum mechanics. This is illustrated by the cosmological-constant problem, where the prediction from quantum mechanics is 120 orders of magnitude larger than the observed value — possibly the largest discrepancy in physics. It is clear that some theory adjustments are needed. Some experimental guidance would be extremely helpful in resolving these issues.

The antimatter gravity experiment is particularly promising in this regard because if we discover "antigravity" (i.e., that antimatter "falls" upward), this may answer several questions at once. Antigravity could explain the apparent absence of naturally occurring antimatter, since the repulsive force would cause matter and antimatter to segregate in the early universe, leading to domains in which one or the other dominates. Furthermore, the net gravitational force from such a system of domains would be repulsive, and this would cause the expansion of the universe to accelerate. Thus a single, perhaps counterintuitive, result – the observation of a repulsive force between matter and antimatter – would simultaneously furnish possible explanations both of the baryon asymmetry of the universe and of dark energy.

Should the initial measurement show that antimatter falls down, there are still some interesting possibilities. For example, antimatter could fall faster than matter if there are gravivector and graviscalar forces that cancel for matter but add for antimatter. A sufficiently precise difference measurement between matter and antimatter would be sensitive to a fifth force that is too weak to have been detected in equivalence-principle experiments. Interferometric techniques have been used to measure the local gravitational force to better than one part in 10^{10}, and similar techniques could be used to measure the difference between the gravitational forces on hydrogen and antihydrogen.

We have the opportunity to measure the gravitational force on antimatter for a very modest cost by taking advantage of Fermilab's ability to accumulate large numbers of antiprotons. Once the apparatus is commissioned, the initial measurement could most likely be made with the antiprotons from a single store. Yet this experiment has the potential to create a revolution in the way we think about the universe. Regardless of the outcome, the antimatter gravity experiment is one that the general public can understand

and appreciate — while not the reason we do experiments, the potential public-relations value should not be underestimated.

7.2.8 Additional Physics

Besides the $X(3872)$, the experiment should have competitive capabilities for studying the additional charmonium-related states mentioned above. The very large inclusive hyperon samples should enable new and precise measurements of hyperon semileptonic and other rare decays. The APEX experiment vacuum tank and pumping system could be reinstalled, enabling a substantial increase in sensitivity for the antiproton lifetime and decay modes.

The bottomonium system has not benefited from $\bar{p}p$ formation studies but is potentially accessible if the Antiproton Accumulator (or perhaps a new storage ring) can be configured for colliding beams. The $\bar{p}p$ widths of bottomonium states are unknown. If they can be shown to be sufficiently large, $\bar{p}p$ formation could lead to the discovery of bottomonium singlet states, which have so far eluded observation, as well as precise measurements of the many states already observed. The current data sets of the B-factories could provide the first measurement or a stringent upper limit on the coupling between bottomonium and the $\bar{p}p$ system.

Antiprotons have a range of potential applications outside of particle physics, to e.g. medicine, homeland security, and nuclear physics. In future these might motivate the construction at Fermilab of an optimized facility for antiproton trapping, including a new storage ring and decelerating linac as touched upon above. (We mention this for completeness; the detailed discussion of such a facility is outside the scope of this report.)

7.3 Experimental Strategy

The variety of measurements discussed here cannot all be carried out with any one apparatus, nor in any one operating mode. We anticipate operating a "medium-scale" spectrometer at a variety of beam momenta in order to carry out the program of charmonium, charm, and hyperon measurements; this program will require a large duty factor and long running times. In parallel, smaller experiments using trapped antiprotons, or antihydrogen trapped or in flight, will be able to take data occasionally for R&D, with more extended data-acquisition periods as needed.

7.3.1 Charmonium, Charm, and Hyperon Measurements

Many of the measurements discussed here can be made with an improved version of the E835 detector. The key improvement is the addition of an analyzing magnet, e.g., a solenoid surrounding or inserted into the barrel calorimeter. The use of an existing magnet from a previous experiment seems feasible, although a custom magnet may prove superior. Charged-particle tracking can be provided using scintillating fibers (for which a very capable readout system will become available once the DØ experiment finishes),

with vertex reconstruction by means of silicon pixel detectors as developed for BTeV. The MICE experiment has demonstrated the efficient tracking of minimum-ionizing particles using fibers only 350 μm in diameter; this approach minimizes both the scattering and energy loss of the charged particles of interest, as well as the premature showering of photons to be measured in the electromagnetic calorimeter.

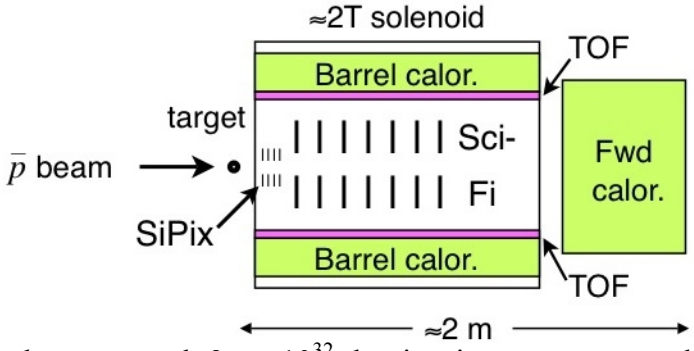

For operation at the proposed 2×10^{32} luminosity, some upgrading of the E835 calorimeter may be required. The shower light pulse develops promptly via Cherenkov radiation in the highly segmented E835 lead-glass calorimeter, but the response of the E835 photomultiplier tubes is slower than is desirable. The PMTs could possibly be replaced with faster photodetectors that have recently become practical. This could also overcome the degradation in performance that would result if the PMTs were required to operate in a significant magnetic field. Alternatively, use of a new calorimeter could be considered.

Triggering on events of interest should be based on a combination of charged-track multiplicity, particle transverse momentum and energy, and separated decay vertices. The anticipated interaction rate is about 10 MHz. A factor 10–100 bandwidth reduction by the first-level trigger would allow the remaining events to be read out into buffer memory and processed at trigger-level 2 in an on-line computer farm, with the *O*(10%) that pass level-2 requirements sent to archival media for off-line analysis. Due to the low energies and multiplicities, the needed data-acquisition bandwidth and sizes of the computing farm and resulting data set are expected to be small in comparison with those of CDF, DØ, and the LHC experiments.

7.3.2 Antihydrogen Measurements

The gravitational force on antimatter will be measured by directing a low-velocity beam of antihydrogen through an atomic interferometer and measuring the gravitational phase shift. The antihydrogen can be made by accelerating cold, trapped antiprotons to a velocity of a few kilometers per second and directing them through a positron plasma. A similar technique has been demonstrated to make a beam of antihydrogen at CERN's AD. A transmission-grating atomic interferometer could have a net transmission exceeding 10%, and could measure sub-micron phase shifts with a reasonable number of antihydrogen atoms. Such an interferometer has been in use with a sodium beam at MIT for over a decade. (Sodium has a much smaller wavelength than hydrogen at the same velocity, so the gratings for the MIT interferometer are much finer than would be needed in this experiment.)

The atomic interferometer would permit a 1% measurement of the gravitational force on antimatter very soon after the apparatus is shown to be working. A precision difference measurement between matter and antimatter would require a longer-term program, and the highest precision would require a laser-based interferometer such as has been used to measure local g to better than one part in 10^{10}. Such a measurement with antihydrogen would be sensitive to possible new forces much weaker than gravity that might couple differently to matter and antimatter.

7.4 Antiproton Summary

There is clearly the opportunity at Fermilab upon completion of the Tevatron program to mount a vital, varied physics program using the Antiproton Source. Such a program can answer a number of interesting physics questions while providing continuity for researchers during the construction of Project X and the larger experiments that it will support.

8. Conclusions

In order to maintain the discovery potential, scientific productivity, and vitality of the field during the next two to three decades it is necessary that the Fermilab research program pursues these same objectives.

This book has presented a set of flexible options for the accelerator-based Fermilab program and its scientific goals. The options rely on a new high-intensity proton source (Project X) as a national project with international collaboration and relevant experiments to it. The physics program exploiting the opportunities provided by Project X is compelling, rich, and robust. It has exciting opportunities in neutrino, muon, kaon, charm, and antiproton physics. The strength and uniqueness of Project X includes

- Delivering over 2 MW beam power in the wide range of proton energy between 60 and 120 GeV for neutrino oscillation programs.
- delivering 100 – 200 kW 8 GeV beam for rare decay and precision programs in parallel with 2 MW neutrino oscillation experiments.
- providing excellent beam structures by reconfiguring the existing rings. This would enhance significantly sensitivities of rare decay and precision experiments.
- providing potential upgrade paths to multi-MW at 8 GeV.

Some of the physics program at the intensity frontier can already be started with the existing source at Fermilab, and would benefit from physics results in the near term and a much higher intense proton source in the future. The program is continuous with current world leading programs in neutrinos.

A high-intensity proton source based on a superconducting linear accelerator would further develop the US and broader community capability to build the ILC and other accelerator projects in the future. Furthermore, such an accelerator provides a capable and upgradable platform for the field. It may also serve as the front end to the devices that might be indicated by the development of our physics understanding during the coming decades, whether for a neutrino factory, muon collider, or other machines at the frontier.

The community of users of an intense proton source has responded enthusiastically to the possibilities enabled by increased capabilities at the intensity frontier. Their active participation in working groups and workshops bodes well for the field if we can find the resources to follow through with the important opportunities presented in this book.

Working with the community and its Physics Advisory Committee, Fermilab will propose programs selected from among the high intensity source based opportunities.